Ion Exchange Resins and Functional Fibres: A Comparative Study for the Treatment of Brine Waste Water

Bongani Ndhlovu Yalala
BSc Hons (Applied Chemistry) NUST

A thesis submitted in partial fulfillment of the requirements for the degree of MAGISTER OF SCIENTIAE in the Department of Chemistry, UNIVERSITY OF THE WESTERN CAPE.

SUPERVISOR: Dr. Leslie Petrik

November 2009

Ion Exchange Resins and Functional Fibres: A Comparative Study for the Treatment of Brine Waste Water

KEYWORDS

Amberlite 252 RFH
Amidoxime-modified polyacrylonitrile
Adsorption
Adsorption isotherms
Adsorption kinetics
Brine
Calcium
Copper
Freundlich isotherms
Ion exchange
Langmuir isotherms
Magnesium
Polyacrylonitrile (PAN)
Pseudo-first order rate expression
Pseudo-second order rate expression
Sodium

Abstract

To improve the adsorption capacity of polyacrylonitrile (PAN) fibres, hydrophilic amidoxime fibres were prepared by subsequent conversion of the cyano groups to an amidoxime group by reacting with hydroxylamine at 80°C at an optimum amidoximation time of 2 hrs. The amidoxime fibre was hydrolyzed/alkali treated in a solution of sodium hydroxide to enhance or improve the adsorption properties. This was followed by characterization of the amidoxime and hydrolyzed fibres using Scanning electron microscopy (SEM); Fourier transform Infrared Spectroscopy (FT-IR) and exchange capacity (cationic and anionic). SEM showed that the hydrolysis process made the surface of Amidoxime fibre rougher than that of Polyacrylonitrile fibre. FTIR revealed that the hydrolyzed Amidoxime fibres contained conjugated imine (-C=N-) sequences.

The adsorption properties of Amidoxime and hydrolyzed Amidoxime fibres for Ca^{2+}, Mg^{2+}, Na^{+} and Cu^{2+} ions from brine wastewater were investigated by the batch technique. Comparative batch studies using Amberlite 252 RFH versus Amidoxime and hydrolyzed Amidoxime fibres was carried out. Various parameters such as fibre dose, pH of the solution, contact time and adsorption experiments were studied to understand the adsorption phenomena, loading capacity of the fibres and kinetics of adsorption for Ca^{2+}, Mg^{2+} and Na^{+} ions from the simulated brine solutions. Comparative batch results indicated that the hydrolyzed Amidoxime fibre was very effective in adsorbing copper over the other metal ions showing good selectivity towards Cu^{2+} ions. Adsorption followed this order: $Cu^{2+} > Mg^{2+} > Ca^{2+} > Na^{+}$. The binding capacity to Cu^{2+} ions is influenced by pH and the highest value of Cu^{2+} ions adsorption is obtained at pH 6.

Based on the results of the binding capacity of the amidoxime and hydrolyzed amidoxime fibres for Ca^{2+}, Mg^{2+} and Na^{+} ions in adsorption kinetics experiments, it was shown that the adsorption equilibrium could be reached within 10-15 mins. Two

adsorption kinetics models (Pseudo-first order and pseudo-second order) were used to test the adsorption kinetics data. The adsorption kinetics data proved to follow a pseudo-second order reaction mechanism. Two adsorption equilibrium isotherms models (Langmuir and Freundlich) were used and their parameters were estimated by fitting model equation to data from the batch experiments. The mechanism for the adsorption of Ca^{2+}, Mg^{2+} and Na^{+} was found to follow the Langmuir isotherm and second order rate. The adsorption capacities for Ca^{2+}, Mg^{2+} and Na^{+} ions were indicating that the monolayer adsorption occurred on the adsorbents.

Functionalization enhanced the sorption of amidoxime fibres by an increase of 20 % in the cationic exchange capacity. This was achieved by the part conversion of the cyano groups into the carboxylic acid groups. The fibres showed faster kinetics largely due the available exchange sites on the surface of the fibres hence the equilibration was achieved much quicker.

Declaration

I declare that ***Ion Exchange Resins and Functional Fibres: A Comparative Study for the Treatment of Brine Waste Water,*** is my work, that it has not been submitted before for any degree or examination in any other university and that all the sources I have used or quoted have been indicated and acknowledged as complete references.

Bongani Ndhlovu Yalala **November 2009**

Signed:……..

Acknowledgements

First, I would to thank my supervisor, Dr. Leslie Felicia Petrik, for giving the opportunity to pursue my studies under her guidance, her constant support, interest and supervision throughout this research. Dr. Gillian Balfour, who found time to read early editions of this thesis and improve it immensely with her profound feedback. Dr. Nuran Boke, for her immense contribution in the adsorption work. Her priceless feedbacks that led to a comprehensive experimental design. Mr. Bruce Hendry, who helped clarify the scope of this work and for his profound insights on ion exchange experiments. Many thanks go to the Environmental and Nano Science (ENS) group for the support offered during my MSc studies.

This work was made possible by sponsorship from Coaltech and National Research Foundation (NRF). Their funding has made it possible to understand and appreciate the importance conserving, pollution prevention, treatment and recovery water. From the Chemistry department my sincere gratitude is extended to Timothy Lesch for his instrument skills, Andile Mantyi for his assistance with chemical procurement. A special thanks to Averil Abbott for her untiring efforts in organizing and managing the administrative side of things. Your contribution is sincerely appreciated.

My deepest gratitude is reversed for my parents for all their patience, encouragement and help they have accorded me over the years. Their advice, guidance, education and upbringing they have given me that has made it possible to do my MSc. Lastly, I would like to thank my girlfriend, Rose Chakamanga for all her encouragement, help, support, patience and love.

Table of Contents

List of Figures

List of Tables

List of Abbreviations

AMD – Acid Mine Drainage

AOPAN – Amidoxime fibres (functionalized Polyacrylonitrile fibres)

BWRO – Brackish Water Reverse Osmosis

C_e – Equilibrium concentration of the adsorbate (mg/L)

DVB – Divinylbenzene

DWI – Deep Well Injection

ED – Electrodialysis

EDR – Electrodialysis Reversal

HAOPAN – Hydrolyzed Amidoxime fibres

IX – Ion Exchange

MED – Multi-effect distillation

MF – Microfiltration

MSF – Multi stage Flash distillation

MVC – Mechanical Vapour Compression

Q_e – Amount of metal ions adsorbed (mg/g)

RO – Reverse Osmosis

SAR – Sodium Adsorption Ratio

SAC – Strong Acid Cation

SBA – Strong Based Anion

SRO – Spiral Reverse Osmosis

SWRO – Sea Water Reverse Osmosis

TDS – Total Dissolved Solids

TVC – Thermal Vapour Compression

VC – Vapour Compression

UF - Ultrafiltration

International Conference Papers

1. **B. Yalala**, L. Petrik, G. Balfour, R. Vadapalli, B. A. Hendry, 2009. Comparative adsorption of major cations from brines by ion exchange processing using Amberlite 252 RFH resins and amidoxime fibres, International Mine Water Conference, October 19-23, CSIR, Pretoria, South Africa (Oral presentation).

2. **B. Yalala**, L. Petrik, G. Balfour, R. Vadapalli, B. A. Hendry, 2009. Preparation and characterization of poly(amidoxime) fibre for removal of calcium, magnesium and sodium ions from brine wastewater, Proceedings of sustainability through resource conservation and recycling 2009, MEI conference, April 4-5, Cape Town, South Africa (Poster presentation).

"Learn from yesterday
Live for today
Hope for tomorrow
The important thing is not to stop questioning…"
Albert Einstein

CHAPTER 1

1 Introduction

The increased level of environmental contamination as a consequence of industrial development is posing a very serious problem to the global environment. Industrial processes for extracting metals or, more generally, all processes involving metals in their productive cycle generate significant heavy metal pollution. Mine drainage, metal industries, refining, electroplating, dye and leather industries, domestic effluents, land fill leachate, and agricultural runoff all generate wastewater that contain heavy metal ions amongst other metal contaminants.

1.1 Background to Water Scarcity Problems

The gradual deterioration of water quality and the increasing water scarcity is a factor, which must be managed efficiently in order to treat and sustain it in the long run (Rijsberman, 2006). Water scarcity causes enormous problems for the vulnerable populations and societies (Pereira *et al.*, 2002). All industries must be prepared to become involved in the preservation of natural water resources.

The mining industry in particular is under enormous pressure to recycle and re-use water in order to minimize the intake of fresh water from the rivers and from water utility companies and eliminate the continuous decantation of polluted mine water into the environment and local river systems (Bell *et al.*, 2001). The practice in the mining community over the past decades has been the continuous pump-outs of the rising underground mine water into the river systems (Schoeman and Steyn, 2001). This has resulted in the pollution of the surface and ground water bodies, the soil and the vegetation surrounding the mining areas and the catchment areas. A rise in pollution and salinity of the water makes the surface water supply unfit for drinking, agriculture or environmental purposes.

Due to the shortage of fresh water supplies and the growing concern over the role of heavy metals in environmental issues, several water reclamation technologies have been studied and/or implemented to various degrees and these include chemical precipitation, membrane filtration, ion exchange, carbon adsorption, reverse osmosis and co-precipitation/adsorption (Kurniawan *et al*., 2006; Wang *et al*., 2003). Table 1.1 lists the advantages and disadvantages associated with each method.

Table 1-1: Treatment technologies for the removal of heavy metals from wastewaters and associated advantages and disadvantages.

Technology	Advantages	Disadvantages	References
Chemical precipitation	Process simple Not metal selective Inexpensive capital cost	Large amounts of sludge containing metals; Sludge disposal cost; High maintenance	Aderhold *et al*., 1996
Ion Exchange	Metal selective; Limited pH; High regeneration	High initial costs; High maintenance costs	Aderhold *et al*., 1996
Coagulation-flocculation	Bacterial inactivation capability; Good sludge settling & dewatering characteristics	Chemical consumption; Increased sludge volume generation	Aderhold *et al*., 1996
Flotation	Metal uptake; Low retention time; Removal of small particles	High initial capital costs; High maintenance and operation costs	Rubio et al., 2002
Membrane Filtration	Low solid waste generation; Low chemical consumption; Small space equipment; Possible to be metal selective	High initial capital cost; High maintenance & operational costs; Membrane fouling; limited flow-rates	Madaeni an Mansourpamesh, 2003; Qin *et al*., 1992
Electrochemical treatment	No chemical required, can be engineered to tolerate suspended solids; Moderately metal selective treat effluent >2000 mg/dm^3	High initial capital cost; Production of H_2 (with some processes); Filtration process for flocs	Kongsricharoern and Polprasert, 1995; Kongsricharoern and Polprasert, 1996.
Adsorption	Wide variety of target pollutant; High capacity; Fast kinetics; Possible selective depending on adsorbent	Performance depends on type of adsorbent; Chemical derivatisation to improve its sorption capacity	Crini (2005)

Currently water treatment processes, for instance, at power stations include water recovery through desalination, ion exchange regeneration for water softening to produce boiler feed water and cooling systems which produce blow down. While in mines, desalination, particularly reverse osmosis, treats rising underground water to potable levels. However, desalination technologies have problems associated with managing the inorganic waste products (sludges and brines) that are being produced. Most treatment systems produce brines that are of relatively high concentration and consequently are costly to dispose of or to convert into useful byproducts.

Brines and salinity build-ups are a direct consequence of the drive to save water through recycling and other recovery processes. Heavy metal contamination also exists in aqueous waste streams from mining operations. These pose a risk of metal contamination in groundwater and surface water. Heavy metals are not biodegradable and tend to accumulate in living organisms, causing various diseases and disorders. Significance progress has been made during the past few years with improved desalination technologies in industry and mining. However, the desalination technologies that are available are prohibitively expensive (often exceed the cost of water treatment) or unsatisfactory because of the long term liability and associated risks brines pose to water resources. The main limitation is the low efficiency in the removal of trace levels of metal ions. It is therefore necessary to develop cost effective ways and a holistic integrative solution to manage brines for long term sustainability as it relates to pre-treatment, beneficiation, disposal and concentration of the brines. The selection of the wastewater treatment method is based on the concentration of waste and the cost of treatment. Adsorption by ion exchange resin is one of the popular methods for the removal of major, minor and heavy metals from the wastewater and aqueous media (Yavuz *et al*., 2003).

Ion exchange resins have been developed as a major option for treating wastewaters over the past few decades (Szlag and Wolf, 1999). Non-specific sorbents, such as activated carbon, metal oxides, silica and ion-exchange resins have

also been used (Kantipuly *et al.*, 1990). Specific sorbents consisting of a ligand i.e. ion-exchange material or chelating agents, that interacts with the metal ions specifically and a carrier matrix that may be an inorganic material (i.e. aluminium oxide, silica or glass) or polymer microspheres (i.e. polystyrene, cellulose, polyhydroxyethyl methacrylate) have been considered for more specific removal (Kabay and Egawa, 1993; Denizli *et al.*, 1998). Selectivity is achieved by new types of ion exchangers with specific affinity to definite metal ions or groups of metals. Chelating ion-exchange resins which are also known as complexing or specific ion resins are designed to have high specificity for an ion or groups of ions. These types of ion-exchange resins adsorb metal ions through a combination of ionic and coordinating interactions instead of the simple electrostatic interactions in conventional cation or anion ion exchange (Harland, 1994). As a consequence, chelating resins offer greater selectivity than conventional resins.

1.2 Objectives of the Study

The treatment of brine (eutectic freeze crystallization-EFC, electrolysis, evaporative concentration and other concentration processes) requires the removal of $Ca^{2+}$and Mg^{2+}. The removal and recovery of Ca^{2+}, Mg^{2+} and Na^{+} ions from the waste water has received considerable attention because they are environmental pollutants, there are health implications and high costs associated with their removal and waste water treatment for both industrial and domestic consumption. Thus the overall objective of this study was to develop functional material to address the $Ca^{2+}$and Mg^{2+} ion contaminants in the brines as they affected the crystallization of NaCl during the eutectic freeze crystallization process in the treatment of brines.

The objective was addressed by investigating the performance of the functionalized chelating fiber (amidoxime-AOPAN) in removing Ca^{2+} and Mg^{2+} from brine solutions and comparing its performance to the conventional commercial resin (Amberlite^{R} 252 RFH). Adsorption of heavy metal ions, specifically Cu^{2+} was used to test the effect of the presence of minor/trace quantities of toxic elements on the

adsorption process of $Ca^{2+}$and Mg^{2+} by both Amberlite 252 RFH and Amidoxime (functionalized PAN-AOPAN) fibres.

The objective of this study was to investigate the performance of the functionalized chelating fibres in removing Ca^{2+}, Mg^{2+} and Na^{+} ions from brine solution and compare its performance to the conventional commercial resin (Amberlite 252 RFH). This study thus seeks to establish answers to the following research questions:-

a) Finding the best route to functionalizing the Polyacrylonitrile (PAN) fibres giving rise to the amidoxime fibres;
b) Ion exchange capacity, equilibrium isotherms and kinetics (mixing and fluid flow effects) investigation of the fibres/solution interface to attempt to understand the processes involved between the metal ions and the functional groups on the fibres;
c) Fibres/solution ratio: the optimum mass of metal ion uptake per volume of effluents.
d) The time variable (agitation period), to determine the optimum time for the system to reach equilibrium;
e) Performing equilibrium investigations (by varying initial metal concentration), to evaluate selectivity as well as the dominating reaction used for metal retention;
f) Comparing the ion exchange capacity of the functionalized fibres in terms of adsorption processes, to that of a selected commercially obtained organic resin exchanger (Amberlite 252 RFH) to determine the efficiency of the fibres;
g) Establish the effects of the presence of competing ions, to observe how they influence metal removal.

1.3 Research Approach

The amidoxime fibres (AOPAN) were used in the treatment of the modelled brine solutions prepared from brine effluent streams simulated to correspond to brines from Emalahleni Water Reclamation desalination plant. The plant is fed by acidic, saline mine waters from four coal mines in the Witbank area. Various parameters such as fibre dose, pH of the solution, contact time, and adsorption experiments were studied to understand the adsorption phenomena, loading capacity of the fiber, and kinetics of adsorption of Ca^{2+}, Mg^{2+} and Na^{+} from the brine solutions.

The research perspective encompasses the following:

a) Functionalization of the Polyacrylonitrile (PAN) fibres and its characterization;
b) Comparative batch adsorption experiments comparing Polyacrylonitrile (PAN) fibers with Amidoxime fibres using Amberlite 252 RFH resins as a standard.

1.4 Problem Statement

Brines are problematic effluents created by water desalination processes, oil and gas production, coal and gold mine drainage and evaporative cooling in power stations and process industries. Such brines are usually mixtures of many salts and disposal is environmentally problematic and costly due to the following reasons:

a) Surface water reservoirs and ground water sources can be polluted by brines, hence violating current environmental policies and legislature and rendering the current disposal methods as ineffective;
b) The increase, in volume and quantity, in the production of brines and its constituents result in an increase in disposal costs;
c) Escalating costs are associated with waste water remediation in a bid to augment fresh water supplies and it is necessary to reduce the actual costs of disposal in an environmental friendly manner.

1.5 Delimitation of Research

In the current study, the following areas were investigated:

a) Functionalization of the Polyacrylonitrile fibres and its characterization;
b) Comparative batch adsorption experiments of Amidoxime fibres against Amberlite 252 RFH resins;
c) Competitive adsorption of Ca^{2+}, Mg^{2+}, Na^{+} and Cu^{2+} ions from their binary, ternary and quaternary solutions by PAN, AOPAN and hydrolyzed AOPAN;
d) Synthetic solutions of calcium chloride ($CaCl_2$), magnesium chloride ($MgCl_2$) and sodium chloride (NaCl) based on the concentrations and elemental composition of the brines (major cations) in question was used in the above mentioned experiments.

In the current study the following areas were **not** investigated:

a) The polymerization of copolymers to produce different blends of Polyacrylonitrile (PAN) fibres and the Amberlite resins;
b) The characterization by determining the pore volume, pore radius and surface area of Polyacrylonitrile, Amidoxime and Amberlite resins was not considered.
c) The removal of toxic metals (heavy metals) other than Cu^{2+} ions fell outside the scope of the investigation.

1.6 Thesis Outline

The rest of the thesis is divided into the following chapters:

Chapter 2: *Literature Review*

A thorough and concise review of literature surrounding the production of brines and their impact on the environment, the treatment methods employed in brine effluent/waste water treatment, ion exchange and adsorption processes as an alternative method of treatment, and the use of Polyacrylonitrile (PAN) fibres as the starting raw material are presented. The main points are then interlinked in a brief summary section.

Chapter 3: *Methodology*

The sample preparation procedure for the functionalization of Polyacrylonitrile by hydroxylamine, the characterization of the amidoxime fibres using characterization tools: SEM, Fourier Transform Infra-red Spectroscopy (FT-IR), Cation and anion exchange capacity and qualitative test of amidoxime functional groups are presented.

Various batch adsorption experiments are presented with detailed experimental protocols concisely described, while all necessary calculation formulas are presented. *Chapter 3* gives an insight into the

type of data which can be extracted and the benefits it provided to the study and also justifies the choice of characterization tools and adsorption methodology used in the study.

Chapter 4: *Results and Discussion:*

In this chapter, the results of the characterization of Amidoxime fibres, in which the degree of functionalization was assessed, are presented. In addition, the adsorption characteristics of Polyacrylonitrile, Amidoxime and alkali treated Amidoxime fibres are also presented. The results and graphs that describe the adsorption, kinetics, and equilibrium of the adsorption process for both Amberlite resins and Amidoxime fibres are presented and extensively discussed here.

Chapter 5: *Conclusions and Recommendations*

The conclusions for the study on the metal removal capacity of the ion exchange adsorbents are discussed and directions for future work are suggested. Recommendations are made, anomalies noted, and the larger relevance and implications of the study are discussed.

CHAPTER 2

2 Literature Review

2.1 Introduction to Water Scarcity

Water is the essence of life as it is required in all aspects of life i.e., human consumption, agriculture and industrial use. It is a scarce resource, not only in arid and drought prone areas but also in regions where rainfall is abundant, which must be managed efficiently in order to treat and sustain it in the long run (Rijsberman, 2006). Water scarcity causes enormous problems for the populations and societies (Pereira *et al*., 2002). All must be prepared to become involved in the preservation of natural water source.

Natural fresh water bodies have limited capacity to respond to increased demands and to receive the pollutant charges of the effluents from expanding urban, industrial and agricultural uses. In regions of water scarcity the water resources are already degraded, or subjected to processes of degradation in both quantity and quality, which adds to the shortage of water. Water conflicts still arise in water stressed areas among local communities and authorities on the preservation of natural ecosystems. Uses such as domestic and urban uses, or activities that alleviate poverty and hunger, such as uses in industry, energy and food production are given first priority and the preservation issues are neglected. Water scarcity may result from a range of phenomena and these may be produced by natural causes (arid and semi-arid climates and droughts), may be induced by human activities (desertification and water management), or may result from the interaction of both (Pereira *et al*., 2002). Presently many water resources are polluted by industrial effluents, domestic and commercial sewage, acid mine drainage, agriculture runoff and litter (Davies *et al*., 1993). For countries that do not have much water to begin with, thus any pollution could have serious future consequences. There is a generally consensus that the need

for water and water supplies is rapidly increasing as a direct result of the growing population, improved standards of living and industrial expansion.

South Africa‘s freshwater supply is almost stretched to its limit (Schlacher and Wooldridge, 1996). Less than 10% of South Africa‘s rainfall is available as surface water, one of the lowest conversion ratios in the world (Anon, 1986). The distribution of the rainfall varies significantly and the availability of the water resource is uneven with approximately 60% of river flow arising from 20% of the land area (east coast). The country’s ground water resources are equally limited. Over-abstraction of ground water sources associated with deep pump irrigation has resulted in reduced freshwater supply to villages and caused lakes and rivers to dry up.

The country is currently categorized as water stressed with an annual fresh water availability of less than 1 700 m^3 per capita (the index for water stress). The current estimate by Food and Agricultural Organization (FAO) is 1.154 m^3 per capita/year. Vast expanses of South Africa are considered arid and semi arid land with 65% of the country receiving less than the minimum amount of rainfall required for successful dry land farming (<500 mm/year) (Anon, 1986). A continued lack of adequate rainfall has given rise to an increase in water demand, which is experienced by both urban and rural communities, probably resulting in increased conflict over its allocation and a further stress on this resource leading to scarcity. Typical conflicts are those between rapidly growing urban areas that claim water for agriculture or conflict between agriculture and environment as agriculture seeks to expand or look for new resources to replace those given up to urban areas. The rural (49 % in population) communities have had to augment their water sources in order to be able to continue with their agricultural activities. However, the sharply increased water and chemical use that fuelled the Green Revolution has contributed to environmental degradation and threatened the resource base upon which human population depend on for food and livelihood.

The pollution of South Africa's scarce water resources through mining is arguably one of the greatest challenges facing the country. In South Africa, the mining sector contributes between 20-30 % of the country's mineral sales, and is the second largest coal exporter in the world (Lloyd, 2002). South Africa's generating technology is largely based on coal fired power stations, with about a million tons of coal finding its way into South African homes. Supplying electricity plays a pivotal role in South Africa, in which it makes up 25 per cent of final energy demand in the country's economy (Lloyd, 2002). According to the Department of Water Affairs and Forestry (DWAF), mining and power generation accounts for more than 10% of the total of 20 x 10^9 m^3 water used annually in South Africa (Eskom, 2000). The main heavy metal-laden waste which emanates directly from coal mining operations, even decades after the decommissioning of a mine, is acid mine drainage (AMD) and since mining sites are usually close to natural streams, thousands of kilometers may be affected and as such, toxic metal pollutants enter our waterways. The underground mine systems of coal and gold mines are interconnected and rely on responsible and collective mine-water management to sustain their individual operations (Bell *et al*., 2001). Most mine-water is pumped to the surface to allow continued deep underground mining operations. Some of the water is stored and treated, before reuse and the remaining water is normally released into surrounding streams and rivers as mine-brine waste water or AMD. A rise in pollution and salinity the surface water makes it unfit for drinking, agriculture or environmental purposes.

Currently South Africa is running a campaign to improve and increase the quantity and quality of potable water supplied for both domestic (6000 L per family per month) and industrial uses. This situation has resulted in portable water demand levels soaring which will probably lead to scarcity. In South Africa, major contributing factors of water scarcity, range from limited fresh water supplies, and pollution of water resources through mining activities (brines and AMD), human population growth and increased demand for water from industry, mining and

domestic sectors (Rijsberman, 2006). To meet this demand, water reclamation has been identified as a viable alternative to augment water supply. Various sources have been identified and these include industrial waste waters, underground and mine waters, brackish, saline and brine waste waters.

2.2 Brine

Brine is water saturated or near saturation with dissolved salts that include sodium, calcium, potassium, chlorides, sulphates and nitrates ions and high total dissolved solids (> 1,500mg/kg TDS) (El-Manharawy & Hafez, 2003**)**. Reject brine, also referred in the literature as concentrate or wastewater, is a byproduct of the desalination processes, mine water and power generating station pump outs. All these processes generate saline effluents that require handling and disposal. The continued discharge and surface disposal of these waters has led to a significant ground and surface water pollution resulting in salinity levels in excess of the Department of Water Affairs and Forestry (DWAF)'s limits.

El-Manharawy et al. (2003**)** presents water chemical classification (Table 2.1) based on the grouping of natural waters that acquire similar chemical characteristics in relation to ascending chloride concentration (in mMol/kg).

Table 2-1: Chemical classification system of natural waters based on chloride molar

Class	**Proposed name**	**Chloride (mmol/kg)**	**Major ion concentrations (mmol/kg)**					**TDS (mg/kg)**
			Ca	**Mg**	**Na**	**K**	**SO_4**	
Fresh Water	Very low fresh	<0.5	<1	<0.5	<1.5	<0.2	<0.5	**<300**
	Low fresh	0.5-1.0	<2	<1	<3	<0.3	<1	**300-600**
	Medium fresh	1.0-1.5	<2.5	<1.5	<5	<0.4	<1.5	**600-1000**
CLASS A: Low Chloride	High fresh	1.5-3.0	<3	<2	<10	<0.5	<2	**1,000-1,500**
	Low Brackish	3.0-10.0	<5	<5	<20	<1	<5	**1,500-2,000**
	Medium brackish	10.0-25.0	<10	<6	<40	<1.5	<10	**2,000-4,000**
CLASS B: Medium Chloride	High brackish	25.0-50.0	<29	<10	<70	<3	<20	**4,000-7,000**
	Low salty	50.0-100	<25	<10	<100	<4	<25	**7,000-10,000**
	Medium salty	100-200	<30	<20	<200	<6	<30	**10,000-15,000**
CLASS C: High Chloride	High salty	200-500	<25	<35	<400	<10	<40	**15,000-30,000**
	Seawater	500-600	<20	<60	<500	<10	<50	**30,000-40,000**
	Very salty seawater	600-700	<20	<80	<600	<15	<60	**40,000-50,000**
	Sub-brine	700-800	<20	<100	<800	<30	<70	**50,000-60,000**
CLASS D:	**Brine**	**>800**	**>20**	**>100**	**>800**	**>30**	**>70**	**>60,000**

Natural brines are commonly found in the interior of the earth, and they are also found on the earth's surface, mostly as a by-product of the oil and gas production wells; hence they are known as oil-field brines. Historically, brines would be dumped into a pit and commonly they would appear to "evaporate" or otherwise go away (Canter *et al.*, 1987). However in many cases, brines would simply seep downward into the subsurface rocks and contaminate the local aquifer. Because groundwater in most places moves slowly, perhaps only several millimeters a year (Canter *et al.*, 1987), many years might pass before nearby water wells became contaminated. Both past and present brine disposal practices can contaminate groundwater. The most commonly practiced disposal option for brines include surface water bodies, sewer streams, evaporation ponds, land application including percolation and deep well injection (DWI). Waste minimization (wastewater evaporators) to surface water, concentration into solid salts, irrigation of plants tolerant to high salinity (halophytes)

and co-disposal with wastewater treatment plant effluent or power plant cooling tower water are new concepts (Khedr *et al*., 2008).

2.2.1 Sources of Brines

The source of brine waste water stream studied in this research was an effluent waste stream from Emalahleni Water Desalination Plant, which uses the reverse osmosis technology. Its feed water source is a large volume of excess underground mine water with a significantly high salt concentration from four fully operational coal mines. These mines have water quality associated with calcium, magnesium, sulphate ions (neutral type of water) and its slightly acidic (associated with iron, manganese and aluminum metals). Annandale *et al*., (2002) states that Kleinkopje colliery currently has some 12 million m^3 of stored underground mine water and is estimated to be generating at a rate of 14 ML/d. The Emalahleni Water Desalination Plant (Figure 2-1) gives a great opportunity to study this type of brine water considering that during its purification activity it also concentrates the salts and also handles large volumes of salty water hence highlighting the need for environmental friendly disposal methods. The high concentration and large volume of mine water gives an opportunity to try low cost adsorbents with great adsorption capacity and greater kinetics.

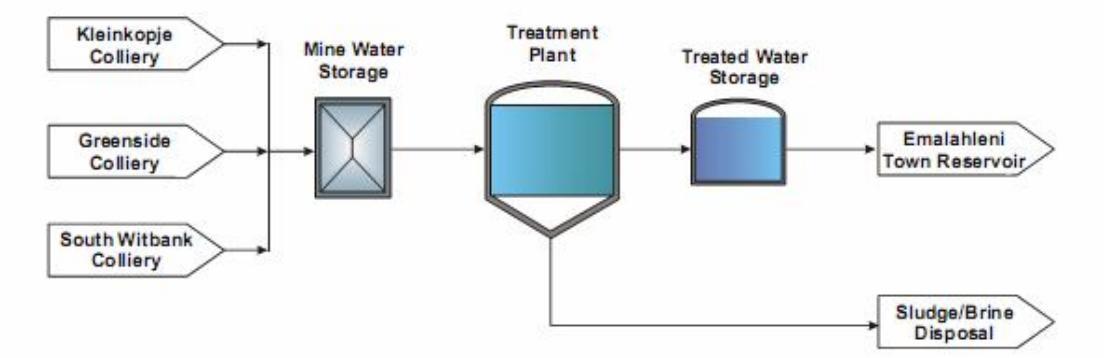

Figure 2-1: Schematic of the Emalahleni desalination plant

In the following section, sources of brine waste water streams from coal mines, power stations and desalination processes will be described in detail. The

focus on these particular sources has been determined by a careful study of various brine sources and where found to be the largest contributors to surface waterway pollution.

2.2.1.1 Saline Streams from Coal Mines

Coal is the most abundant energy source in the world and it's a major source of hydrocarbons. Coal in South Africa is mined in Gauteng, Free State, Mpumalanga and KwaZulu Natal Provinces. Most environmental problems in coal mines can be attributed to the mining methods used in the 1930s and 1940s, notably the practice of pillar robbing (Pereira *et al.*, 2002). The majority of coal deposits are found in Mpumalanga and in the northern Free State provinces. In Mpumalanga it is generally found at shallow depths and in thick seams, which make them easier and usually cheaper to mine hence it's the most cost effective and efficient way of generating electricity. However in KwaZulu-Natal, the seams are deeper and thinner, but of a higher quality.

A lot of mining activity has been done by the coal mines in the upper Olifants River catchment area, which stretches across the Witbank and Middleburg areas in the Mpumalanga province. Most coal mines in this water catchment area have a water quality associated with calcium-magnesium-sulphate rich, neutral type of waters (see Table 2.2; Annandale *et al.*, 2002) and some mines have additional problems of acidic types of waters yielding pHs below 3 (Gunther and Mey, 2007). The saline mine waters have a TDS range around 4000 mg/L, conductivity varying between 2000 µS/cm and 6500 µS/cm, and acidity is associated with iron, manganese and aluminum concentrations (Gunther and Mey, 2007; Burhrmann *et al.*, 1999). Underground coal mines have to deal with excess quantities of underground water (Burhrmann *et al.*, 1999). The mines are continuously expanding and therefore there is a constant influx of water into the mine, creating an increasing demand for water to be pumped out. When mining is completed in a section, that mine section is closed

and the pumping equipment is removed. Eventually the mine roof collapses, which in turn breaks the aquifers causing underground water to flow into the mine. In 1992, an estimate of about 130,000 tons of salt was discharged from coal mines, and 200,000 tons discharged from gold mines, at an average total dissolved salt concentration of 2 g/L (Annandale *et al.*, 2002). This water has high salinity and as per the South African environmental legislation these saline waters, AMD, circumneutral waters should be treated before being discharged.

Table 2-2: Typical mine water quality from 3 Coal mines (Landau and Kleinkopje Colliery, Witbank**)**

Water	**pH**	**Electrical conductivity (mS/m)**	**Ca^{2+} (mg/L)**	**Mg^{2+} (mg/L)**	**K^{+} (mg/L)**	**Na^{+} (mg/L)**	**HCO_3^{-} (mg/L)**	**Cl^{-} (mg/L)**	**SO_4^{2-} (mg/L)**
Lime-treated mine drainage Landau Colliery	6.0	156	287	19	11	7	10	3	998
Kleinkopje (Jacuzzi) Colliery	6.4	288	555	170	-	46	142	19	1986
Kleinkopje (Tweefontein) Colliery	7.1	227	405	196	-	47	68	32	1524

2.2.1.2 Brines from Power Stations

In South Africa, coal is the most abundant source of energy. It is a low grade quality bituminous coal with a low heat value and high ash content (Willis, 1987).

Eskom relies on coal fired power stations to produce approximately 90 % of its electricity and for logistical reasons they were built near the coal mines (Willis, 1987). Eskom uses over 100 million tons of coal per annum (Willis, 1987). Coal mining in South Africa is relatively cheap compared to the rest of the world. These low costs have had an important effect on the nation's prosperity and potential for development. In Europe, by contrast, costs are almost four times higher.

Cooling towers in power stations rely on evaporation process to release heat from process water. To keep the balance of salt concentration, a portion of the water is siphoned off and replaced with fresh water. This discarded water, namely blow down water, is characterized by its hardness and high salt concentration, principally calcium carbonate ($CaCO_3$) and calcium sulphate ($CaSO_4$) (Stratton and Lee, 1975). The blow down water has high turbidity and conductivity, and a pH between 9.6 – 10.5 (Khedr *et al.*, 2008). For large cooling towers, blow downs are usually continuous and amount to 0.5 -3 % of the recirculating water flow rate (Stratton and Lee, 1975). In order to bring the standard of this water to acceptable level for use in the plant, treatment is required to soften it and remove the salts. In some power stations such as Tutuka Power Station, the feed water is a combination of the sites' cooling tower blow down effluent and the neighbouring coal mine's produced water (50% cooling water and 50% mine water) (Khedr *et al.*, 2008; Burhrmann *et al.*, 1999). This is recovered using a number of full scale membrane applications such as Electro dialysis Reversal (EDR) and Spiral Reverse Osmosis (SRO). These processes produce a highly concentrated saline solution as a by-product during regeneration of the membranes. These waters need to be treated before conversion into a useful by-product such as sodium carbonate. Traditionally, cation exchange water softeners are regenerated with excess sodium chloride (NaCl) regenerating material. The sodium ions replace the magnesium and calcium ions trapped on the ion exchange resin. Calcium chloride and magnesium chloride are produced. Those chlorides, along with the excess NaCl, are dumped into the sewers and eventually find their way into the nation's rivers, streams and lakes.

Since all of these materials in the regenerant wastes are soluble, their discharge into a water course adds significantly to the TDS. These high TDS waters must be handled further downstream in order to make it suitable for domestic or industrial consumption. For this reason, pollution control laws already enacted or about to be enacted may in the near future prohibit discharge of high concentration

soluble inorganic salts into waters. Accordingly, it becomes necessary to attempt to prevent such a discharge or regenerant brine from cation exchange water softeners.

2.2.1.3 Brines from Desalination Processes

Desalination is becoming a solution for water scarcity in most arid countries where structural water shortage is a permanent phenomenon. Water scarcity is caused by an ever increasing demand for water to support urban and industrial developments, population growth, improvement in lifestyle and climatic changes (Tsiourtis, 2001). Countries such as Israel, Cyprus and Jordan, which have exploited their limited natural water resources with no more sources to develop, have turned to desalination as an alternative. The falling costs of desalination, which are due to the technological advances in the desalination process, and provision of abundant fresh water from both seawater and from challenging brackish sources have also led to growth in the desalination industry.

Desalination is the separation of fresh water containing a low concentration of dissolved salts from sea, brackish or saline water. In the production of fresh water, the dissolved salts are concentrated to produce a saline stream (concentrate or brine) which must be disposed off. The amount of concentrate produced from a desalination plant is a factor of the desalination process' recovery rate (product water/feed water). One of the disadvantages of the desalination processes in that seawater reverse osmosis (SWRO) plants can produce concentrate that is two times more concentrated than the feed waters while the concentrate produced from the distillation process may have only a 10% salt concentration (Tsiourtis, 2001; Mauguin and Corsin, 2005). According to Awerbuch and Weekes (1990), brackish water Reverse Osmosis plants (BWRO) produced 25% of the total feed water, while groundwater Reverse Osmosis (RO) plants produced 10-25% of the total feed water (Alaabdula'aly and Al-Saati, 1995). Generally acceptable membrane performances of water recovery yields are in the region of 30-60% for Sea Water Reverse Osmosis (SWRO), 60-85% for Blackish

Water Reverse Osmosis (BWRO), 85-97% for BWRO with concentrators and 95-99.5% for salt rejection (Wangnick, 2002). High recovery leads to a concentrating effect of dissolved species in the feed water. The concentrate from membrane desalination processes is characterized by high TDS and has minimal amounts of process-added chemicals. Brackish waters in the salinity range of 2,000 – 5,000 mg/L can be brought up to drinking water quality at a cost of approximately $0.75 - $1.00 per 1,000 gallons compared with sea water desalination costs in the range of $3.00 - $5.00 per 1,000 gallons.

These systems are selected based on operational costs, energy consumption and the type of waste water streams that will be treated. The multi-stage flash evaporation (MSF) and RO processes dominate the market for both seawater and brackish water desalination, sharing about 88% of the total installed capacity (Turek, 2004) (Figure 2.2). Raw water with different qualities has been treated in desalting plants, dominated by seawater and brackish water (Turek, 2004) (Figure 2.3). Seawater is often desalted by various thermal processes and also by reverse osmosis (RO), whereas brackish water is mainly treated by means of RO and ED. Commercially the two most important technologies are based on the thermal and membrane processes. The known thermal processes are multi-stage flash evaporation (MSF), multiple-effect distillation (MED), and vapor compression (VC) distillation processes. The membrane processes are reverse osmosis (RO), electrodialysis (ED), microfiltration (MF), ultrafiltration (UF) and nanofiltration (NF) (Tang and Yong, 2008).

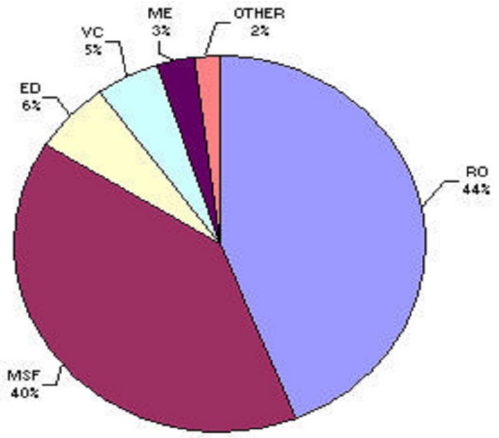

Figure 2-2: Installed desalting capacity by process. (RO = 44%; MSF = 40%; ED = 6%; VC = 5%; ME = 3%; Other =2%).

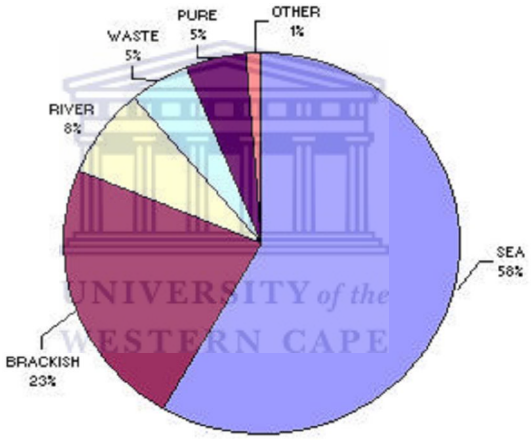

Figure 2-3: Installed capacity by raw water quality. (Sea = 58%; Brackish =23%; River = 8%; Waste = 5%; Pure = 5%; Other = 1%).

Figure 2.2, shows that, of the 100% of desalted water produced around the globe annually, RO (44%) and MSF (40%) are the most widely used technologies. In the US, the primary desalination method currently utilized is RO, while a majority of the large seawater desalination facilities in the Middle East utilize MSF and other distillation technologies.

2.2.2 Treatment Technologies Based On Thermal Processes

About 75% of all desalination facilities in use today employ some variation of the desalination/condensation (Thermal desalination processes) processes due to its simplicity and near universal applicability (Abufaved and El-Ghuel, 2001). Efficiency of the distillation cycle is a function of the difference in temperature (ΔT) of the ambient seawater at the intake to the effluent at the discharge. The lower this differential temperature, the higher the efficiency of the system will be and the lower the specific power consumption will be.

Generally water is evaporated and the resulting vapour is condensed and collected as fresh water. In a multi-effect evaporator, the latent heat released by the condensing water is used to evaporate water at a lower pressure in another vessel (called an "effect") (El-Dessouky *et al*., 1998). MSF evaporation occurs by superheating water under pressure, then releasing this pressure. The pressure release causes water to evaporate spontaneously until it cools to the boiling point.. The heated water is passed through a succession of chambers (called "stages") at lower pressures. Addition of many effects or stages reduces the energy consumption of these processes, hence the names "multi-effect" and "multi-stage flash" distillation. In thermal distillation (particularly MED), 1 kg of steam can produce approximately 15 kg of potable water (Khawaji *et al*., 2008). Mechanical vapor compression (*MVC*) uses a pump to create a partial vacuum over the saline water, which causes the water to evaporate. The vapor is then condensed by reapplying pressure. Thermal vapor compression (*TVC*) operates on the same principle as MVC. However, in this case, a steam-jet aspirator replaces the mechanical pump.

Distillation is capable of removing 99.5% of impurities from water but traditionally the capital cost of the facilities is too high for treating large volumes of water. Distillation systems are more energy intensive (up to four times more) than reverse osmosis systems, but require less pretreatment of the water and are therefore

generally considered to be more robust (Khawaji *et al*., 2008). The process is good for removing hardness, nitrates, sodium, heavy metals, dissolved solids, bacteria and many organics. MSF, MED, MVC are thermal processes which produce distilled water with TDS of 1 – 50ppm.

These processes are major consumers of energy due to high heats of vaporization (evaporating water at 90-120^{o}C) and also the heat loss through the cooling systems (Mohamed and Antia, 1998). However, hybrid designs combining two or more basic desalination technologies have been developed specifically to reduce energy requirements. For example, combining a VC system with single-stage VTE system increases efficiency by about 30% and/or capitalizing on an existing supply of energy provided by power stations (this is particularly feasible for seawater distillation plants, which require low temperature steam as the heat source). The concentrate from thermal processes such as MSF and multi-effect boiling (MEB) is mixed with cold water prior to discharge. The dilution of concentrate results in a final discharged effluent is rarely more than 15% higher in salinity than the receiving water.

2.2.3 Treatment Technologies Based On Membrane Processes

There are two basic types of membrane desalination: RO and ED. In RO systems, pressure is applied to overcome the natural osmotic tendency of water to flow from areas of high concentration to low concentration. The pressure forces water molecules to flow against the osmotic gradient through a series of membranes that are permeable to water, but trap salts.

ED systems exploit the ionic nature of dissolved salts. Saline water is sandwiched between cation-and anion-selective membranes. In this process, only the dissolved solids move through the membranes and not the solvent, so that practical concentrations or depletion of electrolyte solutions is possible. A positive charge is

applied to one side and a negative charge to the other side of the membranes. This electrical charge draws anions through the anion-selective membrane toward the positive charge and the cations through the cation-selective membrane toward the negative charge (see figure 2.4). Fresh water is left behind and is thus desalinized (Valerdi-Perez *et al.*, 2000).

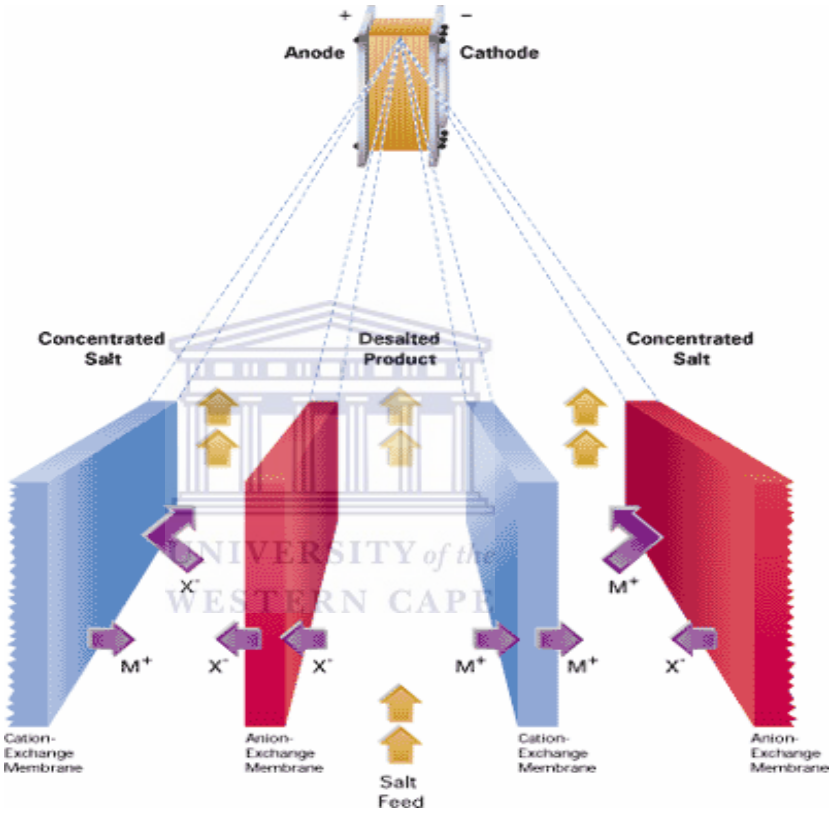

Figure 2-4: Scheme of an electrodialyzer with two cell pairs: migration of ions is caused by the action of an electric field.

Semi permeable and ion specific membrane processes have emerged recently as one of the most promising technologies for advanced water reclamation and wastewater treatment. Integrated membranes systems such as micro-filtration (MF), ultra-filtration (UF), nano-filtration (NF), electro-dialysis reversal (EDR) and RO have been used inter-changeably for either pretreatment (purification) of waste waters or concentration (separation) of ions or metals from the waste streams (Arnal *et al.*, 2005; Nederlof and Hoogendoorn, 2005; Turek *et al.*, 2008; Pak and Mohammandi,

2008 and Sandeep *et al*., 2006). Particle separation in the first two processes essentially involves the use of a sieving mechanism (membrane) that allows particles smaller than its pores to pass through but retains larger ones. NF occupies an intermediate position, allowing the passage of both ions and other entities of a suitable size. It may also be used to remove certain large-sized ions from the solution. However, in the RO process, the membrane allows only the solvent, termed the permeate, to filter through, and retains the solute (inorganic ions as well as the emerging organic pollutants). Currently most desalination plants use a combination of at least two membrane separation techniques to reliably produce high quality water for both industrial and domestic use.

Due to high demand for these processes caused by fresh water scarcity, improvements in the desalination processes for reducing and/or treating the concentrate effluent are being developed and implemented. The larger the capacity of the desalination plant, the larger the reject concentrate being produced. Treating the concentrate is more expensive than the whole water purification process.

2.2.4 Impact on Environment

Reject brine streams contains residues of water softening chemicals (lime), flocculation (aluminum and iron sulphates, silicates), disinfectants (chlorine, sodium hypochlorite), antiscalants, and antifoaming agents. Magnesium, calcium, sodium and chloride are primary contributors to salinity and high TDS levels in water, which can have toxic effects for human and livestock consumption. One of the impacts of land disposal is water pollution that results when concentrated brine is discharged into fresh water sources and unprotected wells. A study in India indicated that seepage from brine caused groundwater contamination of the source well and resulted in an increase in hardness of the groundwater (Mohamed and Antia, 1998).

The chemistry of brine has a significant impact on the environment. Salinity in the soil generally reduces crop growth and this is dictated by the salt tolerance of the plant. This is evidenced by the reduction in plant growth, darkening of the colour of the leaves and scorching of shoots. Dissolved salts increase the osmotic potential of soil water and therefore increase the amount of energy which plants must expend to extract water from the soil. As a result, growth and yield of most plants decline progressively as osmotic pressure increases due to the presence of salts in the soil and the soil water. High solute concentration in the soil solution is conducive for good physical properties in the soil. However, high sodium and chloride levels in clay soils decreases soil permeability, reduces aeration and causes dispersion of soil particles. It can also alter the electrical conductivity of soil, changing the sodium adsorption ratio (SAR) and induce specific ion toxicity. SAR defines the influence of sodium on soil properties by calculating the relative concentration of sodium, calcium, and magnesium (Mickley *et al*., 1993). Although sodium does not reduce the intake of water by plants, it changes soil structure and impairs the infiltration of water, affecting plant growth. Furthermore, it increases irrigation and rainwater runoff, poor aeration and reduces leaching of salts from root zone because of poor permeability.

2.2.5 Disposal of Brines

Disposal of brine is a major problem because of

(a) development and implementation of environmental policies that are protecting the environment from continued pollution hence rendering the current disposal methods as prohibited;

(b) the escalating costs associated with the waste water remediation in a bid to augment fresh water supplies and the actual costs of disposal in an environmental friendly manner, and

(c) the increase in the volume or quantity in the production of the brine wastewater and its constituents.

The single highest producer of brine wastewater is the desalination process, with about 20 - 50% of the total feed water flowing as reject brine. The amount of brine produced, as a percentage of the feed water, depends on the choice of the method, initial salinity of feed water and factors affecting the choice of disposal method. Mickley *et al*. (1993) identified the factors that influence the selection of a disposal method. These include the volume or quantity of concentrate, quality or constituents of concentrate, physical or geographical location of the discharge point of the concentrate, availability of receiving site, permissibility of the option, public acceptance, capital and operating costs, and ability for the facility to be expanded.

Glater *et al*. (2003) cites deep well injection, evaporation ponds, and solar ponds as major strategies for brine disposal, however they are not applicable to very large volumes of wastewater. Various other options exist for the disposal of brine waste water; it includes waste minimization, disposal into surface water bodies, disposal into municipal sewers, pumping into specially designed evaporation ponds, thermal evaporation towards the zero liquid discharge, concentration into solid salts and irrigation of plants tolerant to high salinity (halophytes). Brine disposal at inland sites is generally limited to three categories namely: deep well injection, evaporation ponds and solar ponds (Ahmed *et al*., 2001). Where there are very limited options of using brine on site or to discharge it into disused ponds and pits or the sea, new ways have to be found and implemented for environmentally friendly brine disposal.

2.3 Ion Exchange

Adsorption has been proved to be an excellent way to treat industrial waste effluents, offering significant advantages like the low-cost, availability, profitability, easy of operation and efficiency. For low concentrations of metal ions in wastewater, the adsorption process is recommended for their removal. The process of adsorption implies the presence of an “adsorbent” solid that binds molecules by physical attractive forces, ion exchange, and chemical binding. It is advisable that the

adsorbent is available in large quantities, easily regenerable, and cheap (Kunin, 1976).

IX is a specialty sorption process which is influenced by capacity, sorption affinity for targeted solutes and regeneration or desorption efficiency for any specific application. The sorption efficiency of a target contaminant is strongly dependent on the solute-sorbent interactions and can be enhanced by manipulating sorption site chemistry (functional groups). In essence it is a cyclic process with two major steps: sorption (separation) and desorption (regeneration). Ideally the ion exchange process should be reversible so that the target solutes can be desorbed efficiently. However, in reality, efficiency of desorption (or regeneration) tends to diminish for highly selective sorbents.

IX describes the process, as water flows through a bed of ion exchange material, undesirable ions are removed and replaced with less objectionable ones. It provides a means for transferring one or more ionic species from one liquid phase to another using solid resin. The ionic species in the solid phase (IX resin) are exchanged with those in the liquid phase, hence making it possible to separate, concentrate or recover soluble ionic species. Normally, targeted ionic species may be toxic, precious, or contaminants affecting water purity, are exchanged with less toxic, precious or contaminating ions in solutions. The use of a regenerant on the resin releases the targeted ions into solution, separating the concentrated ions or recovering the precious metals while recovering the IX resin's exchange capacity so that it can be applied again.

These ions can be reversibly exchanged for a stoichiometrically equivalent amount of other ions of the same sign when the ion exchanger is in contact with an electrolyte solution as shown in Equations 2.1 and 2.2. Ion exchange is essentially a diffusion process and is selective, i.e., it takes up certain counter ions in preference to

others. In addition, its usefulness resides in the ability to regenerate quickly with no loss in capacity.

$$\underline{2R\text{-}Na} + CaCl_2\,(aq) \rightarrow \underline{R_2\text{-}Ca} + 2NaCl\,(aq)\ \text{(cation exchange)} \qquad (2.1)$$

$$\underline{2R\text{-}Cl} + Na_2SO_4\,(aq) \rightarrow \underline{R_2\text{-}SO_4} + 2NaCl\,(aq)\ \text{(anion exchange)} \qquad (2.2)$$

The solid (resin) phase is designed R in the above the reactions, and the ions which take part in the exchange (Na^+, Ca^{2+} for cation exchange and Cl^-, SO_4^{2-} for anion exchange) are called counter ions. The counter ions are free to move within the framework-resin and can be replaced with other ions of the same charge. The ions in solution with the same charge as that of the ion exchanger (chloride ion for cationic exchanger and sodium ion for anionic exchanger) are termed the co ions. Carriers of exchangeable cations are called cation exchangers and carriers of exchangeable anions, anion exchangers.

Since the discovery, by Thompson and Way, of the mechanism of ion exchange, a number of important advances have been made in the area of ion exchange systems leading to the development of the specialized polymeric systems designed for the 'selective' removal of unwanted ions. The first industrial application of ion exchange was reported in 1905 where water was softened using sodium-aluminosilicate cation exchange resin. Ion exchange today has a wide variety of important application in industries such as pharmaceutical, food processing, chemical synthesis, biomedical, hydrometallurgy, water treatment (water softening, de-alkalization, de-ionization, toxic heavy metal ions removal), synthetic fiber production and chromatography (Economy *at el*., 2002, Greig, 2000).

IX forms the basis of a large number of chemical processes involving substitutions, separation and removal of ions. In substitution, ions on the resin that are of low or no commercial value are replaced with valuable ions. In separation, ions are

separated according to their affinities between them and the resin as the solution passes through a column packed with the resin.

The ultra pure water production is the biggest, but only one of the many possible applications, many others can be named. First of all, it is the treatment of waste streams where ion exchange materials are most efficiently applied when a relatively small amount of an undesirable substance must be removed from the stream. The main benefits of ion exchange technologies lie in a possibility of removing highly diluted contaminants and in the insensitivity of ion exchange techniques to variations in flow and concentration. These advantages are also decisive in many other separation applications. Moreover, IX processes take over other competing separation techniques when a target substance(s) must be removed from diluted solutions with low or zero residuals. In many cases, such an ion exchange removal can be highly selective.

The wide application of ion exchange resins in pharmaceutics and in food industry is determined by another advantage of these materials. While being chemically active, they are highly stable in both physical and chemical sense and, as a result, do not contaminate the product. They are responsible for majority of the purification and isolation processes and analytical procedures now in general use in the pharmaceutical field (Winters and Kunin, 1949).

An extensive use of ion exchangers and, most often, chelating materials in hydrometallurgy is determined by the possibility of creating highly selective separation systems for a number of ions. Extraction of uranium or noble metals can be mentioned as most common examples (Egawa *et al*., 1992).

The applications in biochemistry and biotechnology could be difficult to describe in brief. Many of them exploit different specific phenomena besides conventionally utilized ion exchange interactions. These phenomena allow designing

of unique methods and technologies to obtain desirable products and by-products from complicated biochemical mixtures (Winters and Kunin, 1949).

Applications of IX materials in medicine are under intensive development. One of the most obvious prospects is a controlled drug release. Certain ion exchange materials can be incorporated in the pharmaceutical recipes to delay consumption of the drug by a patient's body. Due to the high chemical stability, such polymers do not cause any harm or discomfort when, for example, they are taken as pills.

Applications in chemical analysis are wide and somehow different from industrial use. The reason is in the essentially different target of the treatment: obtaining or improvement of the analytical signal instead of a chemical product. Such specificity affects the ways of materials' exploitation, while all processes are based on the same physico-chemical principles.

In the following sections, the synthesis of IX resins, its properties and application based on its structure will be described in detail. The focus is on the polymeric ion exchange resins because of the role they play in water treatment and the potential they hold in application in other fields.

2.3.1 Ion Exchange Resins

IX resins are insoluble solid materials which carry exchangeable cations or anions on fixed sites (Helfferich, 1962) (Figure 2.5). They are mostly available in a moist bead form (granular or powder form) with a particle size distribution typically ranging from 0.3 – 1.2 mm with a gel or macroporous structure. The structure of the resin is generally characterized by the pore-size distribution of the spherical beads and the degree of 'cross-linking' between polymer chains within the bead. Conventional ion-exchange beads (IEBs) consist of three-dimensional covalent networks to which ion

exchange groups are bonded. The network preserves the structural integrity of the material, while the bound ions provide either cationic or anionic exchange sites.

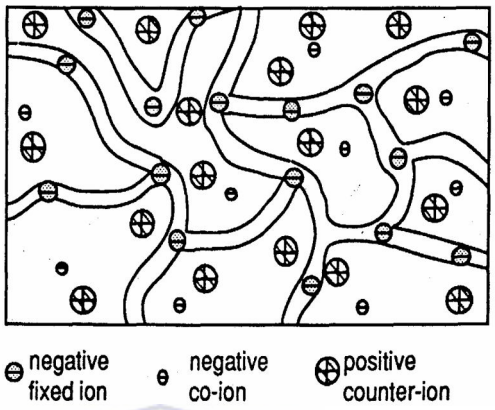

Figure 2-5: A cation exchange resin structure (Zagorodgni, 2007)
.

IX resins (carbonaceous exchangers) were developed around 1930 in order to make use of their exchange capacity (about one third of the total ion exchange capacity of a modern resin) in industrial water treatment applications (Harland, 1994). However, this class of resins lacked uniformity, physical and chemical stability. This was overcome by the further development of the exchangers with large exchange capacity, better chemical, thermal and mechanical stability. The kinetics capability was improved by means of macroporous ion exchangers developed in the 1970s. The range of application of the ion exchange method was remarkably extended first by invention and application of new organic and inorganic ion exchangers and then by the demand for purer water (Calmon, 1984).

During adsorption reaction, the resin is loaded with metal ions and stripped with an appropriate eluent. The amount of metal ion sorbed onto the resin are a function of the concentrations of the competing metals and ligands, the contact time of the sample with the resin and the binding capacity of the resin (stability constants of the metal-ligand species)(Helfferich, 1962). The greater the binding capacity of

the resin the greater the capacity of the resin to overcome the stability of certain ligands, i.e. higher binding capacity lead to sorption of not only free metal ions but also those metal ions in less stable complexes than the resin-metal complex. The resins can be regenerated and reused for continuous processes. A disadvantage of ion exchange process can be slow kinetics. However, increasing the porosity of the resin or decreasing the bead size or crosslinking can help the kinetics by increasing accessibility of the polymer supported ligands to the metal ions. Table 2.3 outlines some of the available resins and their functional groups.

Table 2-3: Functional groups, binding sites and metal ions separated of some common resins

Resin	**Functional group**	**Binding sites**	**Metal ions separated**	**References**
Amidoxime	Hydroxylamine	Amphoteric	Fe^{3+}, Cu^{2+}, Cd^{2+}, Pb^{2+}, Zn^{2+}, U^{6+}	Colella *et al*. 1980; Egawa & kabay, 1992.
Chelex 100	Iminodiacetate	Tridentate	Cr^{3+},	Gode and Pehlivan, 2003
Poly(4-vinylphyridine)	Aminophosphonate	Bidentate	Cu^{2+}, Cd^{2+}, Pb^{2+}, Zn^{2+}, UO_2^{2+}, Ca^{2+}, Mg^{2+}	Wu & Lau, 1996
Amberlite IR-122	Sulphonate	Monodentate	Cd^{2+}, Pb^{2+}, Zn^{2+},	Wu & Lau, 1996
Sephadex SP C-25	Sulphonate	Monodentate	Cd^{2+}, Pb^{2+}, Zn^{2+},	Wu & Lau, 1996
Amberlite CG 50	Carboxylate	Bidentate	$Cr^{3+;}$ Cr^{6+}	Pesavento *et al*, 1994
Retardion 11A8	Quarternary ammonium group and carboxylate	Amphoteric	Cd^{2+}	Samczy ski & Dybezy ski, 1997

According to their material, ion exchangers are divided into two groups:

1. **Inorganic ion exchangers**: Most inorganic materials are crystalline aluminosilicates with cation exchange properties. Characteristic representatives of this group of materials are the *zeolites* (which are the best known in the group) and clay minerals (broadly described as layer lattice silicates). The constitution, channel diameter and ion exchange capacity for various clay minerals, natural and synthesized zeolites are shown in table 2.4.

Table 2-4: Constitution and ion exchange capacities for some clay minerals, natural and synthetic zeolites

Species	**Idealized formula**	**Channel diameter (nm)**	**Exchange capacity (eq/kg)**
Kaolinite	Single layer lattice silicates	-	0.03 – 0.15
Muscovite (mica)	Double layer lattice (non expanding) silicates	-	0.10
Montmorillonite	Double layer lattice (expanding) silicates	-	0.70 – 1.00
Quartz	Dense lattice (3-D)	-	0.05
Analcite	$Na_{16}[(AlO_6)_{16}(SiO_2)_{32}].16\ H_2O$	0.69	4.95
Chabazite	$Ca_2[(AlO_2)_4(SiO_2)_8]_2.13H_2O$	0.37 - .042	4.95
Clinoptilolite	$(Ca,Na_2,K_2)_3[(AlO_2)_6(SiO_2)_{30}].24H_2O$	0.24 – 0.61	2.62
Faujasite	$(Na_2,K)[(AlO_2)_{64}(SiO_2)_{128}].256\ H_2O$	0.74	5.02

Zeolites are the most conventional inorganic ion exchangers, occurring naturally but also synthesized by controlled hydrothermal crystallization from solutions in a wide diversity of variations. They are hydrated aluminosilicates of alkali and alkaline earth metals with crystalline porous structure, having infinite, three-dimensional atomic structures. Zeolites are crystalline, hydrated aluminosilicates. They are further characterized by the ability to lose and gain water reversibly and to exchange certain constituent atoms, also without major change of atomic structure. The precise geometry of the zeolites structures enables them too differentially sorb neutral molecules according to their sizes or structure (molecular sieving activity). This activity is the basis of

many industrial uses such as gas and liquid phase operations to effect separation of hydrocarbons and drying in the petrochemical cracking and reforming reactions.

Whilst, layer lattice clay minerals are finely divided microcrystalline minerals which together with their variable composition limit their choice as ion exchangers in industrial processes. Along with quartz and feldspar minerals, zeolites are three-dimensional frameworks of silicate (SiO_4) tetrahedral in which all four corner oxygens of each tetrahedron are shared with adjacent tetrahedra. If each tetrahedron in the framework contains silicon as its central atom, the overall structure is electrically neutral, as is quartz $(SiO)_2$.

The disadvantages of zeolites over resins for conventional ion exchange applications are largely from their irregular structure, slow kinetics and most importantly their chemical instability in solutions of high and low pH.

2. **Organic ion exchangers**: The majority of organic resins have a matrix of a three-dimensional network of macromolecular hydrocarbon chains. In most cases, this consists of a copolymer of styrene and divinylbenzene (DVB), with the latter providing the crosslinking. The properties of the resins are determined by the ion-exchange groups present on the matrix. In general, these may be divided into three groups: cation exchangers (strong acid or weak acid groups); anion exchangers (strong base or weak base groups); specific ion exchangers (selective chelating groups) as mentioned by Bolto and Pawlowski (1987).

In general, chelating resins are a group of materials having complexing or chelating groups on their surface. Their performance is based

on selective removal of the targeted metal ions from complex solutions by using a chelating group having high affinity for the targeted metal ion. Most the chelating resins and fibres known in literature have been prepared by a two step synthesis process: (a) the insertion of appropriate functional group on the surface of the polymeric support or activation of the polymer or the preparation of the polymer, and (b) the immobilization of a ligand by condensation reaction or coupling reaction (Garg *et al.*, 1998). The chelating groups form complexes with metal ions at certain pH ranges. When a sample containing metal ions is passed over a chelating resin at certain pH values, metal ions form chelates with the chelating agent on the polymeric support and thus are retained by the resin. During elution, the metal ions are removed from the chelate sites on the resins by changing the pH of eluents.

Both inorganic and organic IX resins are able to sorb solvents in which they are placed in, but only to a limited degree. Due to the flexibility of polymer chains molecules, sorbate can penetrate into the polymer mass and the sorption mechanism comprises both adsorption and absorption component. In the adsorption processes the adsorbed species and the solid surface of the adsorbent are neutral. The main differences between ion exchange and adsorption processes are the magnitude of the potential energy barrier and the presence of a desorption step accompanying the ion exchange. Adsorption processes involves the weak Van der Waals forces, while in ion exchange the strong Coulombian forces are involved. Adsorption capacity will be affected by several factors including adsorbent polarity, active groups and pore structure (micro-, meso- and macroporosity).

2.3.2 Synthesis of Ion Exchange Resins

The conventional method of preparation of porous polymeric materials is suspension polymerization with an addition of a monomer/monomer mixture and a monomer-soluble initiator to a stirring reactor containing water with a low amount of a steric stabilizer (Gun'ko *et al.*, 2005). The majority of ion exchange resins are made by the copolymerization of styrene and divinylbenzene (DVB) (Figure 2.6). The styrene molecules provide the basic matrix of the resin, while the DVB is used to crosslink the polymers to allow for the general insolubility and toughness of the resin. The degree of crosslinking in the resin's three-dimensional array is important because it determines the internal pore structure, which has a large effect on the internal movement of exchanging ions (Helfferich, 1962).

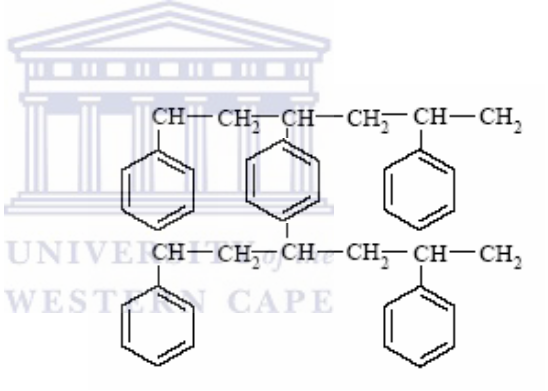

Figure 2-6: Styrene-divinylbenzene copolymer

Formation of styrene-divinylbenzene (DVB) copolymer is through the suspension (pearl) polymerization technique, which involves the addition of monomer mixture dispersion into small droplets in a thoroughly agitated aqueous solution that is kept at a temperature required for polymerization (usually 85ºC - 100ºC) (Chanda and Roy, 2006). A suspension stabilizer is added to prevent the agglomeration of the droplets. The size of the droplets is dependent on the stabilizer, the viscosity of the solution and the agitation. As the polymerization proceeds, the droplets are transformed into polymer beads of the gel-type polymer matrix. After polymerization, polymer beads with pores within its structure are obtained. They are

then chemically activated to perform as ion exchange materials. The activated groups are attached to provide chemical functionality in the bead. These activate groups have a fixed electrical charge, which is balanced by an equivalent number of oppositely charged ions, which are free to exchange with other ions of the same charge. For example, strong acid cation (SAC) resins are formed by treating the beads with concentrated sulphuric acid (a process called sulphonation) to form permanent, negatively charged sulphonic-acid groups throughout the bead.

Highly porous, macroporous (macroreticular) beads are prepared by varying the suspension polymerization technique. An organic solvent is added in which a mixture of the monomers is soluble, but the polymer, when it is formed, is insoluble. As polymerization proceeds, the solvent is squeezed out by the growing polymer regions giving rise to spherical beads with large pores which guarantee access into the interior of the beads even when non-polar solvent are used. The non-solvent is responsible for the formation of meso- and macropores in polymeric particles whereas a good solvent provides the appearance of the microporous structure (Vlad *et al*., 1996).

Styrene-DVB copolymer beads are sulphonated to produce strong acid cationic exchange resins. This method applies to the functionalization of the coating on the glass substrate in the production of the ion exchange fibrous resins. The copolymer beads are functionalized using sulphuric acid at elevated temperatures (150ºC) and pressure, in the presence of a swelling solvent and for a desired degree of sulphonation (Harland, 1994). The sulphonic group is normally introduced into the para-position due to steric effects. The high pressure is to effectively increase the boiling temperature of the solvent to keep the copolymer beads swollen at temperature above the normal boiling point of the swelling solvent without rupturing the beads. After completion of the reaction, the resin is hydrated, converted to a metal salt and is recovered.

Weak acid, cationic exchange resins are prepared by copolymerization of an organic acid or acid anhydride and a cross-linking agent. Generally, an acrylic or methacrylic acid (Figure 2.7) is used in combination with divinylbenzene or similar compounds with at least two vinyl groups. The pearl polymerization can be used if esters, instead of water-soluble acids, are polymerized.

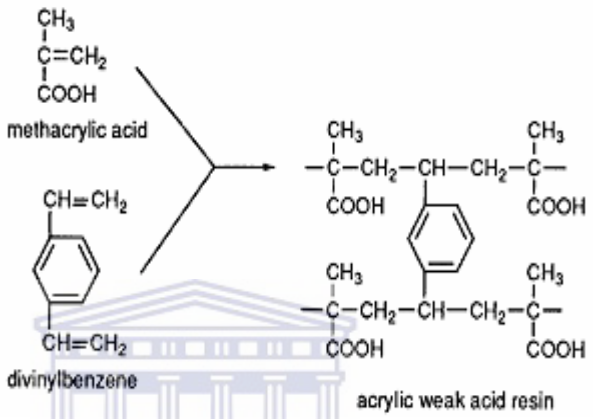

Figure 2-7: Acrylic carboxylic cation exchange resin.

Strong-based anion (SBA) exchange resins are prepared, in a similar way to the strong acid cation resins, by chloromethylating the styrene-DVB copolymer, then aminating the product with a tertiary alkyl amine, outlined in the Figure 2.8. The only difference with SAC resin activation is that the amount of DVB used is less to allow for a more porous bead. The type of amine used determines the functionality of the resin. The common amine used is trimethylamine (TMA), which create a type 1 (SBA) exchanger and the use of dimethylethanolamine (DMEA) produces a type 2 anion resin (Harland, 1994).

Divinylbenzene, a cross-linking agent, provides resin matrix rigidity and resistance to swelling. The degree of cross-linking determines the mesh width of the matrix, the swelling ability of the resin and the mobility of the counter ions in the resins. Highly cross-linked resins are harder and more resistant to mechanical breakdown, and attrition; however they are brittle, susceptible to oxidation, less able

to release large organic molecules during regeneration and exhibit slower diffusion rates (Harland, 1994).

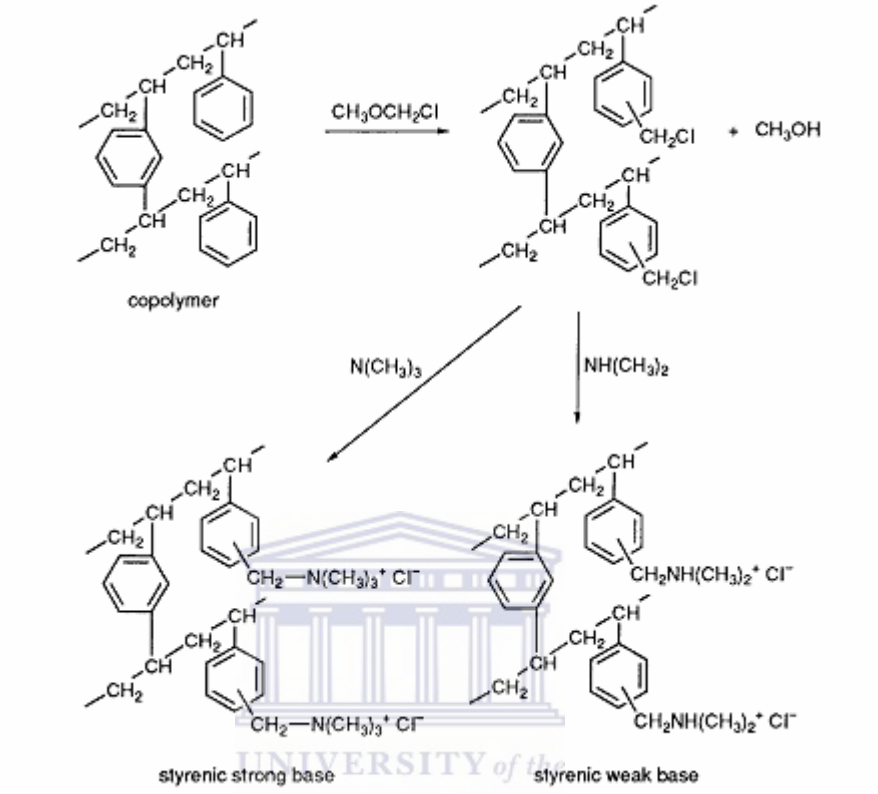

Figure 2-8: Synthesis styrenic anion exchange resins

2.3.3 Properties of Ion Exchange Resins

Many natural and synthetic materials can function as ion exchangers. However, differences in their sorption properties distinguish them as ion exchangers. These properties are summarized in Table 2.5.

Table 2-5: Main properties of Ion exchange Resins (Harland, 1994; Zagorodgni, 2007)

CHEMICAL	**PHYSICAL**
Type of matrix	Physical structure and morphology
Cross-linking degree	Particle size
Type of functional group	Pore size and morphology
Ion exchange capacity	Surface area
Ionic form	Partial volume when swollen

2.3.3.1 Chemical Properties

2.3.3.1.1 Matrix

The framework of ion exchanger, the so-called matrix, consists of an irregular macromolecular, three-dimensional network of hydrocarbon chains, outlined in Figure 2.9. The matrix of the resin is hydrophobic. However, hydrophilic components are introduced by the incorporation of ionic groups such as $-SO_3^-H^+$ (Helfferich, 1962).

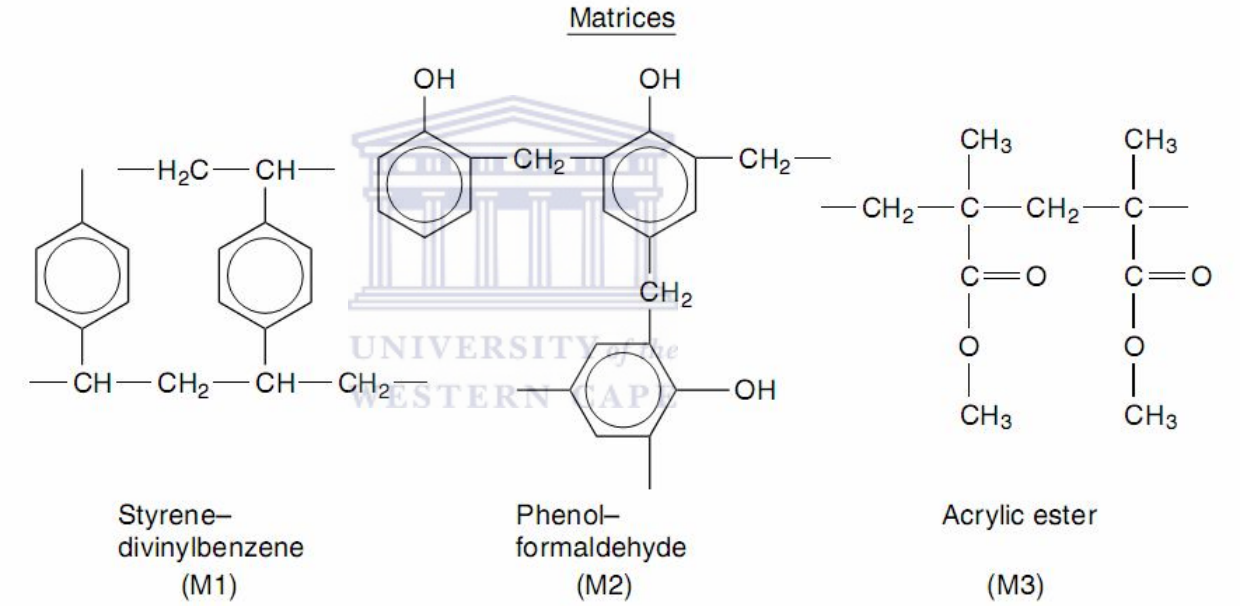

Figure 2-9: Schematic diagrams of matrices.

The common choice is between "styrene-divinylbenzene" or "acrylic-divinylbenzene" copolymer. The most typical example of ion exchange resin is sulphonated polystyrene cross-linked with divinylbenzene, as shown in Figure 2.5. In the case of the cation exchange resins, selection is easily made since the acrylic products are weakly acidic whilst the styrenic resins are strongly acidic. Therefore for cation exchange the choice of copolymer is primarily decided by the process application and operating pH. The situation is very different with anion exchange

resins since the two types of matrix pertain to products of both weak and strong functionality. In the case of anion exchange resins the choice between an acrylic resin and its styrenic equivalent is often made based on the considerations of operating exchange capacity, physical strength, and fouling resistance to complex high molecular weight organic anions (Harland, 1994).

2.3.3.1.2 Degree of Crosslinking

Cross-linking provides the key chemical bonding between adjacent polymer chains which provides the resin with good inherent physical strength. Crosslinking influences not only the solubility but the structure of the matrix, mechanical stability, exchange capacity, water uptake and swelling behavior, volume change in different forms of loading and mobility of the counter ions inside the exchanger, selectivity, and chemical as well as oxidation resistance of ion exchangers (Zagorodgni, 2007). The amount of crosslinking depends on the proportions of different monomers used in the polymerization step. Practical ranges are 1 % to 16 %, with 8 % crosslinking being considered ideal for a general purpose ion exchange resin (Khym, 1974). Exchangers with low degree of crosslinking are soft and mechanically unstable (in the swollen state), while highly crosslinked products are hard, brittle with an increased sensitivity to osmotic influences and can hinder kinetics by making the bead too resistant to the shrinking and swelling necessary during normal operation (Desilva, 1999). This is due to the fact that at low degree of crosslinking (i.e. low proportions of DVB) resins swell strongly in aqueous solutions causing higher porosity and larger surface areas within these resin particles, which leads to faster kinetics. Divinylbenzene (DVB) is widely used as a crosslinking agent.

2.3.3.1.3 Swelling

The volume change which takes place during transference from one medium to another is known as swelling. This swelling is produced by the osmotic pressure in the interior of the ion exchanger against the external, more dilute solution, so that the solvent uptake produces the swelling (Harland, 1994). The amount of swelling is directly proportional to the number of hydrophilic functional groups attached to the polymer matrix and is inversely proportional to the degree of divinylbenzene crosslinking present in the resin (Harland, 1994). Absolute swelling takes place when air-dried resin becomes wet. During absolute swelling a certain quantity of water is taken up by the exchanger.

Swelling is influenced by the following factors: (a) composition of ion exchanger (i.e., the degree of crosslinking), (b) physical strength of the resin matrix, and (c) chemistry of the solution (Harland, 1994). The more crosslinked the resin is, the smaller is the degree of swelling. However, if crosslinking does not exist, the resin can swell without limits in aqueous solutions. The charge density and swelling capacity increase with an increase in the amount of active groups on resin. The swelling decreases with increasing valence. For ions of the same charge, the volume of a swollen resin also depends on both resin and solution chemistry. The volume of the resin increases with increasing volume of hydrated ions. When the ionic groups of a resin are highly dissociated, the resin swells to a greater degree. If the water contains an electrolyte, swelling depends also on the electrolyte concentration. When this concentration increases, the moisture uptake will increase, since the osmotic pressure difference between the external and internal solution is then smaller (Desilva, 1999). Ion exchange resins are generally more swollen by strongly polar solvents than by less polar ones.

2.3.3.1.4 Functional Groups

Ion exchange resins are classified as cation exchangers, which have positively charged mobile ions available for exchange and anion exchangers, whose exchangeable ions are negatively charged (Harland, 1994; Zagorodgni, 2007). Both anion and cation resins are produced from the same basic organic polymers. They differ in the ionizable group attached to the hydrogen carbon network. It is this functional group that determines the chemical behaviour of the resin. The four functional groups commonly found in the four categories of resins are strongly acidic groups, sulphonated group (SO_3^-): weakly acidic groups, carboxylate group (COO^-); strongly basic groups, quaternary amine group [$-N^+(CH_3)_3$]; and weakly basic groups, tertiary amine group [$-N^+(CH_3)_2$] (Zagorodgni, 2007).

Cation Resins

The difference between strong and weak-acid cation resins is dependent upon the pK value of the group attached to the resin matrix. Cation exchange resins are generally quite stable, especially if they are in their salt forms.

Strong-acid cation exchange resins have *sulphonic groups* SO_3^- prematurely fixed to the polymer network to give a negatively charged matrix and exchangeable mobile positive hydrogen ions. Weak-acid resins contain a *carboxylic group* (COO^-H^+). At high pH levels, both groups are completely dissociated and both will exchange cations for their hydrogen ions. The hydrogen ions can be exchanged on an equivalent basis with other cations such as Na^+; Ca^{2+}; K^+; Mg^{2+} to maintain neutrality of the polymer. At low pH solution levels, a pH less than the pK value of carboxyl group, only the sulphonic acid will dissociate because its pK value is lower than that of the carboxyl group.

In the regeneration of the resins, weak-acid resins do not require the same sort of concentration driving force required to convert strong-acid resins to the hydrogen form. This is achieved by keeping the pH of the external solution below the resin pK value for a sufficient period for the reaction to go to completion for the regeneration to be achieved. However, in the strong-acid resin, regeneration will only reach equilibrium and the reaction will not proceed further. The regenerant acid solution must be successively renewed in order to achieve complete resin conversion. Any acids which can produce a pH lower than the pK of the resin will regenerate a weak-acid resin while only strong mineral acids regenerate strong-acid resins.

The strong-acid cation resins are highly ionized in both the hydrogen (R-SO_3H) and salt (R-SO_3Na) form over the entire pH range hence is able to split neutral salts. On the other hand, weak-acid cation resins function in neutral to basic pH range because the functional groups have a high affinity for the H^+ ions. They only dissociate at relatively high pH values (generally pH>3) and thus cannot split neutral salts. However, dependent on resin structure, they split salts with basicities significantly higher than resin pK values, e.g., bicarbonates and carbonates.

The strong acid resin has different affinities for different cations as shown below:

Monovalent cation: $Ag^+ > K^+ > NH_4^+ > Na^+ > H^+$

Divalent cations: $Pb^{2+} > Hg^{2+} > Ca^{2+} > Ni^{2+} > Cd^{2+} > Cu^{2+} > Zn^{2+} > Fe^{2+} > Mg^{2+} > Mn^{2+}$

Trivalent cations: $Fe^{3+} > Al^{3+}$.

Because the exchange reactions are reversible, when the resin capacity is exhausted, it can be recovered through regeneration with a mineral acid (e.g., HCl) with concentrations from 0.5 to 3.0 M.

Anion Resins

Anion resins acquire their properties from the attachment of a nitrogen atom to the resin matrix, to form group with the following amine structures: -C-NH_2 primary amine; -R_1-NH-C- secondary amine; -$R_3^+N^-$ tertiary amine and –R_4N^+ quaternary amine. Strong base and weak base materials are also most stable in their salt forms compared with their hydroxide and free base forms, respectively. The effect of increased temperature is to accelerate the loss of exchange capacity, in which respect acrylic anion exchangers whether weak or strong base, are significantly more unstable than their styrenic counterparts.

Strong-base anion resins are highly ionized and can be used over the entire pH range. The functional sites are derived from *quaternary ammonium groups*. The quaternary ammonium group behaves analogous to a strong acid due to its high degree of dissociation. It is capable of 'splitting' neutral salts in an exchange of an hydroxyl ion for some other anion. It requires an excess of strong base for regeneration to the hydroxyl form (Harland, 1994; Zagorodgni, 2007).

Two types of anion resins are available: (a) Type 1 has three methyl groups around the nitrogen atom and (b) Type 2 has a ethanol group replacing one of the methyl groups. Type 1 is more strongly basic and provides better silicates and carbonate removal as compared to type 2 resins. However, Type 2 resins have greater regeneration efficiency and capacity than Type 1. These resins have their largest swollen volume in the hydroxide form (Harland, 1994; Zagorodgni, 2007).

Weak-base anion resins function in low pH levels where the *primary*, *secondary*, *tertiary amine groups* are protonated and act as positively charged exchange sites for anions. They remove free mineral acids (HCl or H_2SO_4) but cannot split salts.

$$\underline{R_3N} + HCl \leftrightarrow \underline{R_3NH^+Cl^-} \quad (2.3)$$

$$\underline{R_3NH^+Cl^-} + HNO_3 \leftrightarrow \underline{R_3NH^+NO_3^-} + HCl \quad (2.4)$$

After protonation, as shown Equation (2.3), the Cl^- loaded resin is ready for an anion exchange as shown by Equation (2.4), but this will take place only at low pH. Conversion of weak base resin to the free base form is accomplished with any solution which is able to raise the pH to a level higher than the pK value of the amine group. Weak base resins display excellent regenerability and the following are often used: sodium hydroxide (NaOH); ammonium hydroxide (NH_4OH); sodium carbonate (Na_2CO_3) and calcium hydroxide ($Ca(OH)_2$).

2.3.3.1.5 Ion Exchange Capacity

IX capacity is possibly the most important characteristic of an ion exchange material since it is a measure of its capability to carry out useful ion exchange work. Several definitions are employed depending upon the intended application of the data. Ion exchange capacities can be classified as (Kunin, 1960):

1. Anion exchange capacity
2. Cation exchange capacity
3. Breakthrough capacity
4. Saturation column capacity

The capacity is usually expressed on a dry-weight or wet-volume basis.

The dry-weight capacity is the number of exchange sites in milliequivalents per gram of dry resin (milliequivalents (meq) per dry gram). It is sometimes called the intrinsic or specific capacity. In the context of ion exchange equivalent mass is, defined as the gram ion mass (or molar mass) per unit ion charge, and dry weight capacity is the prime capacity defining characteristic of a resin as manufactured. The wet-volume capacity is the number of milliequivalents per unit volume of resin

swollen in water and is usually expressed as equivalents per litre of resin (eq/l). The capacity defined in this way is a characteristic of the material and is independent of experimental conditions.

The standard ionic states are hydrogen form and chloride form for cation and anion exchange resins respectively, and to a fair approximation exchange capacity values can be predicted from the equivalent mass of the monomer characterizing the exchanger (Harland, 1994). For example, the empirical formula of the functional monomer for a gel styrenesulphonic acid resin in the hydrogen form may be written $C_8H_6.S0_3H$, with a Relative Molecular Mass (mass of 1 mole) of 184. Thus the unit equivalent mass is 184 g containing one equivalent of exchangeable hydrogen ions from which the anticipated exchange capacity is 1 equivalent per 184 g dry resin, i.e. 5.4 equiv. per kilogram (eq/kg) dry resin in the hydrogen form (5.4 milliequivalents per dry gram, meq/g). However, the real structures incorporate divinylbenzene and are not homogeneous which results in the measured total exchange capacities being a little lower than those given by the afore-described simple model. Similar considerations when applied to anion exchange resins give values appreciably greater than their measured capacities owing to most commercial resins only being 70-85% chloromethylated.

The measurement of dry weight capacity in a standard ionic form is usually carried out by direct titration of the exchanged ion using either a weighed quantity of dried resin or alternatively a known mass of swollen resin whose water content is determined separately. The neutralization of ion exchange resins in their acid and base forms by addition of standard alkali or acid solutions respectively may be easily studied by pH titration (Fisher and Kunin, 1955). The titration curves obtained are similar to those found for conventional acid-base systems. The capacity of the resin is found from the points on the titration curve where the rate of change in pH with titrant addition is greatest. Dependent upon

whether the reacting functional groups are strong (acid or base), weak acid, or weak base, the pH at complete neutralization will be neutral (pH = 7), alkaline (pH >> 7), or acidic (pH << 7) respectively.

Another technology concept is the breakthrough capacity. If the ion exchange material is used in a column process, the operation is discontinued at breakthrough, i.e. when the ion or substance that is targeted to be trapped by the column appears at the outlet. The total volume required to reach the breakthrough point gives the breakthrough capacity. In equilibrium operation, the solution continuously contacts with resin and consequently there is a high driving force for the removal of solute from solution. In order to achieve maximum removal, the resin in the column must be regenerated (Kunin, 1960). The breakthrough capacity depends on the operating conditions and on the properties (including capacity) of the material. The value of breakthrough capacity of the column is always lower than that of an ion exchange capacity characterizing the material loaded in this column.

2.3.3.1.6 Ionic Form

Most ionic forms may be prepared by passing a large excess of an appropriate acid, alkali, or salt solution through a column of resin over 20-30 minutes. The ease of resin conversion generally increases with decreasing particle size, decreasing crosslinking, and decreasing charge of the ion being displaced (Harland, 1994).

Commercially, the most common ionic forms as manufactured are:

1. Strong acid cation

   Hydrogen form, $-S0_3^-H^+$

   Sodium form, $-S0_3^-Na^+$

2. Weak acid cation

   Hydrogen form, -COOH

3. Strong base anion

   Type 1, chloride form, $-CH_2N(CH3)_3^+C1^-$

   Type 2, chloride form, $-CH_2N(CH_3),(CH_2CH_20H)^+C1^-$

4. Weak base anion (tertiary amine)

   Free base form, $-CH_2N(CH_3)_2$

   Chloride form, $-CH_2NH(CH_3)_2^+Cl^-$

2.3.3.1.7 pH Range

The pH range is very much dependent upon the strength of the functional group, but the following guidelines could be applied (Harland, 1994):

1. Strong acid cation: any pH
2. Weak acid cation: > 4
3. Strong base anion: any pH
4. Weak base anion (tertiary): < 9

2.3.3.1.8 Chemical stability

At the macroscopic level, the chemical stability of modern resins at normal ambient temperatures is excellent, being insoluble in all common organic solvents and electrolyte solutions. Two principle exceptions are resin breakdowns caused by sustained exposure to ionizing nuclear radiation and powerful chemical oxidizing agents such as nitric and chromic (VI) acid, chlorate (V) ions, halogens, and peroxy compound (Harland, 1994).

2.3.3.1.9 Thermal stability

Over a temperature range, the stability characteristics of resins in common use may be summarized as follows (Harland, 1994):

- Cation exchange resins are generally quite stable, especially if they are in their salt forms;
- Strong base and weak base materials are also most stable in their salt forms compared with their hydroxide and free base forms, respectively. The effect of increased temperature is to accelerate the loss of exchange capacity, in which respect acrylic anion exchangers whether weak or strong base are significantly more unstable than their styrenic counterparts.

2.3.3.2 Physical Properties

Many of the physical properties of ion exchangers play key roles in the operation of ion exchange unit processes; e.g. a larger resin particle size would cause lower separation kinetics.

2.3.3.2.1 Particle size

Particle sizes of ion exchange resin are usually in the range of 0.04 – 1.2 mm with 0.30 – 0.85 mm being the most common size ranges in large scale applications (Harland, 1994). Particle size plays a major important role in ion exchange kinetics, separation efficiency, pressure drop, and hydraulic expansion. The particle size selected would be a result of a compromise between the reaction kinetics and hydrodynamics. Ion exchange is essentially a diffusion process being controlled by mass transfer resistance. This mass transfer resistance is dependent on the nature of the resin and also on the size of the particle, for example, the hydrostatic resistance (headless) in fixed bed columns would become extremely high if particles are too small. This would lead to serious pressure drops and lower liquid flow-through velocities.

For example, condensation type resins are generally broken granules. On the contrary, polymerization-type resins are small beads that are uniformly packed. To measure the grain size a mesh is used to keep out larger particles. In addition, for certain processes grain size is extremely important to efficiency. One such process is separations carried out by chromatography. The major point of grain size is that it determines the fluid resistance of an ion exchange column made from ion exchange resin. This can be the key to success of an industrial operation (Desilva, 1999).

The bead size range of conventional products is 300 μm to 1200 μm with a true mean value of approximately 700 μm (Harland, 1994).

2.3.3.2.2 Porosity

The porosity of an ion exchanger particle plays an important role in the exchanger's capacity. Porosity can be defined as a ratio of volume of voids to total volume of the resin. The porosity of conventional resins range from 20% to 50% while in macroporous resins, it ranges from 5% to 50% (Calmon, 1984). The shape and size distribution of pores in the ion exchange resin particle is influenced by the manufacturing process, the degree of cross-linking and the electrolyte of the solution. To achieve a large surface area, a large number of small pores should be incorporated into the resin. This is achieved through the suspension polymerization, a process described in section 2.2.2. The most substantial contribution to the overall surface area comes from the micropores which have diameters smaller than 2 nm, followed by mesopores with diameters ranging from 2 to 50 nm (Sing *et al.*, 1985). Macropores contribute insignificantly to the overall surface area but are important because they act as transport pores for the adsorbate molecule to diffuse from the bulk into the particle interior (meso and micropores) at reasonably low pressures (Calmon, 1984). The most important property of macroporous resins is their porosity,

which enables ions of high molecular weight to diffuse in and out of the resins beads (Lieser, 1979).

Specific surfaces of typical porous and non porous adsorbents are presented in Table 2.6. The application of porous material relies on the intimate contact with a surface that supports the active sites, such as in catalysis, adsorption, ion exchange, chromatography and solid phase synthesis (Calmon, 1984). The active groups that cause separation during ion exchange are not only on the surface of the resin particles but also in the capillary channels or pores within the particles. This helps explain the selectivity aspect of the ion exchangers because different sizes of pores are suitable for reception of ions of different sizes. Only ions of smaller sizes than the pores size can be exchanged, while the larger ones cannot be exchanged (sieve effect) because they cannot gain access to the relevant sites. Ion exchangers with high porosity and appropriate size distribution to the target ions will ensure both high capacity and separation kinetics can be achieved.

Table 2-6: Specific surfaces of typical porous and non porous adsorbents

POROUS		**NON POROUS**	
Adsorbent	**Specific surface (m^2/g)**	**Adsorbent**	**Specific surface (m^2/g)**
Granular carbons	500 - 2000	Carbon black	100
Activated Carbon	1200	TiO_2 pigment	70 – 80
Silica gel	200 - 600	ZnO pigment	1 - 10
Bone char	60 – 80		
Soils	10 – 100		
Asbestos	17		
Polymeric, Macroreticular	100 - 600		

2.3.3.2.3 Resin Colour, Density and Mechanical Resistance

Ion exchangers can be categorized according to their colours. The strongly acidic cation exchange resins and weakly acidic condensation type resins are brown while acrylic and methacrylic acid polymers are white. Colour density depends on the degree of crosslinking in the resin matrix. Physical appearance is as follows:

a) Gel resins: usually shiny beads, which are clear to transmitted light;
b) Macroporous resins: usually dull beads of opaque or translucent appearance.

The true density of any resin, in its dry or swollen form, depends on the resin type, structure, and degree of crosslinking, ionic form, and swelling capacity. The density of the any dry, water free resin is generally smaller (1200 kg/m^3) for anion exchangers than cation exchangers (about 1400 kg/m^3). However, it is more practical to use the water swollen density due its use in predicting the hydrodynamic behaviour in column or fixed bed systems. Furthermore, it should be noted that bulk density is different than the density of the swollen resin. Generally, the water content of swollen resin is about 40 – 60 %. These densities are important because operation is dependent upon the resins (Harland, 1994).

The mechanical strength varies according to a resin's structure and contributes to the wear resistance of the resin. In column systems, the resins are exposed to a lot of attrition caused by friction between particles resulting in material loss for low wear resistance. Increasing the degree of cross-linking increases the solidity of the resin. However mechanical strength reduces after regeneration with alternate concentrated acid and base.

2.3.3.2.4 Physical Structure

The matrix and functional groups define the chemical properties of the polymer while physical configuration of the material defines surface area, mechanical stability, and

among other characteristics resistance to a liquid flow. Ion exchange polymers differ due to differently distributed density of the gel, as outlined in Figure 2.9.

According to their physical structures, ion exchange resins are divided into five groups:

1. **Gel Resins:** The organic ion exchangers first developed were called gel resins. They have an essentially homogeneous distribution of water throughout the resin matrix (Bolto and Pawlowski, 1987).

   Gel resins (Figure 2.10a) have no permanent porosity instead the pores are formed when the resin swells in water giving a homogeneous distribution of water throughout the resin matrix (Kunin, 1976). The pores formed are usually small sized micropores and mesopores (20-50Aº) per unit volume resulting in higher capacity. These pores collapse upon drying and are virtually non-existent in the dry state. The pore structures are determined by the distance between the polymer chains and crosslinks which vary with the crosslink level of the polymer, the polarity of the solvent and the operating conditions. These resins offer certain advantages: they are less fragile (i.e., greater mechanical and chemical stability), requiring less care in handling, react faster in functionalization reactions and possess higher loading capacities. The gel type resins are generally translucent (Desilva, 1999).

2. **Macroporous resins:** Macroporous resins (Figure 2.10c) are made with large pores that permit access to interior exchange sites. They are manufactured by a process that leaves a network of pathways throughout the bead. They have a heterogeneous structure consisting of two phase: (a) gel regions containing dense polymer chains and a minor amount of solvent, and (b) macroscopic permanent pores containing solution similar to the surrounding region. This sponge like structure allows the active portion of the bead to contain a high

level of DVB crosslinking without affecting the exchange kinetics. Unfortunately, it also means that the resin has a lower capacity because the beads contain less exchange sites (Desilva, 1999). However, these resins exhibit faster diffusion rates, are mechanically stronger due to higher crosslinking and exhibit better chemical stability especially resistance to oxidation (Zagorodgni, 2007).

The pore size range is 50 - 1,000,000 ºA wide with an internal surface area ranging from 7 - 1,500 m^2/g. Macroreticular resins, on other hand, are created to overcome slower diffusion rates in highly cross-linked gel resins. According Kunin (1976) the macroreticular portion of resin may actually consist of micro-, macro- and transitional-pores depending upon the pore size distribution. The exchange takes place on the surface of the macropores or in close proximity to the surface, thus the molecules do not enter the dense gel regions.

Both mesopores and macropores are of no significance in terms of adsorption capacity but they act as transport pores for the adsorbate molecule to diffuse from the bulk into the particle interior. On the other hand micropores with slit-shaped pores, having high dispersive forces acting on the adsorbate molecules, provide a space for storing adsorbate molecules (Do Duong, 1998).

3. Isoporous resins: It is claimed that some of the disadvantages of macroporous resins can be overcome by the synthesis of isoporous resins, in which the matrix has a substantially uniform network, free of highly crosslinked regions (Bolto and Pawlowski, 1987). The isoporous resins (Figure 2.10b) have specially designed homogenous distribution of polymeric chains across the bead with a regular structure of micropores.

4. Microporous resins: Microporous is the term used to describe polymer particles manufactured with a low level of cross-linker. Improved rates of exchange can be obtained by using smaller particles, which make a larger surface area available. Powdered ion exchangers are employed in what has been termed precoat filters. However, because they are very fine particles (even though they are present in a coagulated form) they cause a high pressure loss in operation. Because of the high pressure loss, they cannot be employed in a column system (Bolto and Pawlowski, 1987).

5. Magnetic resins: The difficulties of handling small, rapidly reacting resin beads can be surmounted by incorporating a magnetic filler such as the iron oxide (γ-Fe_2O_3) within the particles. The magnetized resin beads then flocculate strongly to give agglomerates, which have settling rates comparable to those of normal sized beads. The flocs, which are held together by magnetic forces, are readily broken up by agitation so that the fast exchange rates associated with the small size of the resin particles can be achieved. Magnetic resins therefore combine some of the handling characteristics of conventional resin beads with the reaction rates of small particles (Bolto and Pawlowski, 1987). They give excellent kinetics, high capacities and better regenerant efficiencies and are being applied for various water treatment processes.

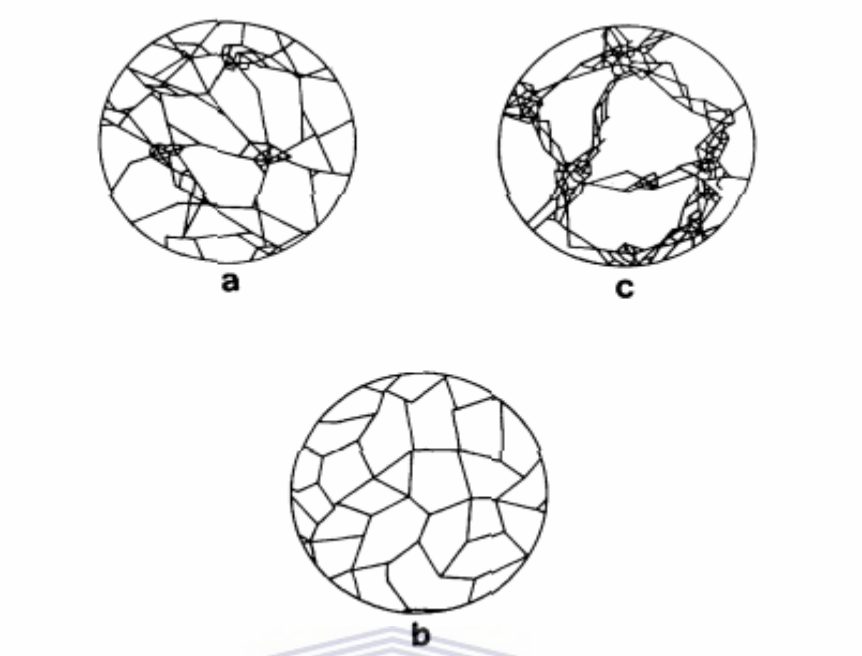

Figure 2-10: Distribution of polymeric chains in ion exchangers: (a) gel-microporous resin; (b) gel-isoporous resin; (c) macroporous resin.

Properties of Ion Exchange Resins – Summary

Given that the primary selection of a resin has been made, Table 2.4 summarizes guidelines concerning the options in relation to matrix, structure, and particle size grading. The list contains characteristics that are most common for all ion exchange materials. One final point: the cost of ion exchange resins has received little comment, but obviously this is a major factor, all other factors being equal. A need to consider matrix modified resins (acrylic) and structure modified materials (macroporous) can increase resin cost anywhere between 16% and 150% compared with standard gel styrenic products depending upon whether comparing anion or cation resins respectively (Zagorodgni, 2007).

2.4 Ion Exchange Equilibria

Sorption is a separation process involving two phases between which certain components can become differentially distributed. Ion exchange resembles sorption because a solid takes up dissolved species stoichiometrically and every ion removed is replaced by an equivalent amount of another ion of the same charge. However, in sorption, a solute is usually taken up non stoichiometrically without being replaced. There are three types of sorption, classified according to the type of bonding involved:

(a) Physical sorption. Adsorption which occurs principally as a result Van der Waal's forces. There is no exchange of electrons in physical sorption, rather intermolecular attractions occur between 'valency happy' sites and are therefore independent of the electronic properties of the molecules involved. The heat of adsorption, or activation energy, is low, i.e. the adsorbate is not held strongly to the adsorbent and therefore this type of adsorption is stable only at temperatures below about 150°C (Zagorodgni, 2007).

(b) Chemical sorption. Chemical adsorption, or chemisorption, involves an exchange of electrons between specific surface sites and solute molecules, which results in the formation of a chemical bond (Zagorodgni, 2007). Molecules are not free to move on the surface. Chemisorption is typified by much stronger adsorption energy than physical adsorption because the adsorbate forms strong localized bonds at specific surface sites on the adsorbate. Such a bond is therefore more stable at higher temperatures.

(c) Electrostatic sorption (ion exchange). This is a term reserved for coulombic attractive forces between ions and charged functional groups and is more commonly classified as ion exchange. In concentrating at the surface, ions of the adsorbate must displace other ions previously affixed to the charged sites. Ion charge and size are the

principal consideration for exchange of this type. For ions of equal charge, however, molecular size determines the order of preference for adsorption, the smaller hydrated ion being able to accomplish closer approach to the adsorption site.

In addition to being ion exchangers, ion exchange materials can also act as sorbents. When they are contacted with an electrolyte solution the dissolved ions are concentrated on both the surface and in the pores of the ion exchange media. In a solution of weak electrolytes or non-electrolytes, sorption by ion exchangers is similar to that of non-ionic adsorbents. In a solution of strong electrolytes sorption equilibrium results, owing to the electrostatic attraction between the ions in solution and the fixed ionic groups on the ion exchange media. Sorption equilibrium is normally represented by 'sorption isotherm' curves.

2.4.1 Solvent Sorption

When resinous exchangers are placed in solution containing an electrolyte, the following features are observed:

(a) the ion exchange resin swells up by imbibing the polar solvent (commonly water) from the external phase,
(b) some electrolyte penetrates the exchanger;
(c) an ion exchange reaction may take place when ion exchange resins and an electrolyte co-exist.

The electrolyte distribution process is driven by the affinity of the ionogenic groups and ions for polar solvent. The coiled and packed chains of the matrix (crosslinked polymer) unfold and make room for solvent molecules but the chains cannot separate completely because they are interconnected by crosslinks. At the same time as swelling occurs an internal osmotic pressure develops (swelling pressure) which, when at equilibrium, counteracts any further change in solvent uptake. The amount of swelling is directly proportional to the degree of

divinylbenzene crosslinking present in the resin. As a result, the resins swell but do not dissolve. Equilibrium is attained when elastic forces of the matrix counterbalance the dissolution tendency. Harland (1994) describes the ion exchange equilibria as an energetic process that explains a set of interactions between the following:

(a) counter-ion and fixed ion (coulombic, ion pairing forces);
(b) counter-ion and matrix (London and Van der Waals forces);
(c) ion-solvent (salvation, hydration force);
(d) solvent-solvent (mixed solvent systems);
(e) ion-dipole (polarization effects).

Helfferich (1962) and Khym (1974) lists the following factors as being important in determining the degree of solvent sorption and degree of swelling likely to occur:

(a) degree of crosslinking: low degree of crosslinking, the hydrocarbon network is more easily stretched, the swelling is large and resin exchanges small ions rapidly. Conversely if the crosslinking is large, the polymer matrix is rigid, the pores of the network are narrowed, exchange process is slower and it prohibits large ions from entering its structure;
(b) functional group and counter ion: the osmotic pressure is attributed almost entirely to the hydration of the functional group while the counter ion in an ion exchanger has considerable influence upon the degree of swelling. Resins swell more strongly when their functional groups are completely ionized;
(c) concentration of the solution: resins swell more when the concentrations are low. Any increase in the concentration reduces the osmotic pressure difference between the interior of the resin and the solution, thus reducing the driving force for solvent uptake;
(d) the nature of solvent: polar solvents are better swelling agents because they interact more strongly with ions in the resins.

Often, water is the solvent in the resin and the amount of water in the inside phase is an important factor in determining relative selectivity of the resin for different ions. The higher the water content of the resin phase, the more the inside phase starts to resemble the outside phase. As a general rule, as the water content increases the difference in selectivity between ionic species becomes less (Zagorodgni, 2007).

2.4.2 Solute Sorption

Many forces and interactions have been found by experimentation to affect the sorption of non-electrolytes. Solutes may form complexes or chelates with the counter ions of the exchanger. Temperature variations may not only affect the state of the solute but also the condition of the exchanger. The molecular size of the solute, the degree of crosslinking of the exchanger and the degree of the hydrophobic nature of the polymer will affect the sorption kinetics (Zagorodgni, 2007).

According to Azonava *et al*. (1999) sorbents with the higher values of specific surface areas, with a higher content of micropores and macronet porous structure, exhibit at least 3 times higher sorption activity in comparison with macroporous sorbents. They further explain that the micropores' content in the macroreticular adsorbent is proportional to the sorption capacity of the adsorbent. Hence crosslinked and hyper crosslinked polymer adsorbents, due to high micropore area, are able to trap large quantities of adsorbates repeatedly.

At equilibrium, the concentration of free electrolyte inside the exchanger will be less than that outside. This imbalance in the concentration of electrolyte across the surface boundary of an ion exchanger is explained by the Donnan membrane theory (Zagorodgni, 2007 and Helfferich 1962). The Donnan effect causes the repulsion of the co-ions from the resin and thus prevents electrolyte sorption, since an excess of the electrolyte cannot be sorbed because of electroneutrality requirements (Helfferich,

1962). This theory applies to the unequal distribution of a diffusible electrolyte between two aqueous phase separated by a membrane permeable to water and to both ions of the electrolyte. For such an imbalance to exist there must be present, in addition to a diffusible electrolyte, a large non-diffusible ion on only one side of the membrane. The resin matrix containing the fixed ionic charges constitutes the restricted non-diffusible ion. The boundary surface between the gel-like structure of an ion exchange bead and the surrounding solution acts as the membrane, the water the counter ion of the exchanger and both the ions of the electrolyte are permeable to this membrane. This donnan exclusion is a unique feature limiting the electrolyte sorption by ionic sorbents.

In general, the maximum of solute sorption increases with increasing amounts of micropores in polymer. The kinetics of adsorption on microporous adsorbents is even faster, as the filling of micropores takes place directly and the free kundsen diffusion in transport is restricted. The diffusion of the solutes into the pores is very easy but the diffusion of adsorbates inside the polymer bulk is very slow due to the high degree of crosslinking (Helfferich 1962).

2.5 Chelate Exchangers

A chelate resin/fibre is an insoluble polymer to which is attached a complexing group or groups that bond metal ions within its structure in such a manner as to form a ring in which the metal is incorporated (Zagorodgni, 2007). These groups can achieve high selectivity and specificity and the reaction involves both ion exchange and chemical reactions. The extremely high selectivity makes it possible to remove a specific ion without involving other ions that may be present and to separate specific ions in a fairly pure state (Calmon, 1981).

Extraction of metal ions using chelating resins has several advantages over conventional methods (Garg *et al*., 1999):

(a) Selective determination of metal ions will be possible by using a chelating resin having a ligand possessing high selectivity to the targeted metal ion;
(b) It is free from difficult phase separation, which is caused by the mutual solubility between water and organic solvent layers;
(c) The chelating resin method is an economical method since it uses only a small amount of ligand and extraction solvent and this also increases the sensitivity of the system;
(d) Trace metal ions at as low as ppb can be determined because the targeted ion is enriched on the solid phase;
(e) The concentration of metal ion can be visibly estimated from the color intensity of the solid phase if the metal complex formed possesses adsorption in the visible wavelength region;
(f) Use of carcinogenic organic solvents is avoided and thus the technique is eco-friendly to nature.

2.5.1 Ion Exchange Fibres (IEF)

Recently, functional fibers have been developed as highly effective adsorbents following the success of the ion exchange resins. Polymeric ion exchange fibres, made from low cost glass and/or polymeric material as substrate, have been developed. They were developed to meet the specific need of high performance in ion exchange separation processes. These fibres display a number of important advantages over conventional ion-exchange beads:

(a) Short diffusion passes are predetermined, providing sorption rates that can be up to hundred times faster than that of the conventional granular resins (with a particle diameter usually between 0.25 and 1 mm) (Varshney, 2003).
(b) Fibrous ion exchangers have higher osmotic stability that allows them to be mechanically more durable in conditions of multiple wetting and drying (for example, at cyclic sorption/regeneration processes in treatments of gaseous media) (Varshney, 2003).

(c) They allow designing of packet reactors with pressure drops much lower than in reactors using granular materials (Basta *et al*., 1998).

(d) Fibrous ion exchangers can be easily fabricated into various forms of textile goods such as cloth, conveyer belts, non-woven materials, staples, nets, felts, papers, etc. This opens many unusual possibilities for new technological designs (Varshney, 2003) and exhibits greatly improved contact efficiency with the media. This enhances both the rates of reaction and regeneration.

(e) Simplification of the overall synthesis including faster more efficient functionalization, elimination of toxic solvents, and overall process simplification.

Having established that conventional treatment methods for waste water are quite expensive and suffer from numerous disadvantages, research has focused on the use of fibres, as cheap adsorbents, which have relatively faster kinetics, are able to remove dissolved and complexed metals from such contaminated waters and have excellent chemical stability and mechanical strength (Soldatov *et al*., 1984, 1988 and 1999). These adsorbents are either complexing agents or contain cationic or anionic exchange sites. For complexing agents, separations are based on the different stabilities of the complexes and their different affinities for the resins/fibres. The chelating groups have been introduced into resins/fibres via synthetic techniques or by simple loading. The modified resins/fibres have been used for the selective recovery or pre-concentration of metal ion (Kabay *et al*., 1993 and Hirotsu *et al*., 1988). Chelating resins have ligands that can selectively bond with certain types of metal cations. The following criterion determines the affinity of chelating resins for a given metal: ionic charge, hydrated ionic radius and ligand bonding with exposed electron pairs on nitrogen and oxygen (Szlag and Wolf, 1999). The chelating resin employed in the ion exchange process, in general, is selective and has affinity for heavy metals ions. Selective resins reduce the residual concentration of heavy metals to below the maximum limits. Common cations such as sodium, calcium, and

magnesium are always found in water samples and have the capability to compete with many metal ions to complex with ligands

Fibrous ion-exchangers are known to have a larger effective specific surface area than the granular ion-exchangers. Moreover, these fibrous adsorbents have good kinetic properties, and can be utilized conveniently in different shapes. Additionally, physical and mechanical requirements of strength and dimensional stability have been achieved by use of a glass fiber substrate. The ion exchange fibers have the potential to remove a wide range of contaminant ions from water such as mercury, cadmium, lead, and cyanide ions as well as radioactive ions such as cesium and strontium. However, the ion exchange fibers are not particularly selective to remove specific toxic ions from water in the presence of high concentrations of non-toxic ions such as sodium and potassium. Many organic fibers or modified fibers, such as polyacrylonitrile (Zhou, 1993), polypropylene (Soldatov, 1988), polyvinylchloride (Luo *et al*., 1991), have been used as the precursor fiber for the preparation of ion exchanger fibers. But their applications are limited by the poor thermal stability and the low content of surface oxygen-containing groups (Wei *et al*., 2005).

The development of chelating polymeric resins containing functional groups such as amino, carboxyl, phosphoric, imidazoline, thioamido and amidoxime have achieved separation of metals (Ischtchenko *et al*., 2003; Liu *et al*., 1999 and Liu R *et al*., 2002) Among them, poly (acrylonitrile)-based fibrous adsorbents containing amidoxime groups have demonstrated their ability in separation or adsorption of metals from aqueous solutions due to their higher capacity, higher adsorption rate, good selectivity, recycling ability and better mechanical stability (Colella *et al*., 1980; Bernabé *et al*., 2000). They have an affinity for a variety of metal ions such as Mg^{2+}, Ca^{2+}, Fe^{3+}, Mn^{2+}, Ni^{2+}, Co^{2+}, Hg^{2+}, Ag^{+} and a high tendency to form strong complexes with heavy metal ions such as As^{3+}, Co^{2+}, Cd^{2+}, Cu^{2+}, Cr^{6+}, Mn^{2+}, Ni^{2+}, Hg^{2+}, Pb^{2+}, Zn^{2+} and radioactive metals such as uranium (Colella *et al*., 1980; Hirotsu *et al*., 1986).

2.5.2 Polyacrylonitrile (PAN) Polymers and Fibres

Polyacrylonitrile is synthetic fibre type having acrylonitrile, {–$CH_2CH(CN)$–}, as its principal repeating unit. The grades of polyacrylonitrile discussed here can all be defined as highly technical fibres. They include the homopolymer PAN fibres and copolymer PAN fibres prepared as carbon fibres precursors. Some commercial technical grade PAN polymers used or fibre manufacture are presented in Table 2.7.

Table 2-7: Typical Technical grade PAN fibres

Type	Supplier	Molecular weight	M_w/M_n	Composition, trade name and polymerisation solvent
1	Kelheim	210 000	2.8	AN:MA = 99.5 : 0.5 %; Dolanit 12™ powder; DMF
2	Faserwerk	85 000	2.8	AN : MA = 94.0 : 6.0 %; DolanTM powder; DMF
3	Acordis Grimsby	120 000		AN : MA : IA = 93 : 6 : 1 %; Fibre tow; DMF
4	Monte fibre	300 000	2.5	AN = 100% ; RicemTM powder ; DMAc

M_w: Weight-average molecular weight is based on the fact that a bigger molecule contains more of the total mass of the polymer sample than the smaller molecules do.
M_n: Number-average molecular weight is total weight of all the polymer molecules in a sample, divided by the total number of polymer molecules in a sample.
M_w/M_n molecular mass distribution,

Fibres from type 1 are used in hot gas filtration, type 2 is used for outdoor awning material, type 3 as a carbon fibre precursor and type 4 is used for water and hot gas filtration applications.

Polyacrylonitrile fibre (PANF) with an abundance of cyano-groups that can be easily transformed into various functional groups (carboxyl, amide, amidoxime, etc.) is one of the most suitable materials for the preparation of chelating fibres. As a result, a variety of chelating fibres based on PANF have been synthesized (Vatutsina *et al.*, 2007; Shunkevich *et al.*,, 2005; Liu *et al.*, 2002; Liu *et al.*, 1999a; Lian *et al.*,

2005; Moroi *et al*., 2004; Gupta *et al*., 2004; Shin *et al*., 2004; Liu *et al*, 1999; Gong *et al*., 2001; Chang *et al*., 2001; MaComb and Desser, 1997 and Soldatov *et al*., 1999). These materials are industrially produced under trademarks FIBAN (Soldatov *et al*., 1988) and VION. Several varieties of ion exchangers of this type containing weak base amino groups and carboxylic acid groups have found an application in air purification from acid gases (Soldatov *et al*., 1986; Soldatov *et al*., 1996). They also can be used as efficient sorbents of cationic and anionic species of the heavy, transition and noble metals from aqueous media (Soldatov *et al*., 2004). Up till now, many of the reported chelating fibres are not viable due to their low stability or economy problems.

The effectiveness of this chelating fibre has been proved by using it to treat actual sewage water, where the concentration of Cd^{2+} was reduced from 0.540 to below 0.001 mg/L. This level easily meets drinking water standards (0.003 mg/L) issued by the World Health Organization. Moreover, this chelating fibre is also very effective at treating other metal ions such as Cu^{2+}, Ca^{2+}, Zn^{2+}, Mg^{2+}, Pb^{2+}, Ni^{2+}, Ag^{+} and Hg^{2+}(Zhang *et al*., 2009)

2.5.3 Amidoxime Fibres

A crosslinked poly(acrylamidoxime) chelating adsorbents, which contains so-called amidoxime chelating functional group, has been studied for nearly 20 years. Various kinds of fibrous adsorbents containing the amidoxime chelating functional group have been synthesized by the methods of suspension polymerization and irradiation-induced graft polymerization of poly(acrylonitrile) followed by functionalization with hydroxylamine (HAN) in ethanol solution (Kabay *et al*., 1993).

According to Egawa *et al* (1994) the reaction mechanism of polyacrylonitrile with hydroxylamine to convert it to poly(amidoxime) is illustrated in Figure 2.11.

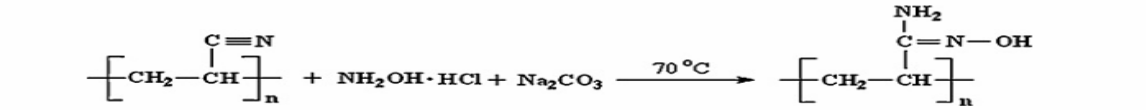

Figure 2-11: The reaction mechanism of poly(acrylonitrile) fibre (AN: MA = 99.9 : 0.1 %) with hydroxylamine to convert to amidoxime.

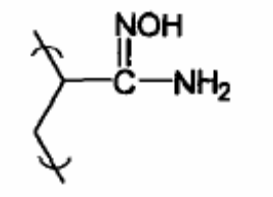

Figure 2-12: Polymeric amidoxime

Studies of the adsorption of uranium from seawater with spherical resin or bead and fibrous fiber or non-woven fabric chelating adsorbents containing amidoxime group indicate that it has a very high selectivity, strong adsorption ability and large loaded capacity for many metal ions, especially for U^{6+} at pH 6.0. Furthermore**,** it is easy to operate and considerable safe to the environment. So the fibrous polymeric adsorbent containing the amidoxime chelating functional group is considered as the most promising materials for recovering uranium from seawater. However, the adsorption mechanism of U^{6+} on amidoxime fibre has not been fully understood due to the isomerization of the amidoxime chelating functional group and variable U^{6+} species in aqueous solution. It is reported that amidoxime polymeric adsorbent usually shows amphiprotic compound characteristics because of two possible isomerization equilibriums of the amidoxime chelating functional group described by (Omichi *et al.*, 1986): Based on this isomeric change, the adsorption properties and mechanism of U(VI) on the FPAO are different usually at different acidic conditions, which results in forming the different complexes.

2.6 Adsorption Isotherms

Equilibrium data, commonly known as adsorption isotherms, are basic requirements for the design of adsorption systems used for the removal of organic pollutants. The Langmuir, Freundlich are the most frequently used two-parameter models in the literature describing the non-linear equilibrium between adsorbed organic pollutant (adsorbate) on the adsorbent (q_{eq}) and organic pollutant in solution (C_{eq}) at a constant temperature.

The Langmuir Model

The Langmuir equation is valid for monolayer sorption onto a surface with a finite number of identical sites. It is probably the best known and most widely applied sorption isotherm. It has produced good agreement with a wide variety of experimental data and is given by Equation 2.9:

$$q_e = \frac{q_o b C_e}{1 + b C_e} \qquad (2.9)$$

where q_e is the amount adsorbed (mg/g), C_e is the equilibrium concentration of the adsorbate (mg/L), and parameters q_o and b are Langmuir constants related to maximum adsorption capacity (mg/g) (monolayer capacity) and bonding energy of adsorption (L/mg), respectively, which are functions of the characteristics of the system as well as time (Langmuir, 1918).

Plots of $1/q_e$ versus $1/C_e$, were obtained from $\frac{1}{q_e} = \frac{1}{q_o} + \frac{1}{b q_o C_e}$ which was the linearized form of the Langmuir equation. The values of monolayer capacity (q_0) and Langmuir constant (b) have been evaluated from the intercept and the slope of these plots.

The adsorption capacity can be correlated with the variation of surface area and porosity of the adsorbent. Higher surface area and pore volume will result in higher adsorption capacity. The Langmuir equation is used for homogeneous surfaces. One can readily deduce that at low sorbate concentrations it effectively reduces a linear isotherm and thus follows Henry's law. Alternatively, at high sorbate concentrations, it predicts a constant – monolayer – sorption capacity.

The Freundlich Model

The Freundlich model assumes neither homogeneous site energies nor limited levels of sorption. The Freundlich equation has the general form shown in Equation 2.10:

$$q_e = k_F C_e^{1/n} \qquad (2.10)$$

where q_e is the amount adsorbed (mg/g), C_e is the equilibrium concentration of the adsorbate (mg/L), K_F ((mg/g)*(mg/L)^n) and n are the Freundlich constants related to adsorption capacity and adsorption intensity, respectively (Freundlich, 1926).

Plots were obtained from $In\,q_e = In\,k_F + \frac{1}{n} In\,C_e$ which was the linearized form of Freundlich equation. ln q_e versus ln C_e linear plots would give the value of 1/n as slope and k_F as an intercept. The value of k_F can be used as alternative measure of adsorption capacity, while 1/n determines the adsorption intensity.

2.7 Kinetics of ion exchange

Ion absorption onto solid ion-exchange and chelating adsorbents is generally considered to involve liquid−solid phase reactions. Kinetics of adsorption or IX is in many cases strongly influenced by diffusion resistance in particles of adsorbent. The ions first diffuse through the solution to the surface of a solid adsorbent, followed by the diffusion of ions within the solid phase. Then the chemical reaction between ions and functional groups takes place, and finally the exchanged ions diffuse to the surface of

the adsorbents and into the solution. The absorption kinetics is governed by the slowest of these processes. When ion diffusion from the solution to the adsorbent surface is the slowest step, the absorption kinetic is liquid-film diffusion controlled. If the ionic diffusion inside the solid adsorbent is the slowest step, the absorption is particle diffusion controlled. In some cases, the chemical reaction is the slowest step; then the absorption process is chemical reaction controlled (Streat, 1984).

The adsorption kinetics normally includes two phases: a rapid removal stage followed by a much slower stage before the equilibrium is established (Ho and Mckay, 1999. The rate law has three primary requirements:

(a) Knowledge of all the molecular details of the reaction including the energetics and stereochemistry;
(b) Interatomic distances and angles throughout the course of the reaction;
(c) The individual molecular steps involved in the mechanism.

The rate at which, sorption takes place is of most importance when designing batch sorption systems. Consequently, it is important to establish the time dependence of such systems under various process conditions. Traditionally, the kinetics has been described by the first-order equation typical of that derived by Lagergren (1898).

2.7.1 Pseudo-first order

A kinetic model for sorption analysis is the pseudo first order rate expression of Lagergren in the form described in Equation 2.5 and 2.6:

$$\frac{dq}{dt} = k_1(q_e - q) \qquad (2.5)$$

$$\log(q_e - q) = \log q_e - \left(\frac{k}{2.303}\right) \times t \qquad (2.6)$$

where q_e is the amount of metal ion (M^{n+}) sorbed at equilibrium (mg/g), q_t amount of M^{n+} sorbed at time t (mg/g) and, k_1 the rate constant of pseudo-first order sorption (1/min). The value of k_1 can be obtained from the slope of the linear plot of log (q_e - q_t) vs. t.

2.7.2 Pseudo-second order model

When the applicability of the first order kinetics becomes untenable (for example, q_e obtained on the basis of the pseudo-first order reaction equation is not the same as the one obtained experimentally), the second order equation is applied with a view to obtain k_2, the second order rate constant as shown in Equation 2.7 (Ho and Mckay, 1998):

$$\frac{dq}{dt} = k_2(q_e - q)^2 \qquad (2.7)$$

The integrated form of the equation (2.7) under the boundary conditions of q = 0 and $q_t = q_t$ at t = t in the linear form (shown in Equation 2.8) makes it possible to obtain q_e and k_2 from the plots of t/q_t vs. t.

$$\frac{t}{q_t} = \left(\frac{1}{k_2 q_e^2}\right) + \left(\frac{1}{q_e}\right) \times t \qquad (2.8)$$

2.8 Summary

Water scarcity has led to various desalination technologies being implemented to augment fresh (portable) water supplies. However, these technologies come with a disadvantage in the form of a concentrated brine stream which is becoming increasing costly to dispose off. The higher the percentage recovery, the higher the concentration levels of the brines produced. Its constituents are generally made up of major cations, anions, minor elements and trace metals. Of interest are the major cations whose concentration lies in the following regions: Mg^{2+} (200 mg/L); Ca^{2+} (500 mg/L) and Na^{+} (1500 mg/L). Various technologies have been implemented in treating brines streams but most these methodologies are being over whelmed by the quantities of the brines being produced. A school of thought has led to the use of cheaper natural adsorbents in the treating of waste waters including brines. Fibre adsorbents have proved to be greater performers in terms of their kinetics and are able to remove dissolved and complexed metals from such contaminated waters and have excellent chemical stability and mechanical strength. These adsorbents are either complexing agents or contain cationic or anionic exchange sites and separations are based on the different stabilities of the complexes and their different affinities for the metal ions.

CHAPTER 3

3 Experimental Setup

3.1 Materials

3.1.1 Ion Exchange Resin and Fibres

The cation exchange resin Amberlite 252 RFH (from Rohm & Haas) and functionalized Polyacrylonitrile PAN poly(amidoxime) fibres (PAN fibres made by Montefibre SpA in Porta de Maghera, Italy) were used in this study. Amberlite 252 RFH is a strong acidic cationic resin having functional sulphonic groups in a styrene-divinylbenzene matrix. The amidoxime chelating fibres were obtained from the commercially available synthetic polyacrylonitrile fibre (99.9% acrylonitrile and 0.1% vinyl acetate) PAN by a one-step reaction with hydroxylamine in methanol (3 wt %) at 80°C for 2 hours. These fibres have a 6 mm length and 1.5 dtex. Their physical properties and specifications as reported by the suppliers are shown in Table 3.1.

Table 3-1: General description and properties of resin and fibre

	Rohm & Haas	**Montefibre SpA**
	Amberlite 252RFH	**amidoxime**
Functional group	Sulphonic	Amidoxime
Matrix	Styrene-divinylbenzene copolymer	Acrylonitrile-vinyl acetate copolymer
Structure	macroporous	fibrous
Bulk density	780 g/L	1.18 g/cm^3
Capacity	1.7 mol/L (H^+ form) ≥1.65 equiv./L (H+ form)	1.96 : 1.35 meq/g (Anionic : Cationic)

3.1.2 Chemicals

The grade and supplier of chemicals used in this study are described in Table 3.2 below:

Table 3-2: Chemicals used in this study

Chemicals	Percentage Purity	Suppliers
Calcium chloride	99% AR	Merck Chemicals
Hydroxylamine hydrochloride	99% AR	Kimix
Magnesium chloride	98 % AR	Merck Chemicals
Potassium hydroxide	99% AR	Merck Chemicals
Sodium chloride	99 % AR	Merck Chemicals
Sodium hydroxide	99 % AR	Merck Chemicals
Hydrochloric acid	32 % AR	Merck Chemicals
Methanol	99 % AR	Merck Chemicals
Nitric acid	55 % AR	Merck Chemicals
Phosphoric acid	85 % AR	Kimix
Sulphuric acid	98 % AR	Merck Chemicals
Copper chloride	99 % AR	Merck Chemicals
Potassium hydrogen phthalate	99 % AR	Merck Chemicals
Potassium dihydrogen phosphate	99 % AR	Merck Chemicals

3.1.3 Preparation of Stock Solutions

The concentration range of 100 – 1000 mg/L of $CaCl_2$, $MgCl_2$ and NaCl solutions used in the experiments were determined from the major metal ion concentration in the brine waste water collected from Emalahleni treatment plant. All solutions were prepared from analytical grade chemicals and deionized water was used as a solvent. Stock solutions of 1000 mg/L of calcium ions (Ca^{2+}), magnesium ions (Mg^{2+}) and sodium ions (Na^{+}) were prepared by dissolving 3.6682 g of $CaCl_2.2H_2O$; 8.3645 g of $MgCl_2.6H_2O$ and 2.5435 g of NaCl in 1 litre of deionized water, respectively. The working solutions containing 100 – 800 mg/L Ca^{2+}, Mg^{2+} and Na^{+} ions, respectively, were prepared by appropriate dilution of the stock solutions immediately prior to their use.

3.2 Instrumentation

A GFL model thermostated water bath shaker was used for shaking the solutions at desired temperatures. The pH was measured using a glass electrode (micro ohm pH meter). Its calibration was carried out using standardized Merck buffer solutions (pH 4 and pH 7). A scanning electron microscope (Hitachi X650, Scanning Electron Micro analyzer) at 10-20 kV was used to examine the surface morphology of PAN, poly(amidoxime) and alkali treated poly(amidoxime) fibre surfaces before and after functionalization. The infrared spectra were measured by the Perkin-Elmer Spectrum 100 FT-IR spectrometer with a specially designed compartment to cater for solid samples. An atomic absorption spectrophotometer (AAS), model PU9100 Philips AAS, was used for the quantitative determination of the concentration of calcium, magnesium, sodium and copper ions. Sample preparation, standards preparation, preparation of the calibration curve for the analysis of Ca^{2+}, Mg^{2+} and Na^{+} is given in Appendix A.

3.3 Preparation of Chelating Fibre Containing Amidoxime Groups

The preparation of the fibre containing amidoxime group is based on the treatment of nitrile groups with hydroxylamine solution giving rise to a selective functional group (Egawa *et al.*, 1992).

3.3.1 Preparation of 3% Hydroxylamine (NH_2OH) Solution

About 110 g of hydroxylamine hydrochloride ($NH_2OH.HCl$) was dissolved in 900 mL methanol (MeOH) solution. 55 g of sodium hydroxide (NaOH) was dissolved in 300 mL MeOH solution. After dissolving the two substances separately in MeOH, the NaOH in MeOH solution was slowly added drop wise using a separation funnel to a methanolic hydroxylamine hydrochloride solution. After the mixture was stirred sufficiently on a magnetic stirrer (in a water bath kept at 30 ^{o}C) sodium chloride

precipitated. The hydrochloric acid (HCl) of $NH_2OH.HCl$ was neutralized by the NaOH solution and the resulting solution was separated from the NaCl precipitate through decantation. Solubility of $NH_2OH.HCl$ in MeOH decreased at low temperature hence dissolution was carried out at 30 °C.

$$NH_2OH.HCl + NaOH \rightarrow NH_2OH + NaCl + H_2O \quad (3.1)$$

A sample solution (1 mL) was taken from NH_2OH-MeOH solution, diluted up to 50 mL using deionized water and this solution was titrated with 0.5 N HCl to calculate the concentration of NH_2OH in the solution using the following formula:

$$[NH_2OH](wt\,\%\,NH_2OH) = 33\times\left[\frac{(0.5\times F_{HCL}\times V_{HCL})}{1000}\right]\times 100 \quad (3.2)$$

If wt % of NH_2OH is higher than 3 %, the solution should be diluted with MeOH to achieve the exact 3 wt% NH_2OH. The final concentration of NH_2OH should be checked again with pH titration.

3.3.2 Functionalization of Polyacrylonitrile (PAN)

10.00 g of fibre was placed into a pyrex reactor which was tightly closed and properly sealed or placed into a round bottom glass flask under a reflux condenser. Then the above-prepared hydroxylamine solution was added to the flask containing the fibre and the reaction was carried out at 80 ºC for 2 hrs shaking gradually. After completion of the reaction, the fibre was separated from the solution by filtration and washed several times with deionized water until no further NH_2OH remained in the solution. (This was checked with 0.001 mol/L Potassium permanganate-$KMnO_4$ solution, in the presence of NH_2OH, the violet colour of $KMNO_4$ turned yellow).

3.3.3 Alkali treatment/Hydrolysis

Dried functionalized fibers were treated with 1.0 mol/L NaOH solution prior to using them for adsorption experiments in order to enhance the adsorption capacity. For this, 3 ± 0.06 g of fibre was treated with 200 mL of 1.0 mol/L NaOH solution at 30 ^{o}C in a water bath, shaking for 24 hrs. After completion of the hydrolysis period, the treated fibers were washed with deionized water until no alkalinity remained in the washings and then dried at 40 ºC to a constant weight prior to use in adsorption experiments (the washings were checked with phenolphthalein indicator from Merck Chemicals).

3.4 Fibre Characterization

3.4.1 FT-IR Analysis

Infra-red spectra of PAN, amidoxime, alkali-treated amidoxime fibres were carried out with an FT-IR spectrometer to determine the functional groups present.

3.4.2 SEM Analysis

A scanning electron microscope (Hitachi X650, Scanning Electron Micro analyzer) at 10-20 kV was used to examine the surface morphology of PAN and Amidoxime fibre surfaces before and after functionalization.

3.4.3 Measurement of Anion and Cation Exchange Capacity

Measurement of Anion Exchange Capacity

The anion exchange capacity of the resin was measured by determining chloride in the supernatant by means of argentometry. A 0.5 ± 0.01 g sample of PAN, Amidoxime fibre and hydrolyzed Amidoxime fibres were shaken at 30 ºC for 15 hrs with a 100 mL of 0.1 mol/L of HCl solution. To 10 mL portion of supernatant, a 10 mL of 0.2 mol/L sodium hydrogen carbonate ($NaHCO_3$) solution and a 5 mL 2 %

starch solution was added. The resulting solution was titrated with a 0.1 mol/L silver nitrate ($AgNO_3$) solution using fluorescein indicator. The anion exchange capacity of the fibre was measured by determining the chloride released.

Measurement of Cation Exchange Capacity

The PAN, Amidoxime fibre and hydrolyzed Amidoxime fibres used for the measurement of anion exchange capacity was washed with deionized water until the washings are acid-free, air-dried, and dried at 40 ºC under vacuum. 0.250 ± 0.005 g of the PAN, Amidoxime fibre and hydrolyzed Amidoxime fibres and 25 mL of 0.1 mol/L NaOH solution was shaken at 30 ºC for 15 hrs. A 5mL portion of the supernatant was titrated with 0.1 mol/L nitric acid (HNO_3) solution using methyl orange indicator. After reaching the methyl orange end point, the chloride released was titrated with 0.05 mol/L silver chloride solution using 0.5 mL of 0.05 mol/L potassium chromate solution for the detection of end point. The cation exchange capacity was determined by subtracting the amount of chloride released from the amount of NaOH exhausted.

The amidoxime group is a bidentate ligand and has both an acidic group which loses a proton and a basic lone pair of electrons on the nitrogen which can co-ordinate with the metal ion hence the determination of the anion and cation exchange capacity procedure is different from the resin procedure because it has to accommodate the anion aspect. The normal resin procedure is usually designed for either cationic or anionic exchange capacity. The underlying principle is still the same because we are quantifying the exchange site H^+ or Na^+ for cations and Cl^- or OH^- for anion exchange capacity.

3.5 Cation Exchange capacity for Amberlite 252 RFH

To 0.5 ± 0.01 g of air dried, hydrogen form cationic exchange resin in a 250 mL erlenmeyer flask add exactly 200 mL of standardized 0.1 M NaOH solution that had

been prepared in 5 % NaCl. The stoppered sample was allowed to stand overnight. 50 mL aliquot of the supernatant liquid was back titrated to the phenolphthalein end point with standard 0.1 M HCl. The volume of the acid required to produce a permanent coloration in the indicator is equivalent to the hydrogen ions initially present in the resin phase (Fisher and Kunin, 1955).

3.6 Adsorption Experiments

The adsorption capacity of Amidoxime fiber and hydrolyzed Amidoxime fibre toward Ca^{2+}, Mg^{2+}, Na^{+} and Cu^{2+} ions from metal ion solutions was evaluated by batch adsorption experiments and their performance was compared to the Amberlite 252 RFH resin.

Synthetic solutions were used to study the adsorption behaviour without the interference of the minor or trace metal ions in the brine waste water solutions. The impact of interference of the minor or trace metal ions on adsorption of the major cations was investigated separately as a parameter by adding a know concentrations of Cu^{2+} metal ions.

The first set of experiments were carried out with Ca^{2+}, Mg^{2+} and Na^{+} solutions at a concentration of 100 mg/L in deionized water. The appropriate pH of the solution was attained by using 20 mL of 0.1 mol/L of various phosphate buffer solutions prepared to achieve a particular pH value in the pH range 2-8 (Table 3.3).

Table 3-3: Buffer solutions for influence of pH on adsorption experiments

pH	Buffer solutions
2	100 mL of 0.1 M KH_2PO_4 and 16.0 mL of 85 % H_3PO_4
3	100 mL of 0.1 M $KHC_8H_4O_4$ and 44.6 mL of 0.1 M HCl
4	100 mL of 0.1 M KH_2PO_4 and 1.0 mL of 0.1 M HCl
5	100 mL of 0.1 M KH_2PO_4 and 1.2 mL of 0.1 M HCl
6	100 mL of 0.1 M KH_2PO_4 and 44.6 mL of 0.1 M HCl
7	100 mL of 0.1 M KH_2PO_4 and 66.0 mL of 0.1 M KOH
8	100 mL of 0.1 M KH_2PO_4 and 108.4 mL of 0.1 M KOH

HCl – Hydrochloric acid
H_3PO_4 – Phosphoric acid
KH_2PO_4 – Potassium dihydrogen phosphate
$KHC_8H_4O_4$ – Potassium hydrogen phthalate
KOH – Potassium hydroxide

3.6.1 Batch Adsorption Experiment

The batch experiments for the adsorption of each metal ion (Ca^{2+}, Mg^{2+}, Na^{+} and Cu^{2+}) was carried out in a 100 mL erlenmeyer flask using a tray action shaker in a thermostated water bath at atmospheric conditions. Fixed amounts of resin (0.1 g) and fibre (0.1 g) were contacted for 24 hrs with 50 mL metal ion solution of variable concentration and pH at 30 °C. Blank solutions were treated similarly without the adsorbent and the recorded concentrations at the end of each operation were taken as the initial concentration. The residual Ca^{2+}, Mg^{2+}, Na^{+} and Cu^{2+} ion concentration in the metal ion solution after the desired treatment and time were measured by AAS. The amount of metal ion retained (q, mg/g), (q, mmol/g), (q, mg/g)and percent adsorption (% A) were calculated as shown by (Equations.3.3 and 3.4):

$$q(mg/g) = \frac{(C_o - C_f) \times V}{M} \tag{3.3}$$

$$q(meq/g) = \left[\frac{q(mg/g)}{Equavalent\ weight\ of\ M^{n+}} \right] \tag{3.4}$$

$$q(mmol/g) = \frac{(C_o - C_f) \times V}{Mr \times M} \quad (3.5)$$

$$Adsorption\,(\%) = \frac{(C_o - C_f)}{C_o} \times 100\,\% \quad (3.6)$$

where q is the amount adsorbed (mg/g) or (meq/g) or (mmol/g), C_o is the initial metal ion concentration, C_f is the final metal ion concentration (mg/L), V is the solution volume (L) M is the amount of adsorbent used (g), Equivalent weight of M^{n+} is the formulae weight divided by the charge on metal ion, M^{n+} and Mr is the atomic mass of the metal ion adsorbed (Sang et al., 2008).

3.6.2 Effect of Adsorbent dose

Metal ion binding capacity was measured by the batch equilibration technique with varying adsorbent mass. Various dry adsorbent amounts (0.05-0.25 g for fibres and 0.1-1.0 g for resins) were contacted with 50 mL of 100 mg/L of each metal ion solution (Ca^{2+}, Mg^{2+}, Na^{+}) at 30 ^{o}C for 24 hrs with continuous shaking. After equilibration was completed, the supernatant solution was collected for metal ion determination by AAS. This procedure was repeated for 100 mg/L $Mg^{2+}$and Na^{+} ion solution and all test samples were performed in triplicate.

3.6.3 Effect of contact time

Contact time adsorption experiments were conducted at 30 °C in different erlenmeyer flasks with covers. The flasks were shaken for different time intervals at constant temperature. Various masses of dry adsorbents (0.1 g for fibres and 0.1 g for resins) were contacted with 50 mL of 100 mg/L of each metal ion (Ca^{2+}, Mg^{2+}, Na^{+}) in solution. After a prefixed time the phases were separated by filtration and the supernatant solution was collected for metal ion determination by AAS.

3.6.4 Effect of pH

For the batch technique, triplicate, 0.1000 ± 0.002 g of the dry fibre adsorbent was placed into a series of 100 mL erlenmeyer flasks and the fibres were allowed to equilibrate with 25 mL deionized water for at least 10 mins. After adding 20 mL of 0.1 mol/L phosphate buffer solutions at various pHs in the pH range of 2-8, 20 mL of 0.01 mol/L metal ion solution was added to each flask, 10 mins later. The mixture was shaken for 24 hrs in a water bath at 30 °C. Blank solutions were treated similarly without the adsorbent and the recorded concentrations at the end of each operation were taken as the initial concentration. After equilibration was completed, the supernatant solution was collected for metal ion determination by AAS. Ca^{2+}, Mg^{2+}, Na^{+} and Cu^{2+} ions were studied during the pH study.

3.6.5 Equilibrium Adsorption Isotherms

Sorption isotherms were carried out in a series of 100 mL erlenmeyer flasks. Each flask was filled with 50 mL of different initial metal ion concentrations varying from 100 to 1000 mg/L while maintaining the adsorbent mass and temperature at constant level. After equilibration, the solution was separated and analyzed. Blank solutions were treated similarly without the adsorbent and the recorded concentrations at the end of each operation were taken as the initial concentration. Each of the data sets was used to calculate the adsorption capacity, q_e, of the adsorbent. Finally the adsorption capacity was plotted against equilibrium concentration, C_e. Each experiment was carried out in triplicate under identical conditions.

3.6.6 Adsorption kinetics

Kinetics experiments were conducted by using a fixed mass of adsorbent (0.1 g for fibres and 0.1 g for resins) and employing metal ion concentration in the range 100 mg/L. The samples at different time intervals were taken and filtered. 1 mL aliquots were diluted to 50 mL with deionized water and concentrations determined using the AAS.

3.6.7 Competitive Adsorption

Competitive adsorption of Ca^{2+}, Mg^{2+}, Na^{+} and Cu^{2+} ions from their binary, ternary and quaternary solutions, as set out in Table 3-4, were investigated by following a similar procedure as described above (section 3.6.1). In 1L flasks, 1000 mL metal solutions were prepared according Table 3-4 with pH adjustment for all copper solutions. A solution (50 mL) containing 200 mg/L of each metal ion in a saturated sodium chloride solution was shaken for 24 hrs in a water bath at 30 °C. Solutions containing Cu^{2+} ions were performed at an optimum pH of 6.0 while the remaining solutions were carried out at their natural pH. After equilibration was achieved, the concentration of the metal ions in the remaining solution was measured by AAS.

Table 3-4: Metal solutions used to study competitive adsorption behavior

System	Solution mixture
Binary	200 mg/L Ca^{2+} + Saturated NaCl
	200 mg/L Mg^{2+} + Saturated NaCl
Ternary	200 mg/L Ca^{2+} + 200 mg/L Mg^{2+} + 200 mg/L Na^{+}
	200 mg/L Ca^{2+} + 200 mg/L Mg^{2+} + Saturated NaCl
Quaternary	200 mg/L Ca^{2+} + 200 mg/L Mg^{2+} + 200 mg/L Na^{+} + 200 mg/L Cu^{2+}
	200 mg/L Ca^{2+} + 200 mg/L Mg^{2+} + 200 mg/L Na^{+} + Saturated NaCl

Chapter 4

4 Results and Discussion

4.1 Fibre Characterization

The fibre was characterized by the following techniques: Scanning Electron Microscope (SEM), Fourier Transform Infra-red (FT-IR) spectrum, cation and anion capacity measurements. A comparison of the capacities of the fibre and resin was carried out and variables such as contact time, pH, adsorption kinetics as well as competitive adsorption were explored. The results are discussed in this section. A justification of the functionalization time is also discussed in this section.

4.1.1 Functionalization and Analysis of FT-IR spectra

A methanolic solution 3% hydroxylamine was used to functionalize the copolymer fibres. This was achieved by conversion of the nitrile groups to amidoxime groups ($C(NH_2)NOH$) at 80ºC (see section 3.3.2 and Figure 2.9). The conversion of the nitrile to the amidoxime functionality was indicated by the reduction of CN absorption at 2242 cm^{-1} in the FT-IR spectra as shown in Figure 4.1. The amidoxime group is a bidentate ligand and has both an acidic group which loses a proton and a basic lone pair of electrons on the nitrogen which can co-ordinate with the metal ion (Liu *et al.*, 2002 and Lutfor *et al.*, 2000). The functionalized PAN (Amidoxime fibres) were then hydrolyzed in 1.0 mol/L NaOH at 30 ℃ and shaken for 24 hrs (procedure described in section 3.3.3).

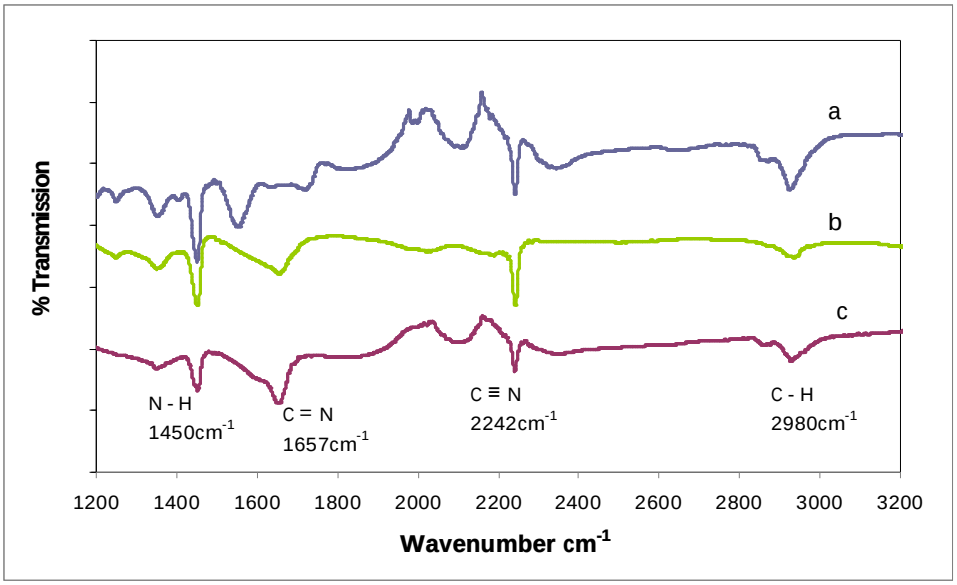

Figure 4-1: The FT-IR spectra of (a) polyacrylonitrile, (b) amidoxime-AOPAN and (c) hydrolyzed amidoxime (HAOPAN).

The key absorption lines in the FT-IR measurements are those due to C≡N stretching mode at wavenumber of 2242 cm^{-1} in the cyano groups, N-H stretching mode at 3100 – 3400 cm^{-1}, in the polyacrylonitrile fibre. The absorptions due to C=N stretching mode at 1657 cm^{-1} and N-O stretching mode at 909cm^{-1} were observed (though not displayed in the figure) in the FT-IR spectra of amidoxime fibre after treatment with hydroxylamine. The relative decrease in the intensity of the characteristic C≡N bonds in PAN is due to a percentage conversion of C≡N to C=N based on the functionalization reaction time, as shown in figure 4.2. Accordingly, the C≡N groups are expected to be replaced with H_2N-C=NOH at the end of the reaction, hence the nitrile group in the amidoxime functionality was indicated by the reduction in absorption of the C≡N groups at 2242 cm^{-1}, appearance of C=N stretching at 1657 cm^{-1} and amide band of N-H at 1450 cm^{-1}, respectively. These results were in agreement with that in the literature (Egawa *et al.*, 1992).

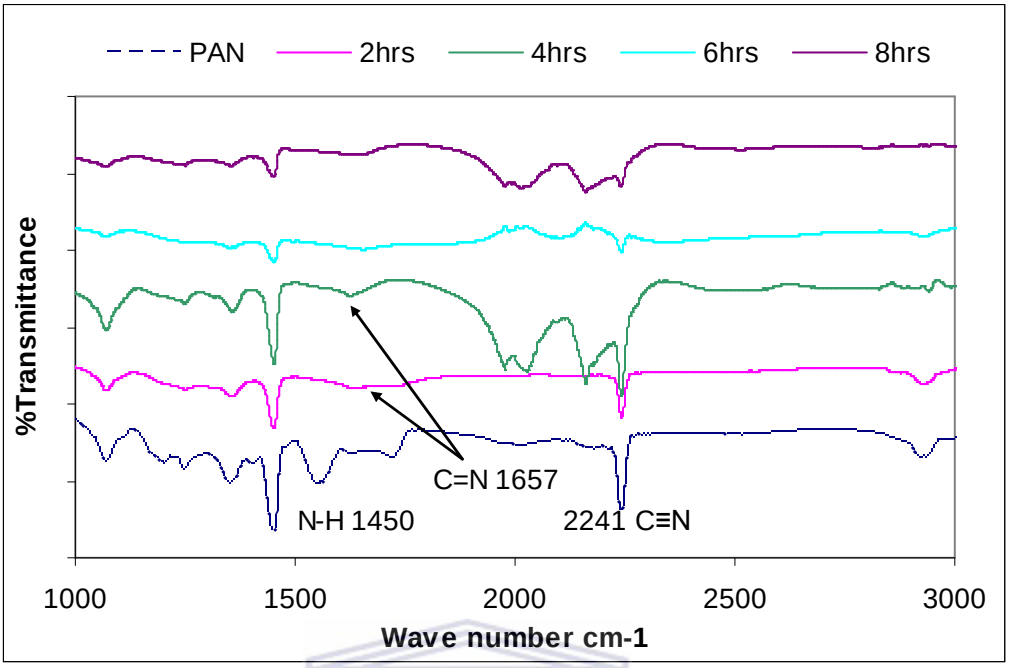

Figure 4-2: Infrared spectra of the amidoximated fibres functionalized at different polymer reaction temperatures.

Figure 4.2 shows the effect of time on the functionalization reaction as determined by comparison of FT-IR of fibres functionalized at different times. An optimum reaction time of 2 hrs was obtained and was there after used throughout the functionalization reaction. This result was confirmed by capacity studied carried out on the fibre samples (section 4.1.2). Having reached the optimum capacity at reaction time of 2 hrs there was no further increase in the capacity of the fibre samples after 2 hrs. This is due to the polymer composition (99.9 AN; 0.1VA) with a compact, well ordered structure resulting in the fibre having excellent resistance to chemical agents, hydrolysis, high mechanical characteristics, optimal heat stability both in dry and wet conditions and extraordinary resistance to light, weathering, mildew and bacteria.

4.1.2 SEM Images

A scanning electron microscope was used to examine the surface morphology of PAN and Amidoxime surfaces before and after functionalization. Figure 4.3.a shows

that the surface of the PAN before the functionalization was relatively smooth and uniform. After functionalization for 2 hrs, the fibre surface was composed of etched strips and stops, became rough and corroded, indicating that the functionalization reaction occurred on the surface of the PAN fibre (Figure 4.3 b).

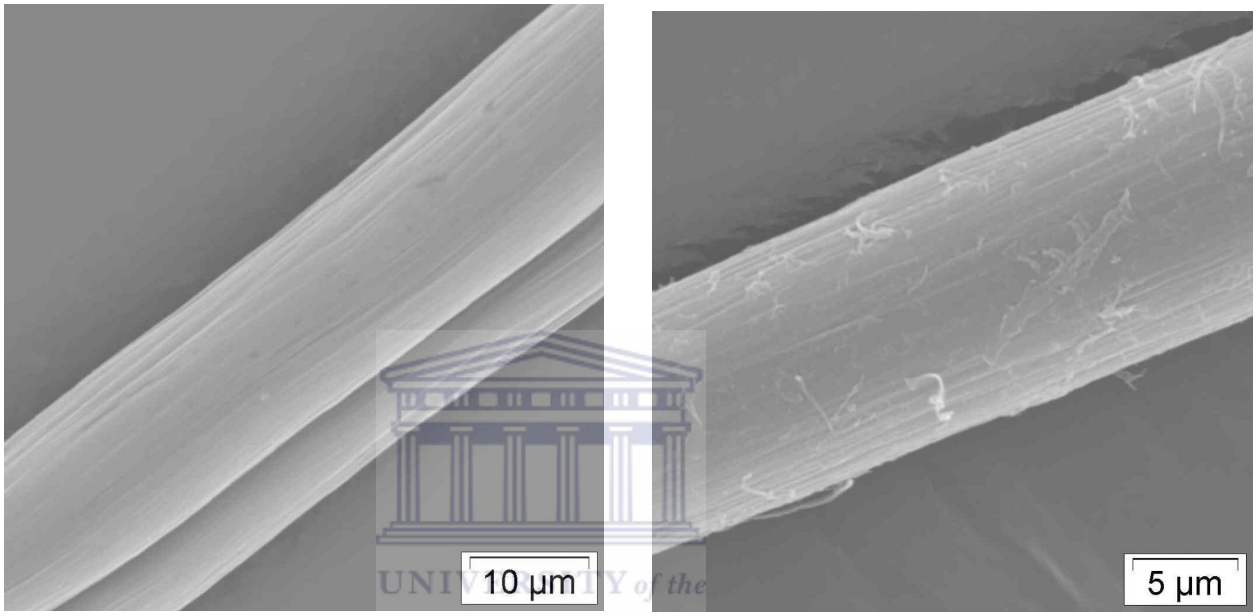

(a) **(b)**

Figure 4-3: SEM images showing the surface morphologies of (a) Polyacrylonitrile, PAN, and (b) Amidoxime (AOPAN).

4.1.3 Exchange Capacity

The capacity of the adsorbent is one of the factors which determine the quantity of adsorbent that will be needed for quantitative removal of a specific metal ion from solution. A comparison of the Amberlite resin capacity and Amidoxime fibres capacity is discussed in this section and their methods of determination are found in sections 3.4.3 and 3.5, respectively. The capacity of the resin and the Amidoxime fibres is reported in Table 4.1 along with the standard deviation of the three determinations.

Table 4-1: Cationic and anionic exchange capacities of amidoxime fibres

	UNTREATED		ALKALI -TREATED	
	Anionic (meq/g)	**Cationic (meq/g)**	**Anionic (meq/g)**	**Cationic (meq/g)**
Amidoxime Fibres	1.96 (± 0.04)	1.36 (± 0.06)	1.85 (±0.05)	1.63 (±0.03)
PAN fibres	1.82 (± 0.13)	1.27 (± 0.15)	-	-

A marginal increase in anion exchange capacity (AEC) and cationic exchange capacity (CEC) was obtained after 2 hrs of functionalization and that alkali-treated improved the CEC by 20 % whereas in the anionic exchange capacity there was a slight decrease. The AEC corresponds to the amount of amidoxime groups introduced and the cation exchange capacity represents the amounts of acidic sites (mainly carboxylic groups) formed by hydrolysis of nitrile and/or amidoxime group during the functionalization and/or alkali-treatment process (Egawa *et al*., 1992). The alkali-treatment of Amidoxime fibres partly converts amidoxime groups into more hydrophilic carboxylic groups, enhancing the swelling of fibre greatly and the anion exchange capacity decreased, which was also observed by Egawa *et al*., (1992). The increased cationic adsorption ability of the resulting fibre after alkaline treating was attributed to changes in the physical and chemical structures of the fibre in alkaline medium, which is consistent with the results reported in the literature (Kabay *et al*., 1993). Egawa et al., (1992 & 1994) and Kabay et al., (1993) were able to functionalize PAN adsorbents within the optimum amidoximation time of 2 hrs and they proved that the alkali-treatment/hydrolysis of amidoxime fibres yields increased adsorption ability due to the changes in the physical and chemical structure of the fibres. However, the fibrous adsorbent containing amidoxime exhibits poor mechanical stability after contact with alkali.

4.2 Batch Adsorption Experiments

Batch adsorption experiments for the adsorption of Ca^{2+}, Mg^{2+} and Na^{+} from synthetically prepared solutions in a concentration range of 100 – 1000 mg/L (similar to the brine waste stream generated from the Emalahleni Water treatment Plant in Witbank, results tabulated in Table 4.2) by Amberlite 252 RFH resin and poly(amidoxime) fibres was carried out. The effects of various process parameters such as, contact time, fibre/resin dosage, pH of the solution, the temperature and the adsorption isotherm, as well as competitive adsorption were studied for the adsorption of Ca^{2+}, Mg^{2+}, $Cu^{2+}$and Na^{+} ions from aqueous solutions.

.**Table 4-2:** Emalahleni brine waste water analysis results from a 3 train RO plant

Brines	**pH**	**Electrical conductivity (mS/cm)**	**Ca^{2+} (mg/L)**	**Mg^{2+} (mg/L)**	**K^{+} (mg/L)**	**Na^{+} (mg/L)**	**NO_3^{-} (mg/L)**	**Cl^{-} (mg/L)**	**SO_4^{2-} (mg/L)**
Stream 1	7.38	8.7	341	177	132	1473	40	753	9633
Stream 2	6.95	12.66	394	283	403	1556	70	1774	16386

The Emalahleni plant desalinates rising underground water from Anglo Coal's Landau, Greenside and Kleinkopje collieries, as well as from the BECSA's defunct south Witbank mine. It comprises of a 3 train module system connected in series, whereby the reject from the first module stream is used as the feed for the second module stream and permeates from the three streams are collected as product water. This water is analyzed by Inductive Coupled Plasma Mass Spectrometer (ICP-MS) in order to determine the elemental composition in the raffinate or brine concentrate. In Table 4.2, the results of the analysis of Emalahleni brine show sodium-chloride-sulphate waters with a considerable amount of calcium, potassium and magnesium concentration. The pH of the water is averagely neutral with an electrical conductivity (EC) that increases from the first raffinate to the second, signifying that these waters are circumneutral. The EC has a direct reflection on the increase in the concentration of the elements in the raffinate.

It is worth noting that several factors namely agitation rate in the aqueous phase, the amount of adsorbent, the sorbent structural properties as well as the metal ions properties such as hydrated ionic radius and initial concentration of metal ions in solution are parameters that determine the adsorption rate. Agitation rate was kept constant while varying the initial metal ion concentration, amount of adsorbent and pH of the solution. This made it possible to compare the properties of the adsorbents.

4.2.1 Effect of contact time

The effect of contact time on adsorption of each metal ion (Ca^{2+}, Mg^{2+} and Cu^{2+}) from their chloride solutions containing 100 mg/L metal ion concentration was studied using Amberlite 252 RFH resin, Amidoxime and hydrolyzed Amidoxime fibres. Various adsorbent masses were added to 50 mL of each individual metal ion solutions and were shaken for 24 hrs at 30 ^{o}C (procedure found in section 3.6.4). Table 4.3 and Figures 4.4; Table 4.4 and Figure 4.5, illustrates the percentage adsorption of each metal ion (Ca^{2+}, Mg^{2+} and Na^{+}) by Amberlite resin and Amidoxime fibres as a function of time. With an increase in contact time from 0 to 20 mins the percentage adsorption increased rapidly and sorption was virtually completed within 25 to 30 mins for the Amberlite resin. A further increase in time had no effect on the adsorption of the metal ions. Therefore, the maximum contact time of 30 mins is suitable for the adsorption reaction by Amberlite 252 RFH to reach equilibrium (Table 4.3 and Figure 4.4). However, in the case of Amidoxime fibres, the maximum contact time needed to reach equilibrium is 15 mins for both hydrolyzed Amidoxime and Amidoxime fibres (Table 4.4 and Figure 4.5; Table 4.5 and Figure 4.6).

Table 4-3: Effect of contact time on adsorption of Ca^{2+}, Mg^{2+} and Na^{+} ions from individual model solution by Amberlite 252 RFH resin.

Time (mins)	Ca^{2+} adsorption (%)	Mg^{2+} adsorption (%)	Na^{+} adsorption (%)
1	50.00	16.47	25.37
5	60.00	36.47	40.30
10	65.00	49.41	46.27
15	70.00	57.64	49.25
20	72.50	64.12	52.24
25	75.00	70.59	52.24
30	80.00	70.59	52.24
40	80.00	70.59	52.24
50	80.00	70.59	52.24
60	80.00	70.59	52.24

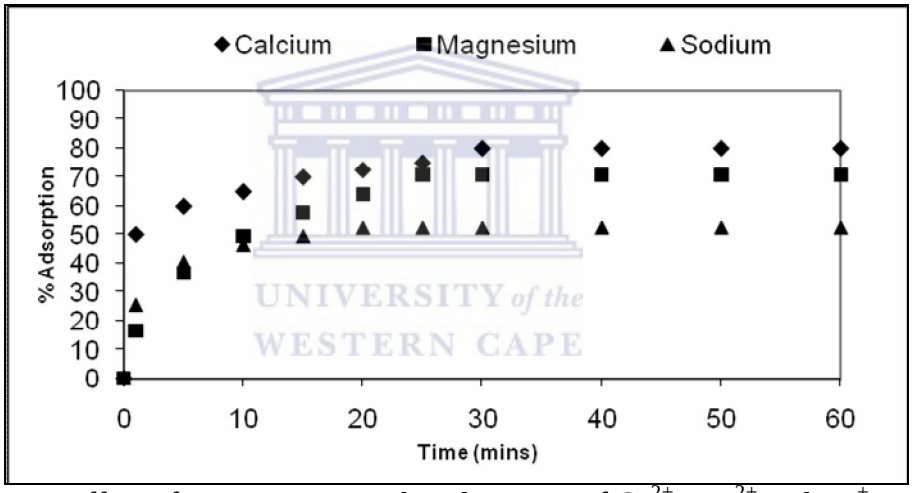

Figure 4-4: Effect of contact time on the adsorption of Ca^{2+}, Mg^{2+} and Na^{+} separately by Amberlite 252 RFH resin (Resin mass, 0.1 g; temp. 30 ºC).

Table 4-4: Effect of contact time on adsorption of Ca^{2+}, Mg^{2+} and Na^{+} ions from individual model solution by Amidoxime fibres.

Time (mins)	Ca^{2+} adsorption (%)	Mg^{2+} adsorption (%)	Na^{+} adsorption (%)
1	14.00	3.26	5.66
5	16.00	9.78	11.95
10	26.00	14.13	13.52
15	32.00	17.39	15.09
20	32.00	17.39	15.09
25	32.00	17.39	15.09
30	32.00	17.39	15.09
40	32.00	17.39	15.09
50	32.00	17.39	15.09
60	32.00	17.39	15.09

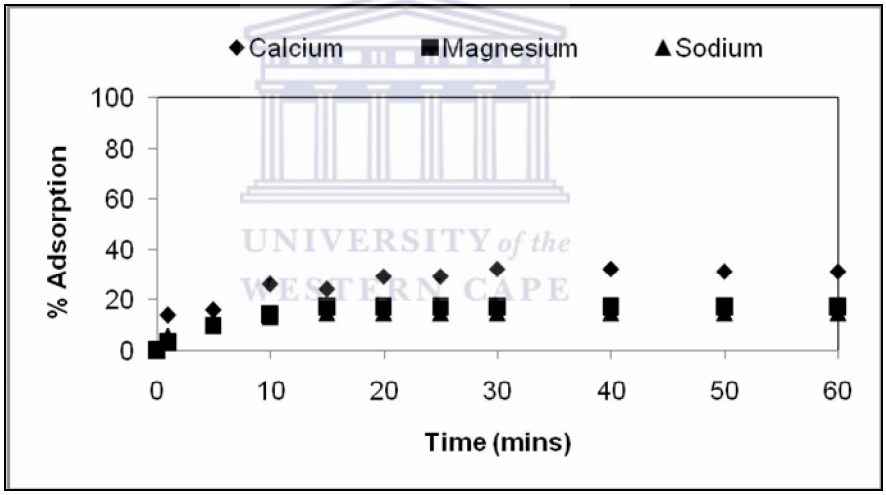

Figure 4-5: Effect of contact time on the adsorption of Ca^{2+}, Mg^{2+} and Na^{+} separately by Amidoxime fibre (Fibre mass, 0.1 g; temp. 30 ºC).

Table 4-5: Effect of contact time on adsorption of Ca^{2+}, Mg^{2+} and Na^{+} ions from individual model solution by hydrolyzed Amidoxime fibres.

Time (mins)	Ca^{2+} adsorption (%)	Mg^{2+} adsorption (%)	Na^{+} adsorption (%)
1	20.00	25.00	27.67
5	30.00	31.52	30.82
10	40.00	35.87	33.96
15	50.00	39.13	33.96
20	50.00	39.13	33.96
25	50.00	39.13	33.96
30	50.00	39.13	33.96
40	50.00	39.13	33.96
50	50.00	39.13	33.96
60	50.00	39.13	33.96

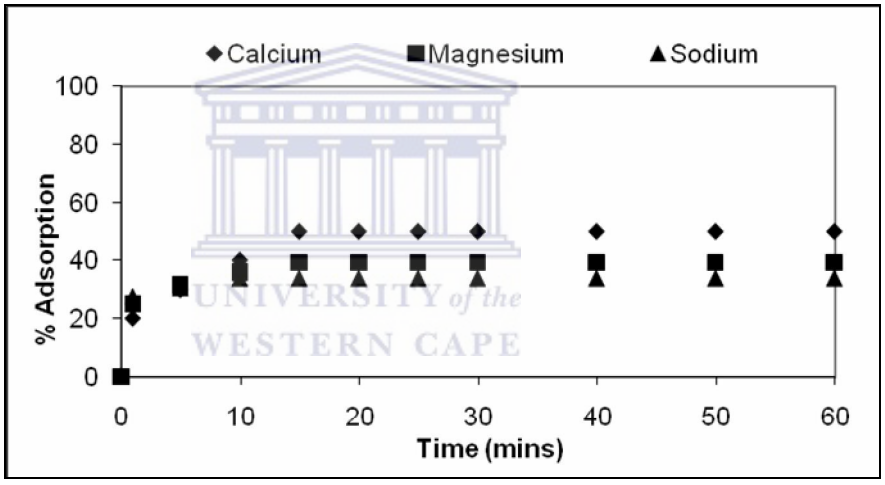

Figure 4-6: Effect of contact time on the adsorption of Ca^{2+}, Mg^{2+} and Na^{+} separately by hydrolyzed Amidoxime fibre (Fibre mass, 0.1 g; temp. 30 ºC).

Table 4.3 and Figure 4.4 shows that the Amberlite resin removed 80 % Ca^{2+}, 70 % Mg^{2+} and 52 % Na^{+} respectively in the first 30 mins, which corresponds to equilibrium removal amounts of 2.14; 2.82 and 1.12 meq/g, respectively. The adsorption equilibria for Ca^{2+}, Mg^{2+} and Na^{+} ions by Amidoxime fibres was attained in about 15 mins, resulting in the adsorption of 32 %, 17 % and 15 % of Ca^{2+}, Mg^{2+} and Na^{+} ions respectively (Table 4.4 and Figure 4.5) which corresponds to equilibrium removal amounts of 0.77; 0.70 and 0.32 meq/g, respectively. On the other hand the hydrolyzed Amidoxime fibres were able to achieve a much higher %

adsorption than the Amidoxime fibres for the same contact time. Percentage figures of 50 %, 39 % and 33 % of Ca^{2+}, Mg^{2+} and Na^{+} ions respectively, were achieved (Table 4.5 and Figure 4.6). This translates to equilibrium removal amounts of 1.35; 1.57 and 0.72 meq/g of Ca^{2+}, Mg^{2+} and Na^{+} ions, respectively. The differences in the contact time between the fibres and resins are as a result of high adsorption rates ascribed to accessibility of exchange sites on the fibres.

Kinetics of metal ion sorption governs the rate, which determines the residence time and it is one of the important characteristics defining the efficiency of an adsorbent (Krishnan and Anirudhan, 2003). The sorption rate is taken into consideration when designing batch sorption systems. Consequently it is important to establish the time dependency of such systems for various pollutant removal processes (Ho *et al.*, 2002). Therefore, the required contact time for sorption to be completed is important to give insight into a sorption process. This also provides information on the minimum time required for considerable adsorption to take place and the possible diffusion control mechanism between the metal ion as it moves from the bulk solution towards the adsorbent surface and through the pore matrix in the case of resin. The metal uptake versus time curves, are single, smooth and continuously leading to saturation suggesting the possible monolayer coverage of metal ions on the surface of the adsorbent (Rengaraj *et al.*, 2001).

The cation exchange capacities (CEC) of Amberlite 252 RFH and Amidoxime fibres determined as set out in section 3.6.3, observed in this study are shown in Table 4.6.

Table 4-6: Cation exchange capacities of Amberlite 252 RFH resin and Amidoxime fibres achieved in the contact time experiment

	Ca^{2+} (meq/g)	Mg^{2+} (meq/g)	Na^{+} (meq/g)
Amberlite resin	2.1428	2.8236	1.1203
Amidoxime fibre	0.7797	0.7018	0.3194
Hydrolyzed Amidoxime fibre	1.3510	1.5737	0.7268

The maximum CEC values were observed for the Amberlite resin followed by hydrolyzed Amidoxime fibre and lastly Amidoxime fibre after 30 minutes for the resin and 15 minutes for the fibres. The order of decreasing capacity is Amberlite > hydrolyzed Amidoxime > Amidoxime fibre for Ca^{2+}, Mg^{2+} and Na^{+} ions in the individual solutions of metal ion mixtures. The greater capacity of the Amberlite resin after 30 mins is explained by the existence of a large number of ion exchange sites per gram of adsorbent whilst the number of ion exchange sites in the fibres is much less. Amongst the fibres, the hydrolyzed Amidoxime fibre has a greater capacity than the Amidoxime fibre. The increased adsorption ability of the hydrolyzed Amidoxime fibre for cations was attributed to changes in the physical and chemical structures (the conversion of cyano groups to carboxylic groups) of the fibre after treatment in alkaline medium (alkali treatment or alkali hydrolysis).

As shown in Figure 4.7, pretreatment of fibre with 1.0 mol/L NaOH for 24 hrs rendered them essentially active. Individual metal ions (Ca^{2+}, Mg^{2+} and Na^{+}) were shaken together with 0.1 g adsorbent at 30 ºC for 24 hrs as a function of time in order to determine the effect of hydrolysis on the uptake of metal ions. The hydrolyzed fibres achieved high Ca^{2+}, Mg^{2+} and Na^{+} loading significantly more quickly than the non treated fibres. Even after 30 mins, the hydrolyzed Amidoxime fibres were 50 % loaded while the non treated fibres (Amidoxime) were 31 % loaded. This is attributed to the increase in the cation exchange capacity and the effect of electrostatic interactions between the metal ions and the hydrolyzed amidoxime fibres. The same

scenario is observed for Mg^{2+} and Na^{+} ions and results are represented in Figure 4.8 and 4.9.

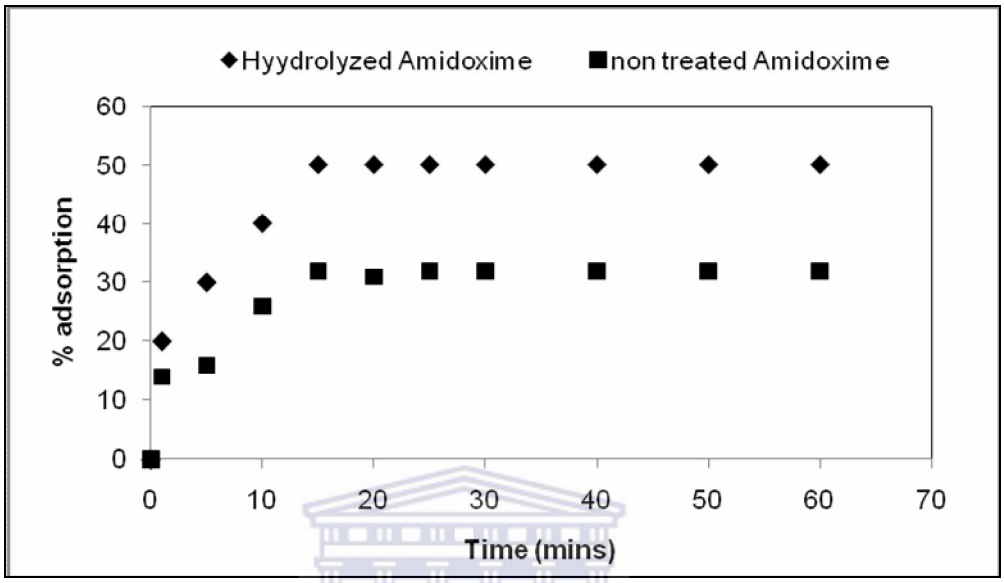

Figure 4-7: Effect of alkaline treatment or hydrolysis on Ca^{2+} loading of Amidoxime fibre using 100 mg/L Ca^{2+} at 30 °C as a function of time.

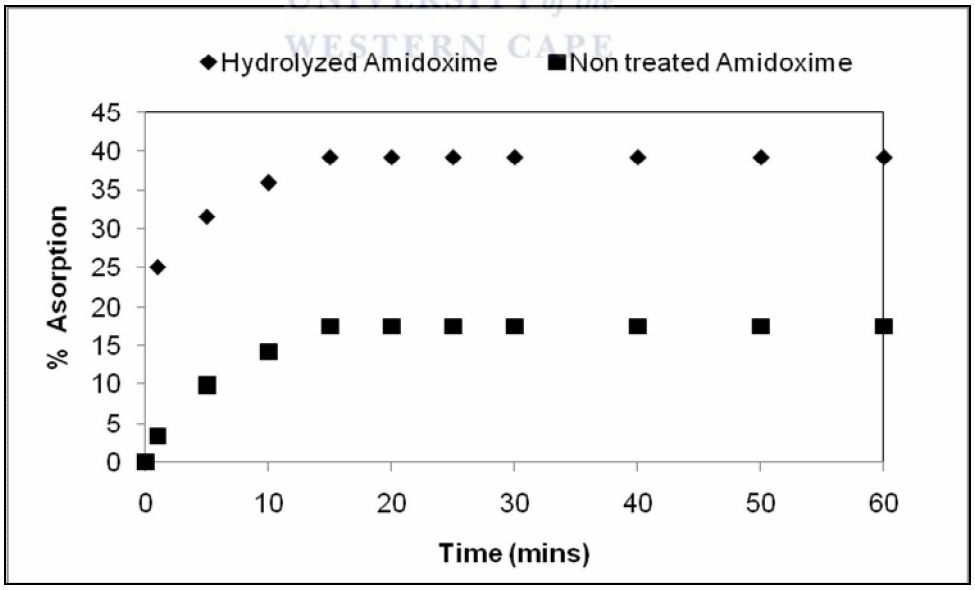

Figure 4-8: Effect of alkaline treatment or hydrolysis on Mg^{2+} loading of Amidoxime fibre using 100 mg/L Mg^{2+} at 30 °C as a function of time.

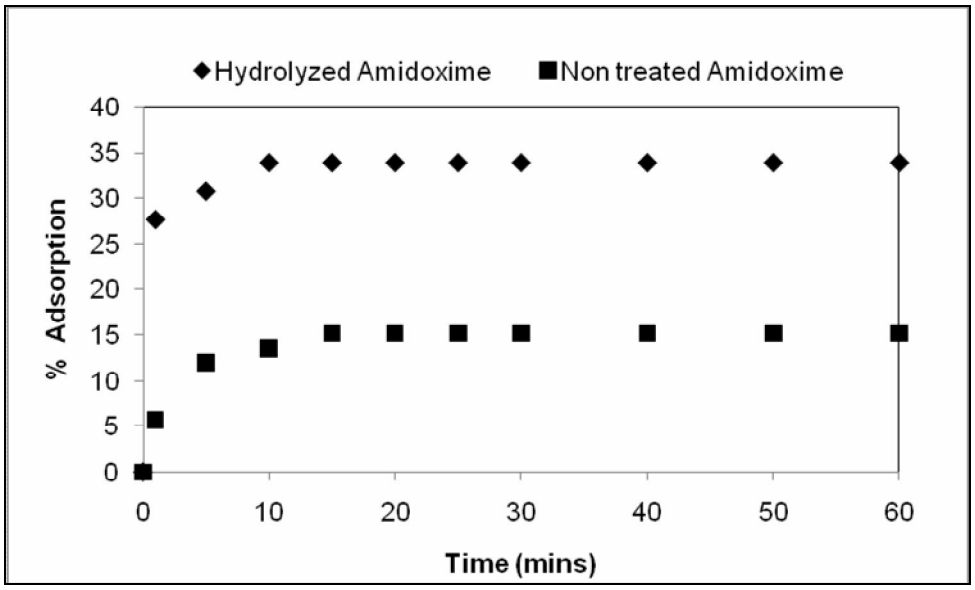

Figure 4-9: Effect of alkaline treatment or hydrolysis on Na^+ loading of Amidoxime fibre using 100 mg/L Na^+ at 30 °C as a function of time.

4.2.2 Effect of fibre/resin mass

The adsorbent dosage is another important parameter, which influences the extent of metal uptake from the solution. The initial concentration of the aqueous feed solution was 0.01 mol/L Ca^{2+} and the experiment was conducted with Ca^{2+} ion solution being shaken separately with the various resin mass for 24 hrs (see procedure in section 3.6.2). The same procedure was repeated for 0.01 mol/L Mg^{2+} and Na^+ ions, respectively.

The results of the effect of Amberlite resin dosage on the adsorption of Ca^{2+}, Mg^{2+} and Na^+ ions from separate solutions are shown in Table 4.7 and Figure 4.10. In this experiment, the feed solution metal ion concentration (0.01 mol/L) and the mixing time (24 hrs) were kept constant and the resin dosage was varied between 0.1 and 1.0 g. It was evident that the amount of metal ion uptake increased from 43.44 to 99.50 % adsorption for the adsorption of Ca^{2+} ions by increasing the resin mass from 0.1 g to 0.5 g. The same effect was observed for Mg^{2+} and Na^+ ions, where metal ion uptake increased from 66.18 and 43.83 to 99.18 and 81.83 % adsorption, respectively.

But Ca^{2+} and Mg^{2+} ions adsorption had a plateau for the resin amounts between 0.5 g to 1.0 g/50 mL. According to these results, optimum resin amount was found as 10 g resin/L for both Ca^{2+} and Mg^{2+} ions.

Table 4-7: Effect of resin mass on adsorption of Ca^{2+}, Mg^{2+} and Na^{+} ions from individual model solution by Amberlite 252 RFH resin.

Resin Amount (g/ 50mL)	Ca^{2+} adsorption (%)	Mg^{2+} adsorption (%)	Na^{+} adsorption (%)
0.1	43.40	66.18	43.83
0.2	67.20	84.28	61.87
0.3	85.90	88.89	69.83
0.4	98.10	99.05	75.39
0.5	99.50	99.18	81.83
0.6	99.50	99.65	81.88
0.7	99.50	99.70	84.05
0.8	99.50	99.78	85.98
0.9	99.50	99.81	87.07
1.0	99.50	99.77	88.06

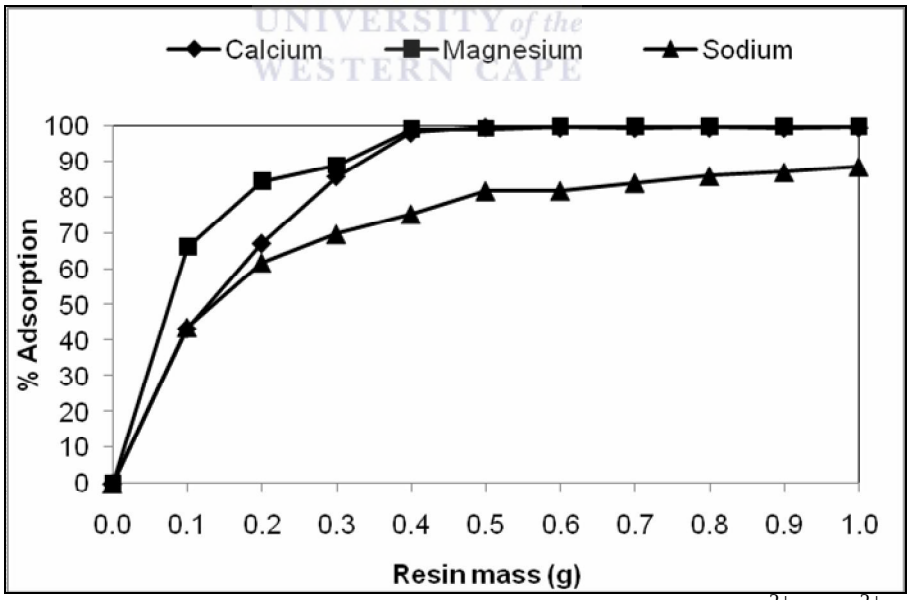

Figure 4-10: Effect of resin mass (g) on the adsorption of Ca^{2+}, Mg^{2+} and Na^{+} respectively, by Amberlite 252 RFH resin, (metal ion concentration, 0.01 mol/L; temperature, 30 °C; volume, 50mL; contact time, 24 hrs).

From Figure 4.10, it is apparent that the percent adsorption of metal ions increases as the adsorbent mass increases from 0.1 g up to 0.5 g due to an increase in the number of available sites or surface sites on the adsorbent at higher mass of adsorbent. Metal ions' removal increased with increasing Amberlite resin mass reaching its peak height at 0.50 g /50 mL or 10 g resin/L (Figure 4.10). It is plausible that the achievement of 100 % adsorption for Ca^{2+} and Mg^{2+} could be attributed to the low concentration of the metal ions in solution and this gives an impression that there are more cationic exchange sites than the cations supplied from solution. Further increase in resin mass has shown negligible effect towards increase in percentage adsorption of Ca^{2+}, Mg^{2+} and Na^{+} ions from solution. In order to see the effect of cationic exchange sites in the adsorption of metal ions, the metal ions in solution must be in excess, so that the limiting factor will be the cationic exchange sites and the maximum adsorption will be reached when the exchange sites are exhausted and not when ions in the solution are exhausted.

Fibre mass was varied from 0.05 to 0.250 g in 50 mL solution for both hydrolyzed Amidoxime and non treated Amidoxime fibres. The results presented in Table 4.8 and Figure 4.11 indicated a slight increase in adsorption of metal ions with increase in fibre mass. According to these results, optimum fibre amount was found as 1 g resin/L for adsorption of Ca^{2+}, Mg^{2+} and Na^{+} ions by amidoxime fibres. Further increase in the fibre dosage has shown a negligible effect towards an increase in percentage adsorption of magnesium and sodium from the solution, probably due to saturation of exchange sites.

Table 4-8: Effect of resin mass on adsorption of Ca^{2+}, Mg^{2+} and Na^{+} ions from individual model solution by Amidoxime fibres.

Resin Mass (g/ 50mL)	Ca^{2+} adsorption (%)	Mg^{2+} adsorption (%)	Na^{+} adsorption (%)
0.05	41.85	27.92	25.07
0.10	41.99	28.21	26.10
0.15	43.78	29.34	26.33
0.20	44.42	29.62	26.81
0.25	44.84	30.19	26.94

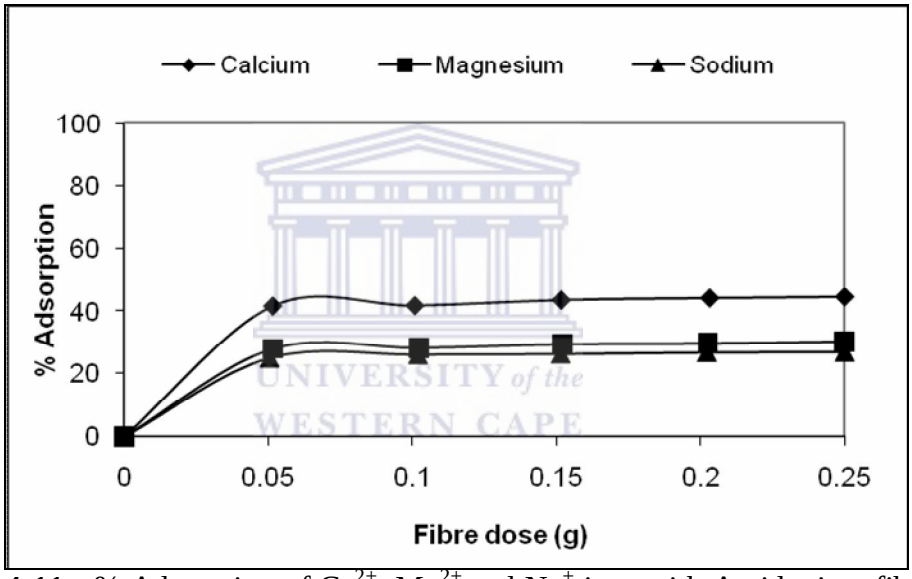

Figure 4-11: % Adsorption of Ca^{2+}, Mg^{2+} and Na^{+} ions with Amidoxime fibres as a function of fibre mass. (Metal ion concentration, 0.01 mol/L; temperature, 30 °C; volume, 50 mL; contact time, 24 hrs).

Table 4.9 and Figure 4.12 shows that there was a slight increase in adsorption of metal ions with increase in fibre dosage. According to these results, optimum fibre amount was found as 1 g resin/L for adsorption of Ca^{2+}, Mg^{2+} and Na^{+} ions by hydrolyzed amidoxime fibres. Further increase in the fibre dosage has shown a negligible effect towards an increase in percentage adsorption of magnesium and sodium from the solution, probably due to saturation of exchange sites.

Table 4-9: Effect of resin mass on adsorption of Ca^{2+}, Mg^{2+} and Na^{+} ions from individual model solution by Amidoxime fibres.

Resin Mass (g/ 50mL)	Ca^{2+} adsorption (%)	Mg^{2+} adsorption (%)	Na^{+} adsorption (%)
0.05	51.84	40.26	38.11
0.10	51.97	40.56	39.15
0.15	53.76	41.67	39.37
0.20	54.40	41.96	39.85
0.25	54.82	42.53	39.97

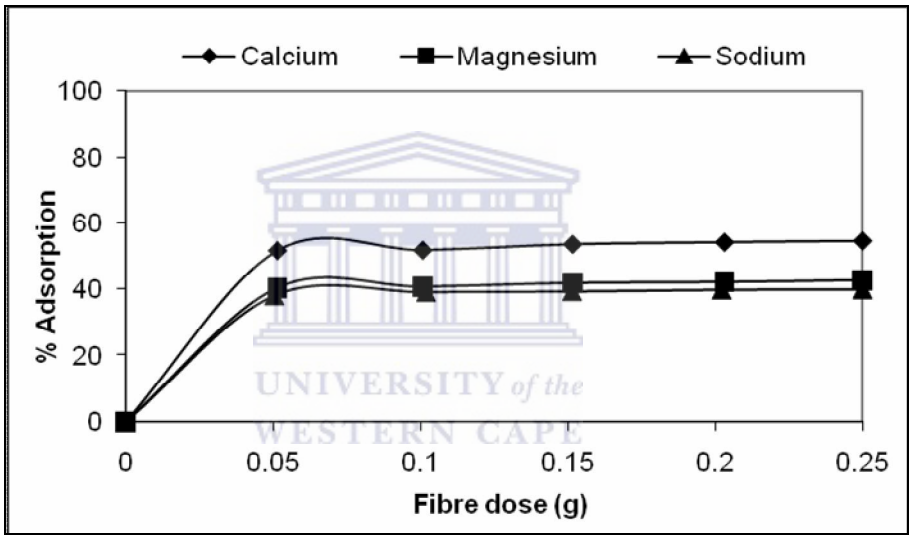

Figure 4-12: Figure 4.12: % Adsorption of Ca^{2+}, Mg^{2+} and Na^{+} ions with hydrolyzed Amidoxime fibres as a function of fibre mass. (Metal ion concentration, 0.01 mol/L; temperature, 30 °C; volume, 50 mL; contact time, 24 hrs).

After hydrolysis of the amidoxime fibres, when used for adsorption of Ca^{2+} ions, there was an increase of 10 % in the adsorption capacity as compared to the previous result obtained from amidoxime in figure 4.11. With Mg^{2+} and Na^{+} ions the observed increase in the capacity adsorption was 12 % after hydrolysis. But when various masses of these adsorbents were used in the fibre mass experiments, results produced showed negligible increase in adsorption with the increase in the fibre dosage. This could be attributed to saturated exchange sites hence little or no adsorption after 0.05 g mass of fibre.

4.2.3 Effect of pH

The pH studies presented in this section were carried out according to the procedure given in section 3.6.4, to see the effect of pH on the adsorption of metal ions from aqueous feed solutions containing 100 mg /L Ca^{2+}, Mg^{2+} and Na^{+} ions with a fixed quantity of Amidoxime fibres. It is well known that pH, besides various physicochemical effects, is an important variable in the ion exchange governed adsorption processes, by which surface charges may be changed or modified. The pH of the metal ion solutions was adjusted to the desired values with phosphate buffer and potassium hydroxide solutions (Table: 3.4 and section 3.6.4). Metal adsorption occurs through a rather strong bond which is a chemical sorption like hydration of ions in aqueous solutions.

The experiment was conducted separately with each metal ion solution being shaken with the 0.2 g Adsorbent for 24 hrs at 30 ºC (see procedure in section 3.6.4). The determination of the uptake and percentage removal of Ca^{2+}, Mg^{2+} and Na^{+} ions separately from the aqueous solution by Amidoxime fibres and hydrolyzed Amidoxime fibres was performed using the procedure set out in section 3.6.4 and the results shown in Table 4.10 and Figure 4.13; Table 4.11 and Figure 4.14, indicate that pH does not play any role in the uptake of these metal ions. The results give an indication that uptake is purely through ion exchange mechanism.

For Amberlite resin, the pH study was not conducted because of the nature and the properties of the resin. It's a strong cation resin, which is highly ionized in both the hydrogen and salt form over the entire pH range, i.e, it completely dissociates both high and low pH levels. Hence its performance is not affected by or influenced by pH.

Table 4-10: Effect of pH on the sorption Ca^{2+}, Mg^{2+} and Na^{+} ions by Amidoxime fibre.

pH	Ca^{2+} adsorption (meq/g)	Mg^{2+} adsorption (meq/g)	Na^{+} adsorption (meq/g)
2	2.98	1.72	0.77
3	3.09	1.91	0.87
4	3.07	1.88	0.85
5	3.18	2.07	0.95
6	3.28	2.23	1.04
7	3.01	1.79	0.81
8	3.00	1.79	0.81

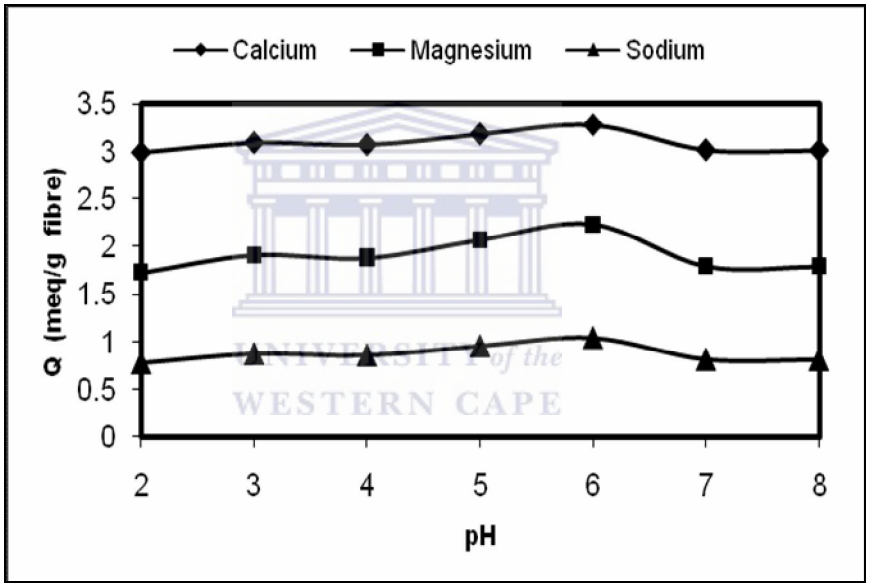

Figure 4-13: Effect of pH on the sorption of Ca^{2+}, Mg^{2+} and Na^{+} ions by Amidoxime fibre. (Fibre mass, 0.2 g; temperature, 30 °C; volume, 50 mL, contact time, 24 hrs).

Table 4-11: Effect of pH on the sorption Ca^{2+}, Mg^{2+} and Na^{+} ions by hydrolyzed Amidoxime fibre.

pH	Ca^{2+} adsorption (meq/g)	Mg^{2+} adsorption (meq/g)	Na^{+} adsorption (meq/g)
2	3.86	3.34	1.47
3	3.95	3.40	1.59
4	3.88	3.42	1.57
5	3.91	3.47	1.67
6	4.09	3.51	1.61
7	3.89	3.50	1.67
8	3.90	3.51	1.67

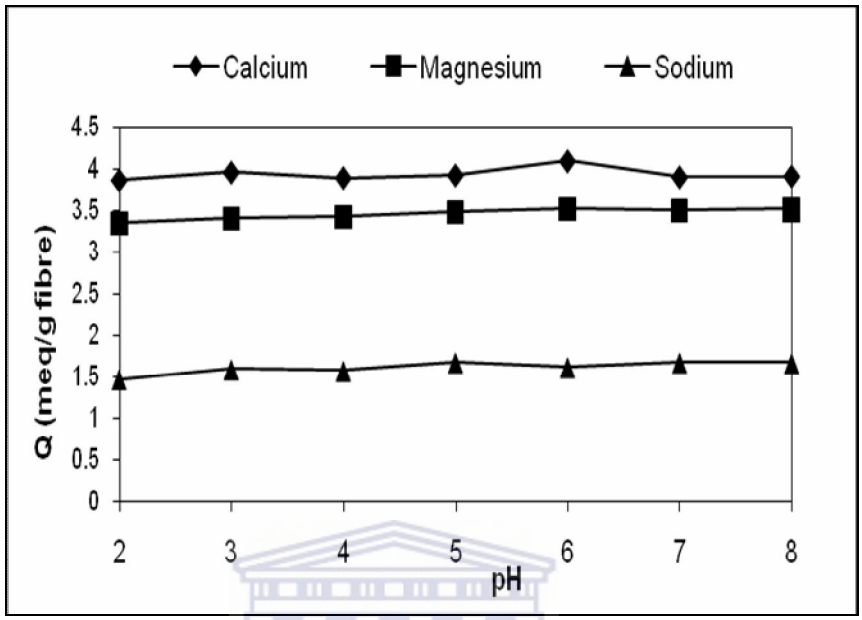

Figure 4-14: Effect of pH on the sorption of Ca^{2+}, Mg^{2+} and Na^{+} ions by hydrolyzed Amidoxime fibre. (Fibre mass, 0.2 g; temperature, 30 °C; volume, 50 mL, contact time, 24 hrs).

The determination of the uptake and percentage removal of copper from the aqueous solution was performed using the procedure set out in section 3.6.4 and is strongly affected by the pH of the metal ion solution as illustrated in Figure 4.15.

Table 4-12: Effect of pH on the sorption Cu^{2+} by PAN, Amidoxime fibre and hydrolyzed Amidoxime fibres.

pH	PAN (meq/g)	Amidoxime fibres (meq/g)	Hydrolyzed Amidoxime (meq/g)
2	0.16	0.17	0.21
3	0.19	0.17	0.23
4	0.21	0.21	0.26
5	0.26	0.27	0.33
6	0.80	1.13	1.25
7	0.34	0.87	1.15
8	0.26	0.72	1.12

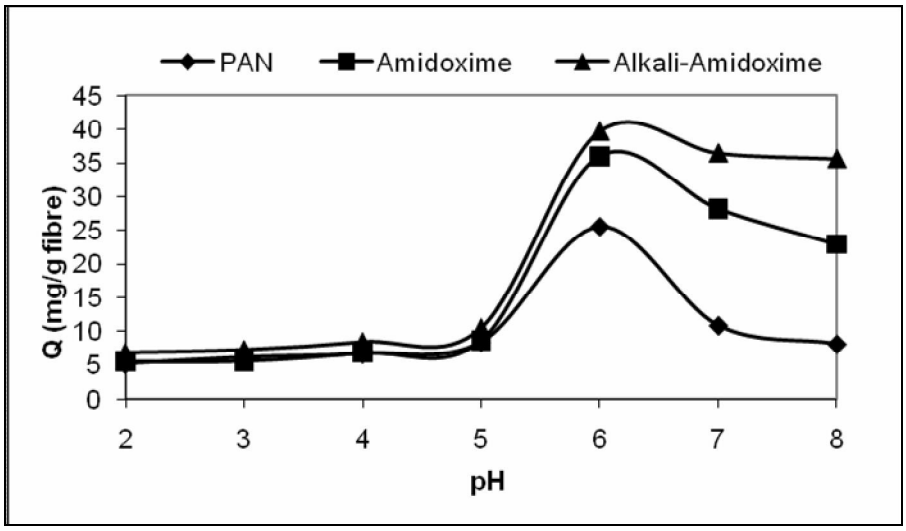

Figure 4-15: Effect of pH on the sorption of Cu^{2+} ions by alkali-treated Amidoxime, Amidoxime and PAN fibres. (Fibre mass, 0.1 g; temperature, 30 °C; volume, 50 mL, contact time, 24 hrs).

It can be seen from Table 4.12 and Figure 4.15, that adsorption percentages are very low in strong acidic medium. After pH 3, the uptake of copper ions increases from 5.22; 5.45 and 6.82 mg/g to 25.5; 35.93 and 39.74 mg/g of PAN; Amidoxime and hydrolyzed Amidoxime fibres, respectively, up to pH 6.0 where after adsorption decreased. No pH values over 8.0 were studied since precipitation of heavy metals occurs. Copper sorption is noted to increase significantly at pH 6, hence this was the optimum pH for Cu^{2+} and this pH was used in the competitive adsorption experiments (very close to the original pH of the solutions). After pH 6.0 the capacity of adsorption decreases in the pH range of 6 to 8. The results presented in Figure 4.15 indicate that pH plays a very influential role in the adsorption of metal ions suggesting a chelating or complexing reaction is taking place. Metal ions, especially heavy metal ions, are adsorbed by forming chelates coordinated by nitrogen atoms of primary amino groups and oxygen atoms of oxime groups. A metallic ion is intermolecularly complexed, being coordinated by two amidoxime groups belonging to different polymeric chains and this is shown in Figure 4.16.

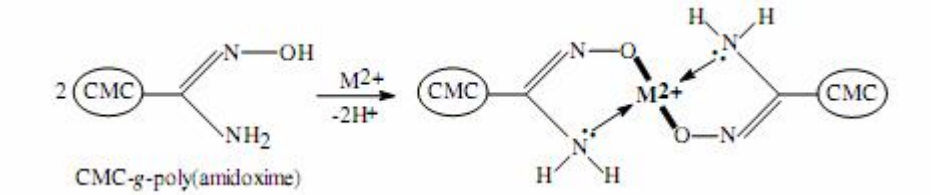

Figure 4-16: A metallic ion coordinated by two amidoxime groups belonging to different polymer chains.

The minimum adsorption observed at low pH (pH 2), in Figure 4.15, may be due to the fact that the higher concentration and higher mobility of H^+ ions present favoured the preferential adsorption of hydrogen ions compared to Cu^{2+} ions (Ajmal *et al.*, 2000). In this acidity region, pH ≤ 3.0, Amidoxime molecule is a proton acceptor, it quickly reacts with a proton, H^+, in the following equation (4.1):

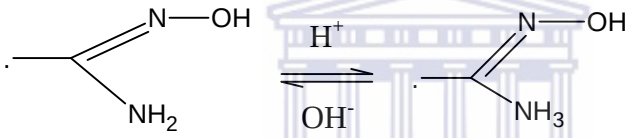

(4.1)

The protonation of $R–C(NOH)NH_2$ results in a quick decrease of the reactivity of AOPAN and ultimate termination of the reaction between AOPAN adsorbent and M^{2+} (metal ions). It would be plausible to suggest that at lower pH value, the surface of the adsorbent is surrounded by hydronium ions (H^+), thereby preventing the metal ions from approaching the binding sites of the sorbent (Wong *et al.*, 2003). This means that at higher H^+ concentration, the sorbent surface becomes more positively charged such that the attraction between biomass and metal cations is reduced (Saeed *et al.*, 2004). So, in our experiment we found that Cu^{2+} was minimally adsorbed by FPAO in this acidity range.

In contrast, as the pH increases, more negatively charged surface becomes available thus facilitating greater Cu^{2+} sorption. It is commonly agreed that the sorption of metal cations increases with increasing pH as the metal ionic species become less stable in the solution. After pH ≥ 3.0, with an increase in basicity of the

aqueous solution, $R–C(NOH)NH_3^+$ as a cation gradually converts to a neutral $R–C(NOH)NH_2$ molecule by reacting with OH^-. However, at higher pH values (pH 7 and pH 8) there is a decrease in the adsorption capacity. This is due to the occurrence of copper precipitation. At pH 7 there are three species present in solution as suggested by Elliot and Huang (1981), Cu^{2+} in very small quantities and $Cu(OH)^+$ and $Cu(OH)_2$ in large quantities. Three species are adsorbed at the surface of adsorbent by ion exchange mechanism with the functional groups present in adsorbent or by hydrogen bonding.

As discussed by Sengupta *et al.*, (1991) most chelating ion exchangers have strong affinities for hydrogen ions because of weak-acid or weak-base functional groups. Consequently, metal ion uptake is drastically reduced under highly acidic conditions (pH < 2.0), because of competition from the hydrogen ions. Bilba *et al.*, (2003) and Lutfor et al., (2000) were able to achieve maximum Cu^{2+} ions adsorption at a pH 6.0.

4.2.4 Adsorption Equilibrium Isotherms

The equilibrium data obtained from the adsorption equilibrium experiments for Ca^{2+}, Mg^{2+} and Na^+ ions on Amberlite 252 RFH resin and Amidoxime fibres, as set out in section 3.6.5, were analyzed using the Langmuir and Freundlich equation. The Langmuir model assumes that the uptake of metal ions occurs on a homogeneous surface by monolayer adsorption without any interaction between adsorbed ions. The model can be represented in the linearised form, which is given as follows (Deng et al., 2003):

$$\frac{1}{q} = \left[\left(\frac{1}{k_l\, q_m}\right)\left(\frac{1}{C_e}\right)\right] + \left[\frac{1}{q_m}\right] \qquad (4.2)$$

where q is the amount adsorbed on the resin at equilibrium (mg/g), C_e is the equilibrium concentration of the adsorbate (mg/L), and k_l is equilibrium constant related to the affinity of the binding sites for the metals or the Langmuir constant. q_m is the resin capacity (maximum possible amount of metallic ion adsorbed per unit mass of adsorbent). The basic assumption of the Langmuir theory is that adsorption takes place at specific homogeneous sites within the adsorbent. It is then assumed that once a metal-ion occupies a reaction site, then no further adsorption occurs at that location.

Freundlich model assumes that the uptake or adsorption of metal ions occurs on a heterogeneous surface by monolayer adsorption. The model is described by the following equation (4.3):

$$q = k_f (C_e)^{\frac{1}{n}} \qquad (4.3)$$

$$In\, q_e = \left(\frac{1}{n}\right) In C_e + In\, k_f \qquad (4.4)$$

The common terms (such as *q and C_e)* in the above equations are described in the Langmuir expression given previously and k_f and n are Freundlich constants that can be related to the adsorption capacity and adsorption intensity, respectively.

In this section of the results, hydrolyzed Amidoxime fibres' adsorption of Ca^{2+} ion results were used to describe the adsorption equilibrium isotherms and its modeling using Langmuir and Freundlich models. The Mg^{2+} and Na^{+} ions adsorption results on both the Amberlite resin and Amidoxime fibres are tabulated in Figure 4.13 and the graphs are presented in the Appendix 7.2. Equilibrium data was obtained for calcium adsorption onto hydrolyzed Amidoxime fibres. The results are tabulated in Table 4.13. The equilibrium relationship for hydrolyzed Amidoxime fibres was

shown in Figure 4.17. The linearised fitting curves of for hydrolyzed Amidoxime fibres are given for Langmuir and Freundlich models in Figure 4.18 and Figure 4.19, respectively. The comparison of experimental and theoretical curves of Langmuir and Freundlich models is shown in Figure 4.20.

Table 4-13: Constant and correlation coefficients of Langmuir and Freundlich isotherms for adsorption of Ca^{2+}, Mg^{2+} and Na^{+}

Adsorbent	**Solution conc 100 mg/l**	**Freundlich isotherms**			**Langmuir isotherms**		
		n	k_f	R^2	q_m	k_L	R^2
Amberlite 252 RFH	Ca^{2+}	2.9878	15.6301	0.8928	140.8451	0.016243	0.9967
Hydrolyzed Amidoxime		0.9837	12.7127	0.9780	204.0816	0.000372	0.9945
Amidoxime		0.9348	21.7867	0.9841	217.3913	0.000280	0.9977
Amberlite 252 RFH	Mg^{2+}	2.8571	7.1086	0.9679	74.6269	0.010140	0.9917
Hydrolyzed Amidoxime		1.3161	2.3364	0.9461	156.2500	0.000929	0.9920
Amidoxime		1.3355	3.1986	0.9507	101.0101	0.001005	0.9917
Amberlite 252 RFH	Na^{+}	2.00441	3.7558	0.9057	128.2051	0.004033	0.9944
Hydrolyzed Amidoxime		2.3491	3.0778	0.9702	188.6792	0.000598	0.9750
Amidoxime		0.91166	21.7562	0.9611	285.7143	0.000248	0.9837

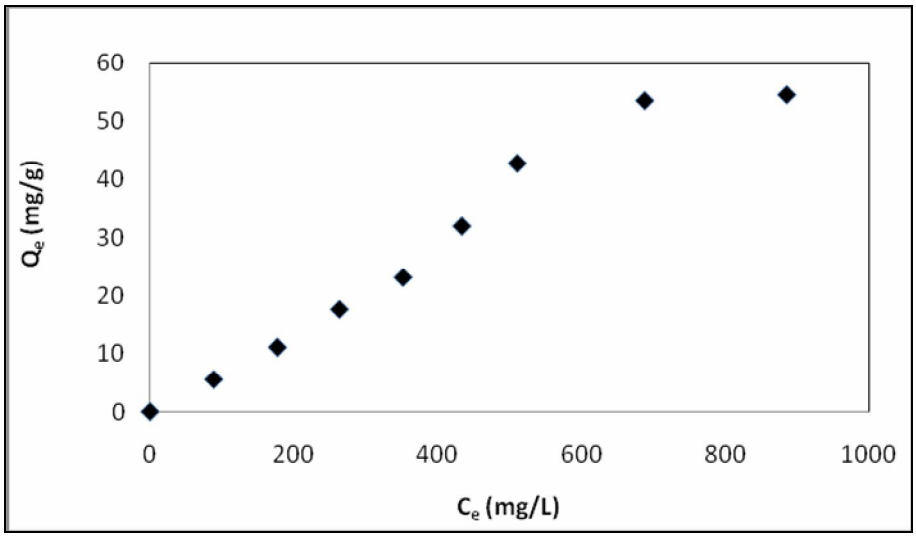

Figure 4-17: Equilibrium isotherm of Alkali-treated Amidoxime fibres for adsorption of Ca^{2+} ions.

The adsorption equilibrium isotherm of hydrolyzed Amidoxime fibres (Figure 4.17) shows that the equilibrium concentration is directly proportional to the adsorption capacity from 100 mg/L to 800 mg/L before flattening out due saturation.

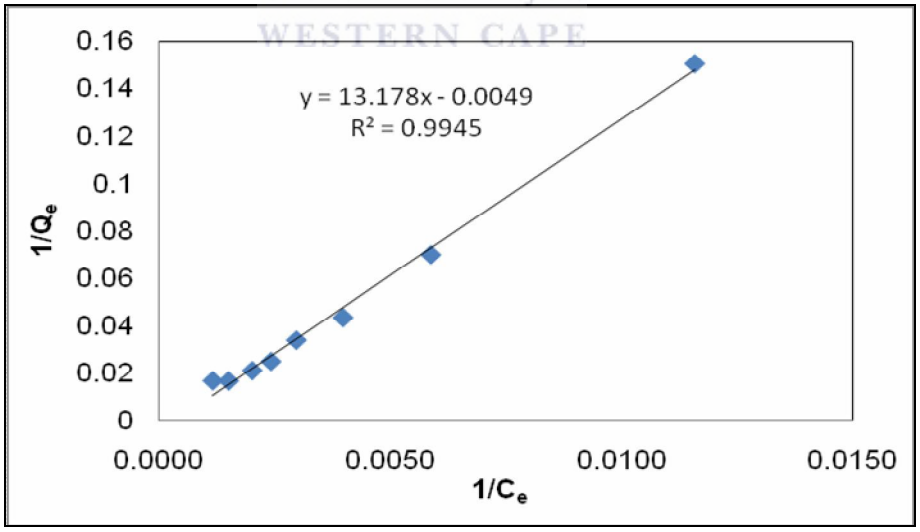

Figure 4-18: Linearized form of Langmuir model of Alkali-treated Amidoxime fibres for adsorption of Ca^{2+} ions.

The linear plot of $1/Q_e$ versus $1/C_e$ suggests the applicability of Langmuir isotherms.

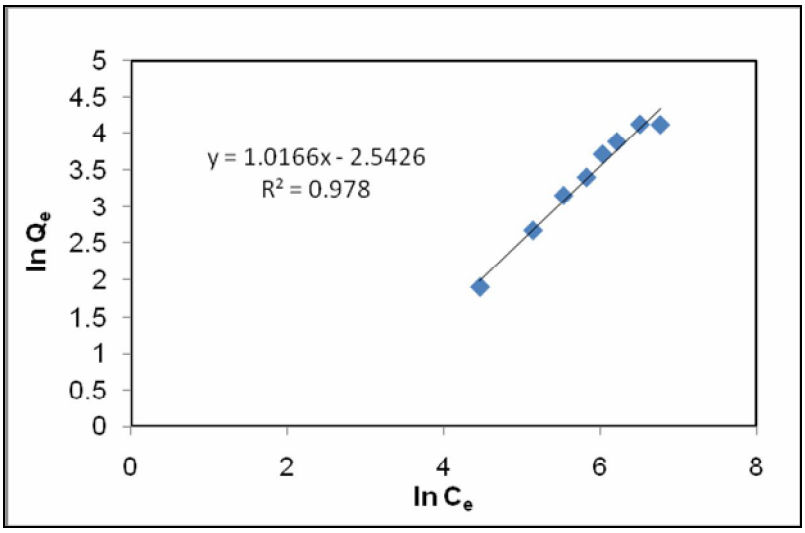

Figure 4-19: Linearized form of Freundlich model of hydrolyzed Amidoxime fibres for adsorption of Ca^{2+} ions.

Linear plot of In Q_e versus In C_e shows that the adsorption of Ca^{2+} obeys the Freundlich adsorption isotherms. However, when you compare the R^2 values the Langmuir has a greater R^2 signifying that the adsorption of Ca^{2+} by hydrolyzed Amidoxime fibres shows a better fit for the Langmuir model than the Freundlich model (Figure 4.20).

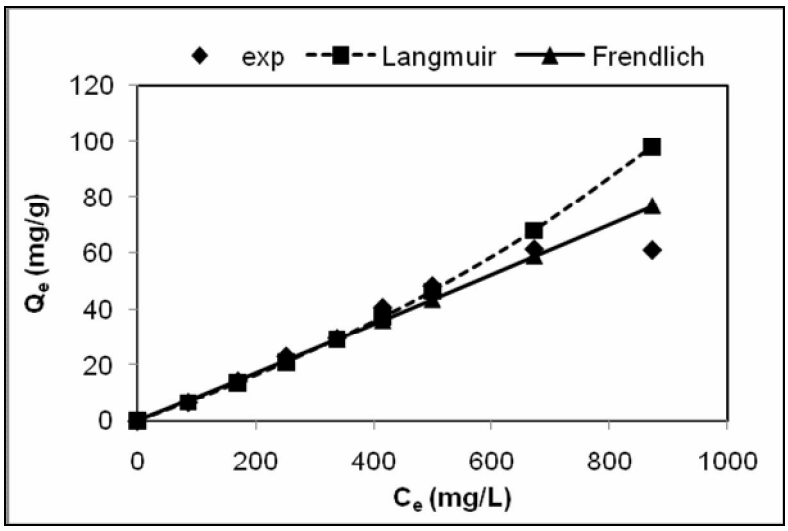

Figure 4-20: The comparison of the experimental and theoretical curves for Langmuir & Freundlich models of Hydrolyzed Amidoxime fibres for adsorption of Ca^{2+} ions.

Figure 4.17, shows that the adsorption of Ca^{2+} ions increased initially with an increase in concentration of the Ca^{2+} ions in solution and then adsorption leveled off. The initial increase in metal adsorption might be due to many available sites on hydrolyzed Amidoxime fibres. The correlation coefficients for the linear regression fit of Langmuir and Freundlich model were found to be 0.9945 and 0.9780 for hydrolyzed Amidoxime fibres (Figures 4.18 and 4.19), respectively. The adsorbent showed a better fit for the Langmuir model than the Freundlich model (Figure 4.20) even though it did not reach experimental points at higher concentration. This can be explained by changes in surface sorption properties during the binding of ions on the inner and outer surfaces, which is more intensive at higher initial concentrations. This results in a lower number of surface sites available for ion exchange. The theoretical curve for Langmuir shows similarity with the equilibrium curve indicates that there is a strong relationship for the data and the Langmuir model mechanism. All the results show that the Langmuir model fitted the results quite well suggesting that the surface of the sorbent is homogeneous.

The comparison of the Langmuir and Freundlich parameters for magnesium and sodium adsorption equilibrium by Amberlite 252 RFH resin, Amidoxime fibres and hydrolyzed Amidoxime are tabulated in Tables 4.13 (graphs are shown in Appendix 7.2).

The R^2 values in Table 4.13 suggest that the Langmuir isotherm provides a good model of the sorption system. The sorption constant, K_L, and sorption capacity, q_m, for calcium are higher than those for magnesium and sodium. As seen from the Table 4.13, q_m (maximum adsorption capacity (mg/g) of the fibres (hydrolyzed Amidoxime and Amidoxime) was higher than Amberlite 252 RFH as a result of high available surface area and also due to their structural differences even if b (bonding energy of adsorption (L/mg)) was nearly the same.

4.2.5 Kinetics of Adsorption

The kinetics of adsorption describes the rate of metal ions uptake on ion exchange resins and this rate controls the equilibrium time. This was determined using fixed amount of adsorbent, 0.1 g and employing metal ion concentration of 100 mg/L and varying the reaction time (see section 3.6.6). Even though the results are tabulated together, this series of experiments were carried separately using one metal ion at a time.

In Figure 4.21, the graph shows that the hydrolyzed Amidoxime fibres have faster kinetics in the adsorption of Na^+ ions than Amidoxime fibres and Amberlite resin. This is attributed to the structure of the fibres where the active exchange sites are found on the surface of the fibres whereas in the resin the exchange sites are found on the walls of pores inside the resin. Kinetics follows the following order: Hydrolyzed Amidoxime fibres > Amidoxime fibres > Amberlite resin.

Equilibrium for the adsorption of Na^+ ions by hydrolyzed Amidoxime fibres and Amidoxime fibres was achieved in 15 mins whereas equilibrium for Amberlite resin was achieved in 20 mins. Thereafter the adsorption proceeds at a slower rate until equilibrium was reached.

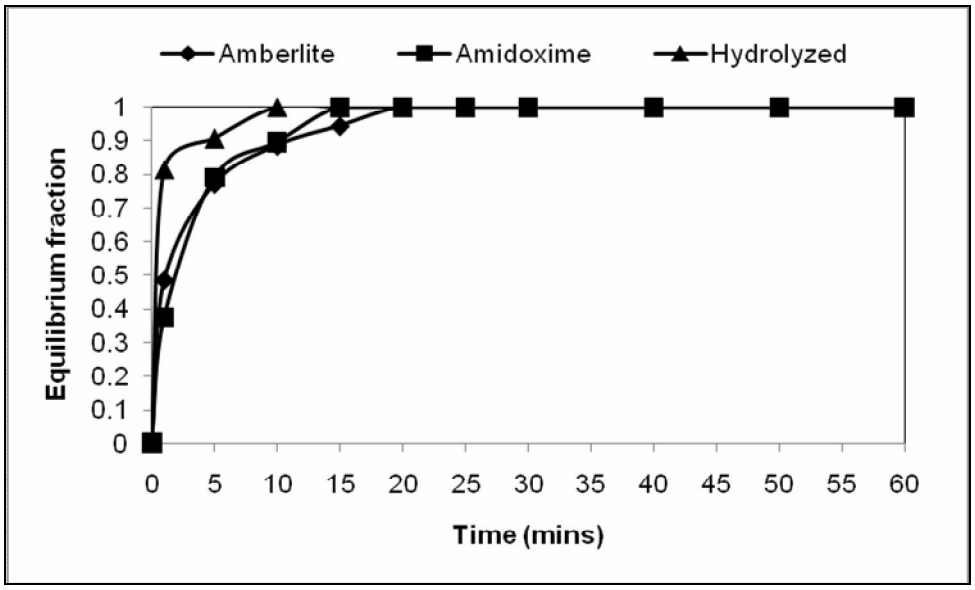

Figure 4-21: The comparison of the kinetics adsorption curves of Na^+ ions adsorbed on Amberlite resin, Amidoxime fibres and Hydrolyzed Amidoxime fibres.

For the adsorption kinetics of Mg^{2+} on hydrolyzed Amidoxime fibres, Amidoxime fibres and Amberlite resin, Figure 4.22, shows that the hydrolyzed Amidoxime fibres have greater kinetics in the adsorption of Mg^{2+} ions than Amidoxime fibres and Amberlite resin. Adsorption kinetics follows a similar trend described for the adsorption of Na^+ ions by hydrolyzed Amidoxime fibres, Amidoxime fibres and Amberlite resin. The same trend is observed for the adsorption kinetics of Ca^{2+} ions by hydrolyzed Amidoxime fibres, Amidoxime fibres and Amberlite resin as shown in Figure 4.23. After 10 minutes, 90 % adsorption of Ca^{2+} and Mg^{2+} and 100% adsorption of Na^+ were achieved by hydrolyzed Amidoxime fibres. For the Amidoxime fibres 80 % adsorption of Ca^{2+} and Mg^{2+} and 90% adsorption of Na^+ respectively, were achieved after 10 minutes. For Amberlite resins, 80 % adsorption of Ca^{2+} and Mg^{2+} and 90% adsorption of Na^+ were achieved after 10 minutes. This shows that the hydrolyzed Amidoxime fibres have faster adsorption kinetics followed by Amidoxime fibres and lastly Amberlite resins.

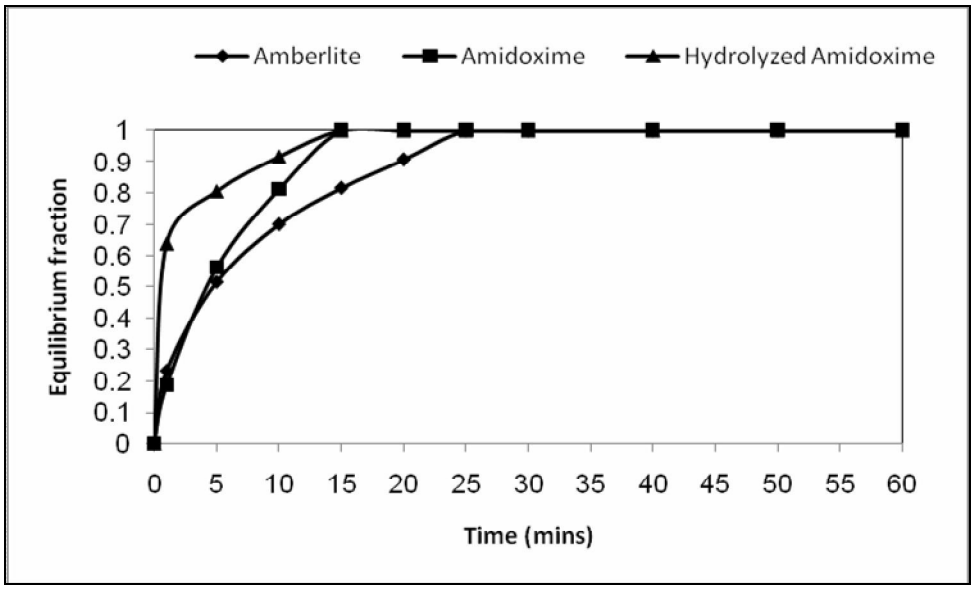

Figure 4-22: The comparison of the kinetics adsorption curves of Mg^{2+} ions adsorbed on Amberlite resin, Amidoxime fibres and Hydrolyzed Amidoxime fibres.

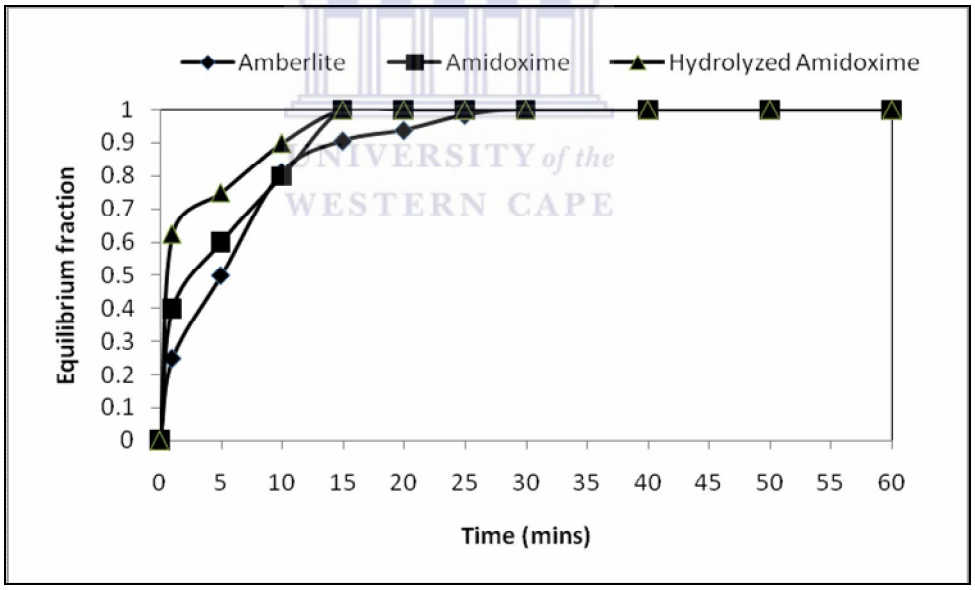

Figure 4-23: The comparison of the kinetics adsorption curves of Ca^{2+} ions adsorbed on Amberlite resin, Amidoxime fibres and Hydrolyzed Amidoxime fibres.

The data for Ca^{2+}, Mg^{2+} and Na^{+} adsorption obtained from the solutions containing each of these metal ions respectively, in various contact time with Amberlite 252 RFH, Amidoxime and hydrolyzed Amidoxime fibres were calculated to determine the order of reaction rate. The kinetics of the adsorption data was

analyzed using different kinetic models such as pseudo-first-order and pseudo-second-order models.

4.2.5.1 Pseudo-first order kinetic model

Well known kinetic expressions, namely pseudo-first and second order were used to fit the adsorption kinetics experimental data (Jha *et al*., 2008). The Lagergren rate equation is the most widely used sorption rate equation for the sorption of solutes from a liquid solution. It can be represented as follows:

$$\frac{dq}{dt} = k_1 (q_e - q) \qquad (4.5)$$

$$\log(q_e - q) = \log(q_e) - \left(\frac{k}{2.303}\right) t \qquad (4.6)$$

where q_e is the amount of metal ion adsorbed at equilibrium (mg/g), q_t amount of metal ion adsorbed at time t (mg/g), k_1 the rate constant of pseudo-first order sorption (1/min). The value of k_1 can be obtained from the slope of the linear plot of log (q_e - q_t) vs. t.

The results of the pseudo first order kinetics are shown in Figure 4.24; 4.25 and 4.26. The plot of log ($q_e - q_t$) versus "time" at different adsorbate concentrations for the adsorption of Ca^{2+}, Mg^{2+}, and Na^{+} onto Amberlite 252 RFH resin and hydrolyzed Amidoxime fibres deviated slightly from the data after a short period. The calculated slopes and intercepts from the plots were used to determine the rate constant k_1 and equilibrium capacity (q_e). These values, k_1, q_e and regression co-efficient are provided in Table 4.14.

Table 4-14: Rate constants for First and Second order for adsorption on Amberlite 252RFH, hydrolyzed Amidoxime and Amidoxime fibres

Adsorbent	Solution Conc. 100 mg/L	First Order Rate Expression		Second Order Rate Expression	
		k_1 (min^{-1})	R^2	k_2 (g/mg min)	R^2
Amberlite 252 RFH	Ca^{2+}	0.084981	0.7467	0.009649	0.9961
Hydrolyzed Amidoxime		0.120447	0.9494	0.026689	0.9983
Amidoxime		0.191610	0.9942	0.096752	0.9993
Amberlite 252 RFH	Mg^{2+}	0.108702	0.9959	0.0006639	0.9963
Hydrolyzed Amidoxime		0.165586	0.9991	0.228125	0.9993
Amidoxime		0.162822	0.9944	0.048027	0.9996
Amberlite 252 RFH	Na^{+}	0.160519	0.9959	0.038704	0.9996
Hydrolyzed Amidoxime		0.231452	0.9828	0.935426	0.9999
Amidoxime		0.213718	0.9469	0.130671	0.9981

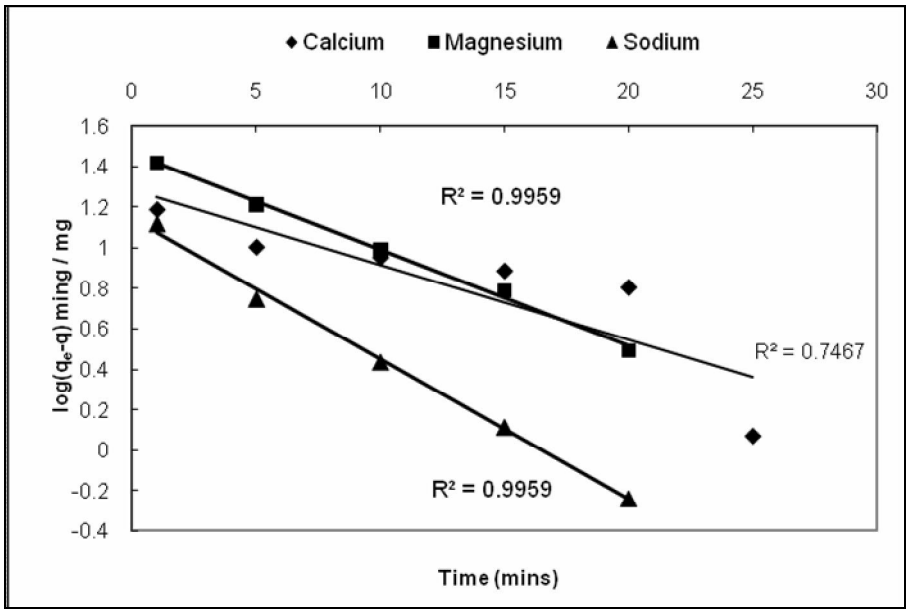

Figure 4-24: Pseudo-first-order kinetics for Ca^{2+}, Mg^{2+}, and Na^{+} onto Amberlite 252 RFH resin (conditions: resin dosage = 2 g/L; concentration: 100 mg/L).

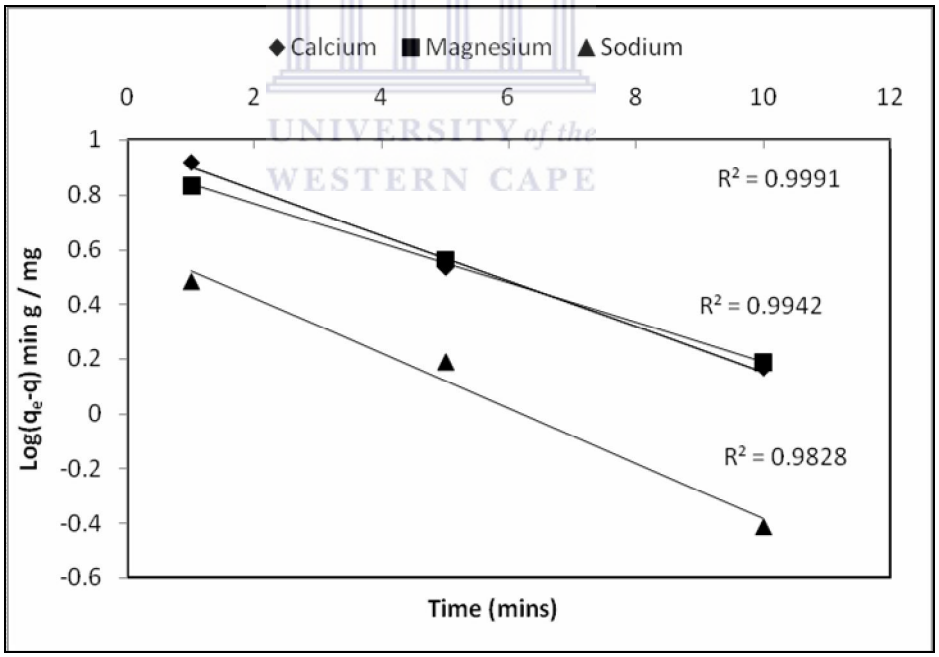

Figure 4-25: Pseudo-first-order kinetics for Ca^{2+}, Mg^{2+}, and Na^{+} onto Amidoxime fibres (conditions: fibre dosage = 2 g/L; concentration: 100 mg/L).

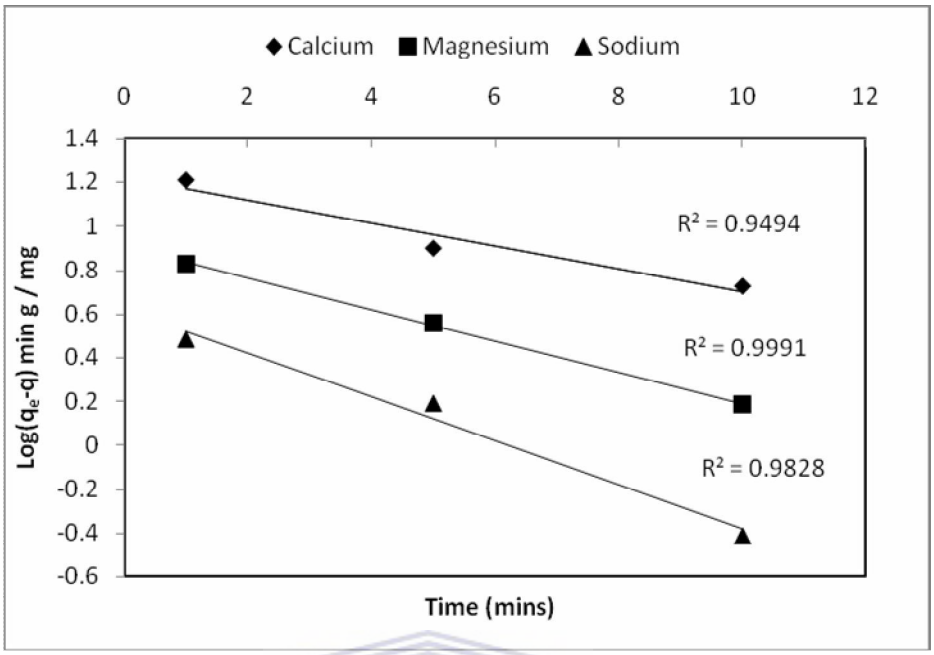

Figure 4-26: Pseudo-first-order kinetics for Ca^{2+}, Mg^{2+}, and Na^{+} onto hydrolyzed Amidoxime fibres (conditions: fibre mass = 2 g/L; concentration: 100 mg/L).

It was observed from (see appendix C) that the Lagergren model fits well for the first 15 min and 30 min for fibre and resin, respectively, thereafter the data deviates from the theory in both the case of the resin and that of the fibres. Thus, the model represents the initial stages where rapid adsorption occurs well but cannot be applied for the entire adsorption process. The rate of sorption was assumed to be proportional to the difference between the maximum capacity, q_c, at equilibrium and the capacity at any time, t, of the sorbed metal ions in a first order at the initial reaction stage. A similar trend was previously observed by Ho and McKay (1998) for dyes on peat particles. Ho and McKay (1998) reported that the sorption data were represented well by the Lagergren first order kinetic model only for the rapid initial phase that occurs for a contact time of 0–30min. This confirms that it is not appropriate to use the Lagergren kinetic model to predict the adsorption kinetics for Ca^{2+}, Mg^{2+} and Na^{+} in the ion exchange process for the entire sorption period, which shows that the model can be applied to a certain extent but is not appropriate to describe the entire process. The first order equation did not apply throughout all the contact times in this work. It was applicable over the initial 1–15 min sorption period

for fibres and 1-30 min sorption period for the resin (see Appendix C for graphical representation).

4.2.5.2 Pseudo Second order kinetics model

The pseudo-second order reaction is greatly influenced by the amount of metal on the adsorbent's surface and the amount of metal adsorbed at equilibrium (Ho and Mckay, 1999). The rate is directly proportional to the number of active surface sites. The pseudo-second order reaction rate expression can be written as shown below taken from equation (4.7)

$$\frac{t}{q_e} = \left(\frac{1}{k_2\, q_e^2}\right) + \left(\frac{1}{q_e}\right) t \qquad (4.7)$$

The product $k_2 q_e^2$ is the initial sorption rate 'h' (Eq. (4.8)):

$$rate = k_2\, q_e^2 \qquad (4.8)$$

where k_2 (g/mg h) is the pseudo-second order rate constant, q_e the amount adsorbed at equilibrium and q_t is the amount of metal adsorbed at time 't'. Plotting t/q against "t" at different adsorbate concentrations (Figures 4.27 and 4.28) provided second order sorption rate constant (k_2) and q_e values from the slopes and intercepts (see Table 4.14).

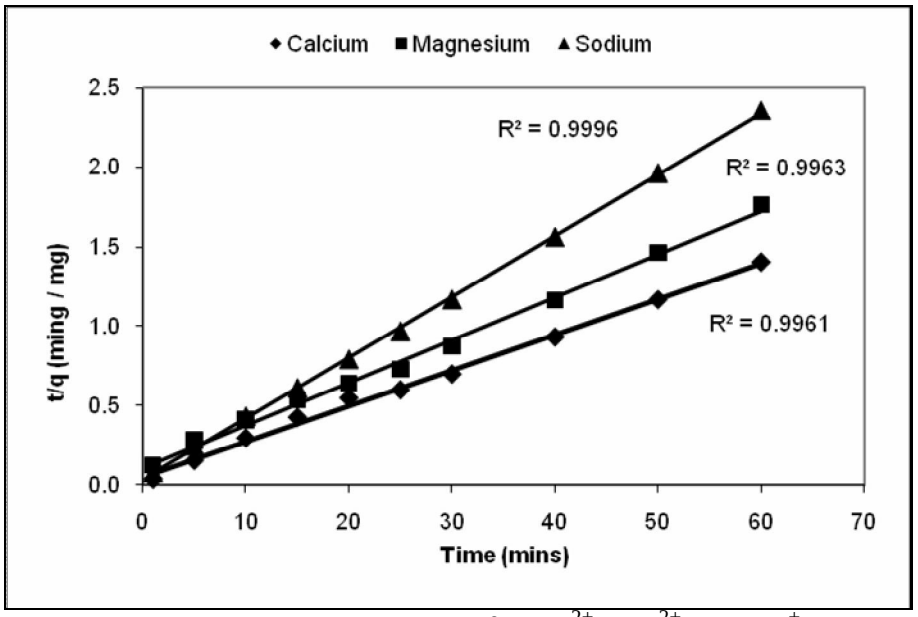

Figure 4-27: Pseudo-second-order kinetics for Ca^{2+}, Mg^{2+} and Na^{+} onto Amberlite 252 RFH resin (conditions: resin mass = 2 g/L; concentration: 100 mg/L).

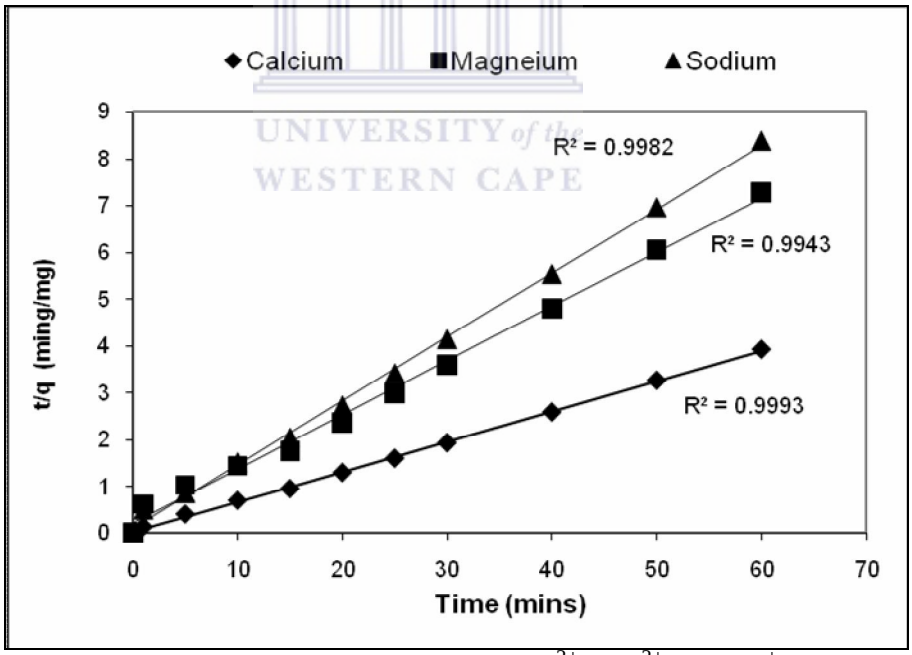

Figure 4-28: Pseudo-second-order kinetics for Ca^{2+}, Mg^{2+} and Na^{+} onto Amidoxime fibres (conditions: resin mass = 2 g/L; concentration: 100 mg/L).

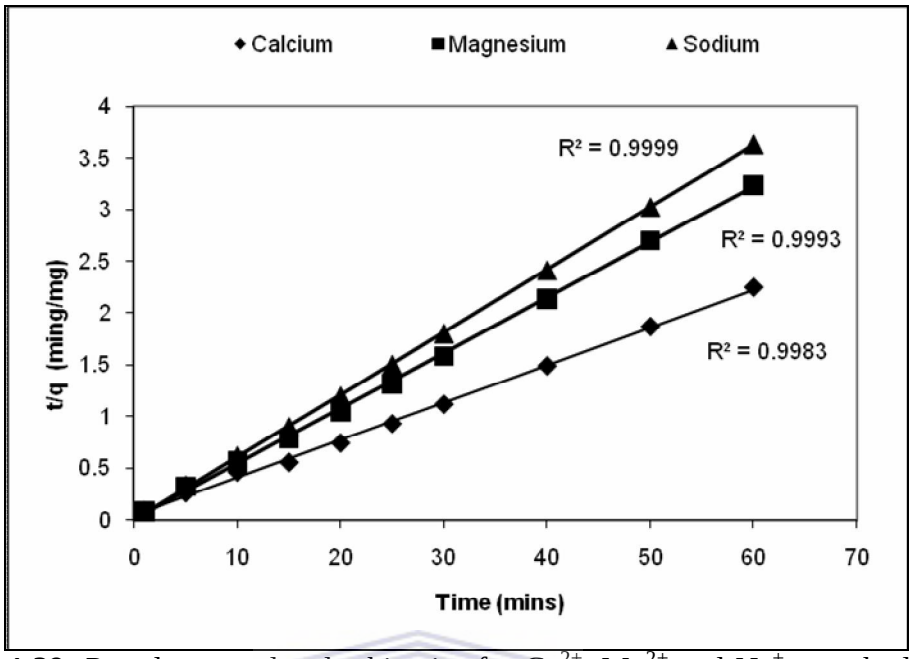

Figure 4-29: Pseudo-second-order kinetics for Ca^{2+}, Mg^{2+} and Na^{+} onto hydrolyzed Amidoxime fibres (conditions: resin mass = 2 g/L; concentration: 100 mg/L).

The graphs, Figures 4.27; 4.28 and 4.29, show plots of the linearized form of the pseudo-second order model (Equation 4.7) for Ca^{2+}, Mg^{2+} and Na^{+} ions onto hydrolyzed Amidoxime fibres, Amidoxime fibres and Amberlite resin. The correlation coefficients for the linear plots of t/q against time from the pseudo-second order rate law are greater than 0.9940 for metal ions. Therefore, the best fit model for all these sorption systems is possibly be the pseudo-second order sorption rate expression.

From Table 4.14, where the rate constants for pseudo first and second order kinetics are given, it showed that the regression coefficient of pseudo-second order was superior to that of the pseudo-first order reaction. This suggests that this sorption system is not a first order reaction and that the pseudo-second order model fits best, based on the assumption that the rate-limiting step may be chemical sorption or chemisorption involving valency forces through sharing or exchange of electrons between sorbent and sorbate and provides the best correlation of the data. The calculated q_e values agree very well with the experimental values, and a regression

coefficient shows that the model can be applied for the entire adsorption process and confirms the chemisorption of Ca^{2+}, Mg^{2+}, and Na^{+} onto ion exchange fibres and resins. Graphs showing the modeling of the first and second order against the experiments kinetics results are presented in the Appendix C (kinetics adsorption).

The maximum adsorption capacities are 1.35, 1.57 and 0.73 mg per g of hydrolyzed amidoxime fibre for Ca^{2+}, Mg^{2+}, and Na^{+}, respectively. The order of affinity based on a weight uptake by Adsorbents is as follows: $Mg^{2+} > Ca^{2+} > Na^{+}$. The maximum adsorption capacities in molar basis are 1.57 mmol Mg^{2+}/g hydrolyzed amidoxime fibre, 1.35 mmol Ca^{2+}/g hydrolyzed amidoxime fibre and 0.73 mmol Na^{+}/g alkali-treated amidoxime fibre. Therefore, there is a difference on the order of affinity on a molar basis due to the molecular sizes of the metal ions, where the Ca^{2+} ion is double the size of the Mg^{2+} ion. The difference in adsorption behaviour of Ca^{2+}, Mg^{2+}, and Na^{+} can be explained by the different affinity of metal ions for the donor atoms (i.e. oxygen and nitrogen) in the amidoxime structure and a difference in the sizes of the metal ions is most probably also the case for the non complexing groups on the amidoxime sample resulting in a relatively high adsorption of Mg^{2+}ions under non-competitive adsorption conditions.

4.2.6 Competitive Adsorption

In this group of experiments, competitive adsorption of Ca^{2+}, Mg^{2+}, Na^{+} and Cu^{2+} ions from their binary, ternary and quaternary solutions were investigated by following a similar procedure as described in section 3.6.1. The initial metal ion concentrations were chosen as 200 mg/L for each metal ion; 0.1 g of adsorbent (dry mass) was added to 50 ml of the binary, ternary and quaternary solutions, respectively. Solutions containing Cu^{2+} ions were performed at an optimum pH of 6.0 while the remaining solutions were carried out at their natural pH.

From Table 4.15, the observed affinity order in adsorption was found to be the same under competitive and non-competitive conditions: $Mg^{2+} > Ca^{2+} > Na^{+}$. In this case

the same order of maximum adsorption has been confirmed as follows: hydrolyzed amidoxime fibres > amidoxime fibres > PAN, which is seen from table 4.13 and 4.14. When Cu^{2+} ions were added to the competitive adsorption, they showed greater adsorption than Mg^{2+}, Ca^{2+} and Na^{+} ions. This is probably due to difference in coordination behaviour for the complexing Cu^{2+} ions on the amidoxime sample resulting in a relatively high adsorption of Cu^{2+} ions under competitive adsorption conditions at pH 6.0. In this case, the amidoxime fibres showed more affinity for Cu^{2+} ions (Figure 4.30). The adsorbents, hydrolyzed Amidoxime fibres, Amidoxime fibres showed greater selectivity for Cu^{2+} ions followed by Ca^{2+}, $Mg^{2+}$and lastly Na^{+} ions. From the pH studies (section 4.2.3), we have been able to see that the adsorption of Cu^{2+} ions is made possible by complexing, which occurs at a pH 6.0 hence the amidoxime fibres have a greater selectivity for the Cu^{2+} ions because of they possess chelating properties.

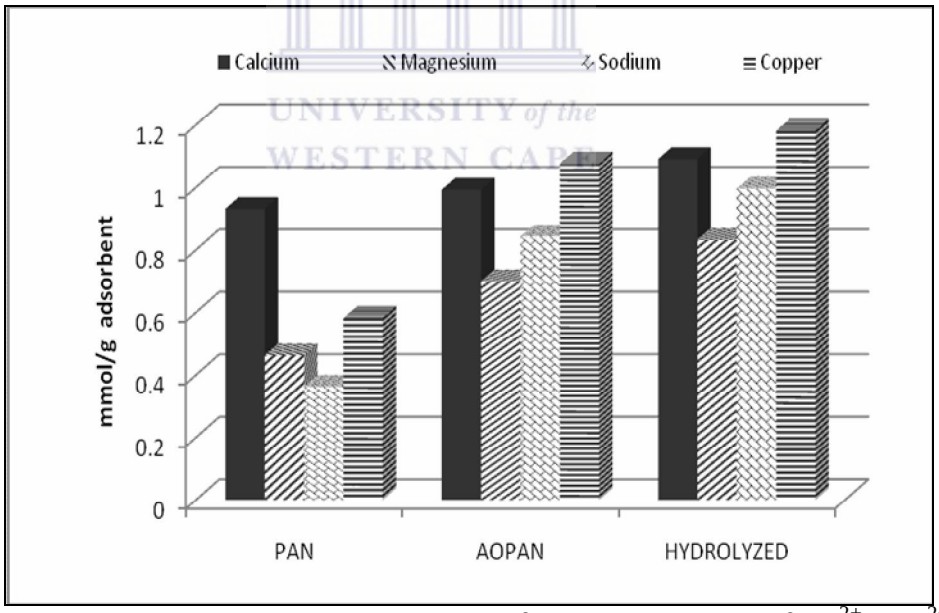

Figure 4-30: Competitive adsorption results for the adsorption of Ca^{2+}, Mg^{2+}, Na^{+} and Cu^{2+} ions on the PAN, Amidoxime fibres and hydrolyzed Amidoxime fibres (0.1 g adsorbent; 200 mg/L of each metal ion; shaken for 24 hrs).

Table 4-15: Competitive adsorption of Ca^{2+}, Mg^{2+}, Na^{+} and Cu^{2+} ions on the PAN, Amidoxime fibres and hydrolyzed

Adsorbent	Solution Concentration 200mg/L	Binary		Ternary		Quaternary	
		mg/g	mmol/g	mg/g	mmol/g	mg/g	mmol/g
PAN	Ca^{2+}	60.0658	1.4986	36.1134	1.8021	37.3530	1.8639
Amidoxime		62.1580	1.5511	42.4723	2.1194	39.7801	1.9850
Hydrolyzed Amidoxime		65.1004	1.6243	44.2606	2.2086	43.7411	2.1827
PAN	Mg^{2+}	41.7810	1.7190	20.5840	1.69.42	11.2495	0.9259
Amidoxime		47.9948	1.9747	26.1767	2.1545	17.0243	1.4012
Hydrolyzed Amidoxime		53.8737	2.2166	30.0130	2.4702	20.2362	1.6655
PAN	Na^{+}			13.0759	0.5685	8.3323	0.3623
Amidoxime				19.3533	0.8414	19.3902	0.8431
Hydrolyzed Amidoxime				23.2562	1.0111	22.9225	0.9966
PAN	Cu^{2+}					36.9829	1.1641
Amidoxime						68.4293	2.1539
Hydrolyzed Amidoxime						75.4420	2.3620

The order of maximum adsorption by the hydrolyzed amidoxime fibres, amidoxime fibres and PAN has been maintained even though the background solutions have been changed. In Figures 4.31 and 4.32, the competitive adsorption was carried out in two different concentrations of NaCl solutions, the first was in saturated NaCl solution (due to the fact that these metal ions are being treated are found in saturated NaCl solution-the brine contains high level of concentration of NaCl) and the second was in 200 mg/L NaCl solution (see procedure in section 3.6.7). The results show that the maximum adsorption has been confirmed as follows: hydrolyzed amidoxime fibres > amidoxime fibres > PAN, which is seen from Figure 4.30 and 4.31, and all adsorbents showed greater adsorption in the following order: $Mg^{2+} > Ca^{2+} > Na^{+}$ ions.

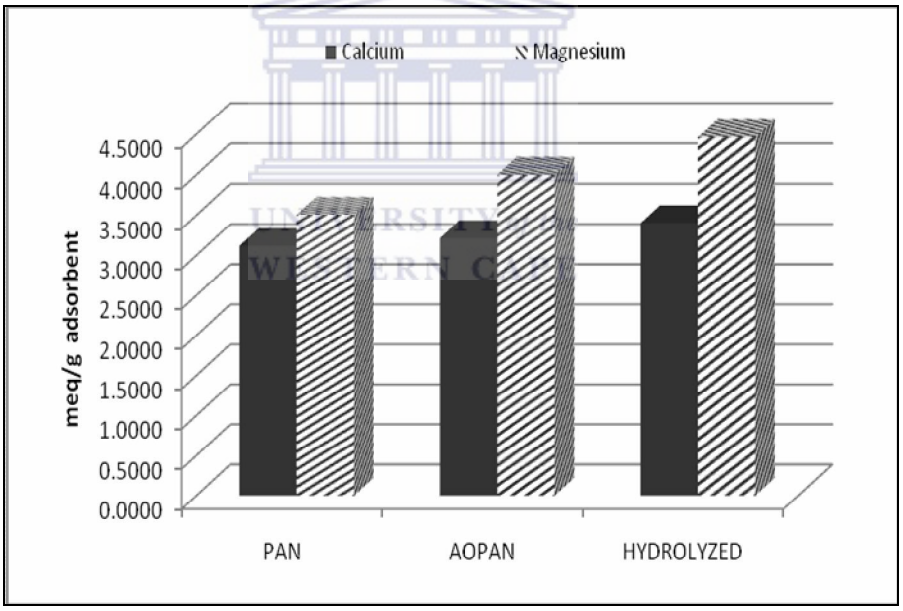

Figure 4-31: Competitive adsorption results for the adsorption of Ca^{2+}, Mg^{2+} ions on the PAN, Amidoxime fibres and hydrolyzed Amidoxime fibres in saturated NaCl solution (0.1 g adsorbent; 200 mg/L of each metal ion; shaken for 24 hrs).

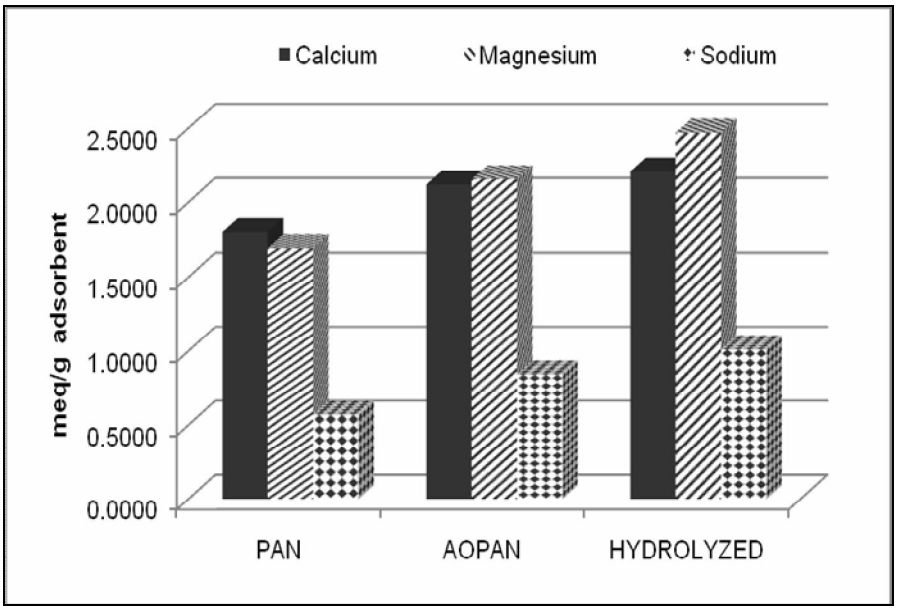

Figure 4-32: Competitive adsorption results for the adsorption of Ca^{2+}, $Mg^{2+}$and Na^{+} ions on the PAN, Amidoxime fibres and hydrolyzed Amidoxime fibres in 200 mg/L NaCl solution (0.1 g adsorbent; 200 mg/L of each metal ion; shaken for 24 hrs).

CHAPTER 5

5 Conclusion

5.1 General Conclusions

This study has been able to prove that amidoxime fibres can compete with the Amberlite resin in the treatment and removal of major ions (Ca^{2+}, Mg^{2+} and Na^{+} ions) from brine wastewaters by taking advantage of their greater kinetics and greater selectivity towards these ions. Adsorption capacities of 1.35 meq/g for Ca^{2+}, 1.57 meq/g for Mg^{2+} and 0.70 meq/g for Na^{+} by hydrolyzed Amidoxime fibres and 0.77 meq/g for Ca^{2+}, 0.70 meq/g for Mg^{2+} and 0.32 meq/g for Na^{+} by Amidoxime fibres and finally 2.14 meq/g for Ca^{2+}, 2.11 meq/g for Mg^{2+} and 1.12 meq/g for Na^{+} by Amberlite 252 RFH resins were achieved for contact time experiments.

The surface of PAN fibres were modified through a 2 hrs functionalization process involving 3 % hydroxylamine in methanol solution. The amidoxime fibres possessed $–C(NH_2)=NOH$ on the surface and had an 8 % improvement on the capacity adsorption. After functionalization, the amidoxime fibre were hydrolyzed in 1 mol/L NaOH solution for 24 hrs at 30 °C in order to enhance the adsorption capacity of the amidoxime fibres. Functionalization enhanced the sorption of amidoxime fibres by an increase of 20 % in the cationic exchange capacity. This was achieved by the part conversion of the cyano groups into the carboxylic acid groups.

The sorption of Cu^{2+} ions on amidoxime chelating sorbent is dependent on the pH of the sample solution due to competitive reaction between amidoxime chelating group and protons in the solutions and it achieved a maximum adsorption of 35.73 mg/g (1.13 meq/g) at pH 6.0. The adsorption capacity of Cu^{2+} ions was further enhanced by alkali treatment/hydrolysis of the amidoxime fibres and a maximum adsorption

capacity of 39.74 mg/g (1.25 meq/g) was then achieved. The amidoxime group acts as a bidentate ligand, coordinating to metallic ions through the nitrogen atoms of the amino groups and the oxygen atoms of the oxime groups. Therefore the sorption of Cu^{2+} ions by amidoxime fibres is favoured by increasing pH.

Two adsorption equilibrium isotherm models (Langmuir and Freundlich) were used and their parameters were estimated by fitting model equations to data from the batch experiments. The mechanism for the adsorption of Ca^{2+}, Mg^{2+} and Na^{+} was found to follow Langmuir isotherm. The adsorbents (hydrolyzed amidoxime, amidoxime fibre and amberlite resin) showed a better fit for the Langmuir model than the Freundlich model hence the adsorption capacities for Ca^{2+}, Mg^{2+} and Na^{+} ions were indicating that the adsorption took place at a specific homogeneous sites within the adsorbents and once the metal ion occupied the site, then no further adsorption occurred at that location (monolayer adsorption).

The hydrolyzed amidoxime fibres and amidoxime fibres had faster kinetics than the resin showing that the adsorption equilibrium could be reached within 10-15 mins. The Amberlite resin showed that the resin adsorption equilibrium could be within 20-30 minutes exhibiting slower kinetics as compared to the fibres. The kinetics of adsorption of the Hydrolyzed amidoxime fibres, amidoxime fibres and amberlite resins were analyzed on the basis of the pseudo-second order mechanism. For all of the systems studied, chemical reaction seems significant in the rate-controlling step and the pseudo-second order chemical reaction kinetics provide the best correlation of the experimental data, whereas the pseudo-first order model proposed fits the experimental data well for an initial period of the first reaction step only. However, over a long period the pseudo-second order model provides the best correlation for all of the systems studied.

The competitive adsorption capacities for each metal ion are as follows: 2.36 meq/g for Cu^{2+}, 2.18 meq/g for Ca^{2+}, 1.66 meq/g for Mg^{2+} and 0.99 meq/g for Na^{+}. It is clear

that the selectivity of the hydrolyzed amidoxime fibres for Cu^{2+} ions were higher than from other ions. Hydrolyzed amidoxime fibres exhibit the following metal ion selectivity sequence under competitive adsorption conditions: Cu^{2+}> Ca^{2+}> Mg^{2+}> Na^{+}. This shows that the amidoxime fibres are found to be excellent adsorbent with high adsorption capacity and selectivity for Cu^{2+} ions.

The hydrolyzed amidoxime fibres exhibit greater adsorption capacity due to the alkali-treatment/ hydrolysis of the fibres; adsorption is affected by pH, particularly for heavy metals, has faster kinetics than Amberlite resins and has greater selectivity for Cu^{2+} ions showing an affinity for heavy metal adsorption.

The removal of metal ions from contaminated environmental aquatic systems is only the first step in any remediation process. As pointed out earlier, one possible advantage of using amidoxime fibres as the ion exchange medium in the remediation process is that the fibres contain an amidoxime group which is a bidentate ligand hence it coordinates to metallic ions, exhibiting greater selectivity for heavy metals and has greater kinetics thus improved equilibration times.

5.2 Recommendation

Apply the amidoxime fibres in the treatment of minor/trace elements. In this study, greater adsorption efficiency was achieved by alkali-treatment/hydrolysis of the fibre and greater selectivity was exhibited by the amidoxime fibres for divalent metal ions particularly heavy metals.

It would be valuable to carryout competitive kinetics adsorption in order to describe kinetics adsorption equilibrium in multi-component systems.

In future, these fibres should be used to treat real brine solutions with the view of analyzing their performance on adsorption of minor elements.

A systematic study of distribution coefficients using Amberlite 252 RFH resin and Amidoxime fibres should pursued. Distribution coefficients form the fundamental base from which ion exchange separations can be planned.

Column studies should also be pursued. Most industrial applications of adsorption processes are usually implemented in the continuous column operation with the capacity of treatment and the recovery factors in mind. These parameters are normally determined the type of adsorbent, the equilibration time (kinetics), the size of the column and the break through curves (capacity of the column).

6 References

ABUFAYED, A.A. and EL-GHUEL, M.K.A., 2001. Desalination process applications in Libya. *Desalination,* **138**(1-3), 47-53.

ADERHOLD, D., WILLIAMS, C.J., EDYVEAN, R.G.J., 1996. The removal of heavy-metal ions by seaweeds and their derivatives. *Bioresource Technology,* **58**(1), 1-6.

AHMED, M., ARAKEL, A., HOEY, D. and COLEMAN, M., 2001. Integrated power, water and salt generation: a discussion paper. *Desalination,* **134**(1-3), 37-45.

AJMAL, M., RAO, R.A.K., AHMAD, R. and AHMAD, J., 2000. Adsorption studies on Citrus reticulata (fruit peel of orange): removal and recovery of Ni(II) from electroplating wastewater. *Journal of hazardous materials,* **79**(1-2), 117-131.

ALAABDULA'ALY, A. I. AND AL-SAATI, 1995. *International Desalination Association Conference*, 1995, pp21.

ANNANDALE, J. G., JOVANOVIC, N. Z., TANNER, P. D., BENADÉ, N., DU PLESSIS, H. M., 2002. The sustainability of irrigation with gypsiferous mine water and implications for the mining industry in south Africa, *Mine Water and the Environment,* **21**, 81-90.

ANON, 1986. Management of the water resources of southern Africa. Pretoria: .

ARNAL, J.M., SANCHO, M., IBORRA, I., GOZÁLVEZ, J.M., SANTAFÉ, A. and LORA, J., 2005. Concentration of brines from RO desalination plants by natural evaporation. *Desalination,* **182**(1-3), 435-439.

AWERBUCH, L. and WEEKES, M.C., 1990. Disposal of concentrates from brackish water desalting plants by means of evaporation technology. *Desalination,* **78**(1), 71-76.

AZANOVA, V.V. and HRADIL, J., 1999. Sorption properties of macroporous and hypercrosslinked copolymers. *Reactive and Functional Polymers,* **41**(1-3), 163-175.

BABEL, S. and KURNIAWAN, T.A., 2004. Cr(VI) removal from synthetic wastewater using coconut shell charcoal and commercial activated carbon modified with oxidizing agents and/or chitosan. *Chemosphere,* **54**(7), 951-967.

BASTA, K., ALIANE, A., LOUNIS, A., SANDEAUX, R., SANDEAUX, J. and GAVACH, C., 1998. Electro-extraction of Pb^{2+} ions from diluted solutions by a process combining ion-exchange textiles and membranes. *Desalination,* **120**(3), 175-184.

BEAUVAIS, R.A. and ALEXANDRATOS, S.D., 1998. Polymer-supported reagents for the selective complexation of metal ions: an overview. *Reactive and Functional Polymers,* **36**(2), 113-123.

BELL, F.G., BULLOCK, S.E.T., HÄLBICH, T.F.J. and LINDSAY, P., 2001. Environmental impacts associated with an abandoned mine in the Witbank Coalfield, South Africa. *International Journal of Coal Geology,* **45**(2-3), 195-216.

BERNABÉ L. RIVAS, HERNÁN A. MATURANA, SANDRA VILLEGAS, 2000. Adsorption behavior of metal ions by amidoxime chelating resin. *Journal of Applied Polymer Science,* **77**(9), 1994-1999.

BOLTO, B. A. AND PAWLOWSKI, L., ed, 1987. *Wastewater Treatment by Ion exchange.* London: McGraw-Hill.

BURHRMANN, F., VAN DER WALT, M., HANEKAN, D., FINLAYSON, F., 1999. Treatment of Industrial wastewater for reuse. *Desalination,* **124**, 263-269.

CALMON, C., 1984. Recent developments in water treatment by ion exchange. *Reactive polymers.Ion exchangers, sorbents,* **4**(2), 131-146.

CALMON, C., 1981. Specific and chelate exchangers: new functional polymers for water and wastewaster treatment. *Journal / American Water Works Association,* **73**(12), 652-656.

CANTER, L. W., KNOX, R. C. AND FAIRCHILD D. M., 1987. Ground Water Quality Protection. Lewis Publishers, INC, CRC Press: .

CHANDA, M. & ROY, S. K., ed, 2006. *Plastics Technology Handbook.* 4th ed edn. United States: Taylor & Francis.

CHANG, X., YANG, X., WEI, X. and WU, K., 2001. Efficiency and mechanism of new poly(acryl-phenylamidrazone phenylhydrazide) chelating fiber for adsorbing trace Ga, In, Bi, V and Ti from solution. *Analytica Chimica Acta,* **450**(1-2), 231-238.

CHAPMAN-WILBERT, M., 1993. *The Desalting and Water Treatment Membrane Manual: A Guide to Membranes for Municipal Water Treatment, Water Treatment Technology Program, Report No. 1,* R-93-15. Denver, United States of America: United States Department of the Interior, Bureau of Reclamation, Research and Laboratory Services Division, Applied Sciences Branch.

COLELLA, M.B. and SIGGLA, S., 1980. Poly(acrylamidoxime) Resin for Determination of Trace Metals in Natural Waters. *Analytical Chemistry,* **52**(14), 2347-2350.

CRINI, G., 2005. Recent developments in polysaccharide-based materials used as adsorbents in wastewater treatment. *Progress in Polymer Science,* **30**(1), 38-70.

DAVIES, B.R., O'KEEFFE, J. H., AND SNADDON, C. D., 1993. *A Synthesis of the Ecological Functioning, Conservation and Management of South African River Ecosystem.*

DEL PINO, M.P. and DURHAM, B., 1999. Wastewater re-use through dual-membrane processes: opportunities for sustainable water resources. *Desalination,* **124**(1-3), 271-277.

DENG, S., BAI, R. and CHEN, J.P., 2003. Behaviors and mechanisms of copper adsorption on hydrolyzed polyacrylonitrile fibers. *Journal of colloid and interface science,* **260**(2), 265-272.

DENIZLI, A., BÜYÜKTUNCEL, E., SAID, Z., GENÇ, Ö. and PISKIN, E., 1998. New dye-ligand: Procion red MX-3B carrying poly(EGDMA-HEMA) microbeads for removal of copper ions. *Journal of Macromolecular Science - Pure and Applied Chemistry,* **35**(6), 919-932.

DESILVA, J., Essentials of Ion Exchange, Presented at 25th W.Q.A. Annual Conference, 1999 .

DOINA BILBA, D., MOROI, G. AND BILBA, N., 2006. Copper (ii) and mercury (ii) retention properties of a polyacrylamidoxime chelating fiber. *Environmental Engineering and Management Journal,* **5**(3), 297-305.

DOUGLAS M. RUTHVEN, 1984. Principles of Adsorption and Adsorption Processes. 2nd edn. New York: Wiley-Interscience.

DROSTE, L.R., 1997. Theory and Practice of Water and Wastewater Treatment. New York,: John Wiley & Sons, Inc, pp. 480-484.

ECONOMY, J., DOMINGUEZ, L. and MANGUN, C.L., 2002. Polymeric Ion-Exchange Fibers. *Industrial & Engineering Chemistry Research,* **41**(25), 6436-6442.

EGAWA, H., KABAY, N., SHUTO, T. and JYO, A., 1992. Recovery of uranium from seawater. XII. Preparation and characterization of lightly crosslinked highly porous chelating resins containing amidoxime groups. *Journal of Applied Polymer Science,* **46**(1), 129-142.

EGAWA, H., NONAKA, T., ABE, S. and NAKAYAMA, M., 1992. Recovery of uranium from seawater. X. Pore structure and uranium adsorption of macroreticular chelating resin containing amidoxime groups. *Journal of Applied Polymer Science,* **45**(5), 837-841.

EL-DESSOUKY, H., ALATIQI, I. and ETTOUNEY, H., 1998. Process synthesis: The multi-stage flash desalination system. *Desalination,* **115**(2), 155-179.

ELLIOTT, H.A. and HUANG, C.P., 1981. Adsorption characteristics of some Cu(II) complexes on aluminosilicates. *Water research,* **15**(7), 849-855.

EL-MANHARAWY, S. and HAFEZ, A., 2003. A new chemical classification system of natural waters for desalination and other industrial uses. *Desalination,* **156**(1-3), 163-180.

ESKOM, 2002. *Annual Report towards sustainability,* South Africa: Eskom.

FISHER, SALLIE AND KUNIN, ROBERT, 1955. Routine Exchange Capacity Detrminations of ion Exchange Resins. *Anal.Chem.,* **27**, 1191-1194.

FREUNDLICH H., 1926. Adsorption. *Journal of Physical Chemistry,* **7**, 57-64.

FRIEDRICH HELFFERICH, 1962. Ion Exchange. McGraw-Hill, pp. 5-9; 35-36; 72-94.

GARG, B.S., SHARMA, R.K., BHOJAK, N. and MITTAL, S., 1999. Chelating Resins and Their Applications in the Analysis of Trace Metal Ions. *Microchemical Journal*, **61**(2), 94-114.

GLATER, J. AND COHEN, Y., 2003. Brines disposal from Land based membrane desalination plants: A critical assessment. , 1-5.

GLEICK, P. H., COOLEY, H., KATZ, D., LEE, E., MORRISON, J., 2006. The world's water, 2006-2007: the biennial report on freshwater resources. Island Press.

GODE, F. AND PEHLIVAN, E., 2003. A comparative study of two chelating ion-exchange resins for the removal of chromium(III) from aqueous solution. *J. Hazard. Mater.*, **100**(1-3), 231-243.

GONG, B., LI, X., WANG, F., XU, H. and CHANG, X., 2001. Synthesis of polyacrylacylaminourea chelating fiber and properties of concentration and separation of trace metal ions from samples. *Analytica Chimica Acta*, **427**(2), 287-291.

GREIG, J. A., SOCIETY OF CHEMICAL INDUSTRY (GREAT BRITAIN), SOCIETY OF CHEMICAL INDUSTRY, ed, 2000. *Ion Exchange at the Millennium: Proceeding of IEX 2000.* World Scientific.

GUN'KO, V.M., LEBODA, R., SKUBISZEWSKA-ZIĘBA, J., GAWDZIK, B. and CHARMAS, B., 2005. Structural characteristics of porous polymers treated by freezing with water or acetone. *Applied Surface Science*, **252**(3), 612-618.

GUNTHER, P. AND MEY W., Selection of mine water treatment technologies for the Emalahleni (Witbank) water reclaimation Project. , 6-14.

GUPTA, M.L., GUPTA, B., OPPERMANN, W. and HARDTMANN, G., 2004. Surface modification of polyacrylonitrile staple fibers via alkaline hydrolysis for superabsorbent applications. *Journal of Applied Polymer Science,* **91**(5), 3127-3133.

HÁBOVÁ, V., MELZOCH, K., RYCHTERA, M. and SEKAVOVÁ, B., 2004. Electrodialysis as a useful technique for lactic acid separation from a model solution and a fermentation broth. *Desalination,* **162**, 361-372.

HARLAND, C.E., 1994. Ion Exchange: Theory and Practice. 2nd edn. Cambridge, England: Royal Society of Chemistry.

HIROTSU TAKAHIRO, KATOH SHUNSAKU, SUGASAKA KAZUHIKO, SEN MANABU and ITAGAKI TAKAHARU, 1986. Binding Properties of a Polymer Having Amidoxime Groups with Proton and Metal Ions. *Separation Science and Technology,* **21**(10), 1101-1110.

HIROTSU, T., KATOH, S., SUGASAKA, K., TAKAI, N., SENO, M. and ITAGAKI, T., 1988. Effect of water content of hydrophilic amidoxime polymer on adsorption rate of uranium from seawater. *Journal of Applied Polymer Science,* **36**(8), 1741-1752.

HO, Y.S., HUANG, C.T. and HUANG, H.W., 2002. Equilibrium sorption isotherm for metal ions on tree fern. *Process Biochemistry,* **37**(12), 1421-1430.

HO, Y.S. and MCKAY, G., 1999. Pseudo-second order model for sorption processes. *Process Biochemistry,* **34**(5), 451-465.

HO, Y.S. and MCKAY, G., 1998. Sorption of dye from aqueous solution by peat. *Chemical Engineering Journal,* **70**(2), 115-124.

IRVING LANGMUIR, 1918. The adsorption of gases on plane surfaces of glass mica and platinum. *Journal of the American Chemical Society,* **40**(9), 1361–1403.

ISCHTCHENKO, V. V., HUDDEERSMAN, K. D., VITKOVSKAYA, R. F., 2003. Part 1. Production of a modified PAN fibrous catalyst and its optimization towards the decomposition of hydrogen peroxide. *Appl. Catal. A-gen,* **242**, 123-137.

JHAMANIS KUMAR, K., 2005. Removal of zinc from aqueous solutions by ion exchange process – A review. *Journal of Metallurgy and Materials Science,* **47**(3), 119-128.

JHA, M.K., UPADHYAY, R.R., LEE, J. and KUMAR, V., 2008. Treatment of rayon waste effluent for the removal of Zn and Ca using Indion BSR resin. *Desalination,* **228**(1-3), 97-107.

KABAY, N. and EGAWA, H., 1993. Kinetic behavior of lightly crosslinked chelating resins containing amidoxime groups for batchwise adsorption of UO_2^{2+}. *Separation Science and Technology,* **28**(11-12), 1985-1993.

KABAY, N., KATAKAI, A., SUGO, T. and EGAWA, H., 1993. Preparation of fibrous adsorbents containing amidoxime groups by radiation-induced grafting and application to uranium recovery from sea water. *Journal of Applied Polymer Science,* **49**(4), 599-607.

KANTIPULY, C., KATRAGADDA, S., CHOW, A. and GESSER, H.D., 1990. Chelating polymers and related supports for separation and preconcentration of trace metals. *Talanta,* **37**(5), 491-517.

KHAWAJI, A.D., KUTUBKHANAH, I.K. and WIE, J., 2008. Advances in seawater desalination technologies. *Desalination,* **221**(1-3), 47-69.

KHEDR, M.G., 2008. Membrane methods in tailoring simpler, more efficient, and cost effective wastewater treatment alternatives. *Desalination,* **222**(1-3), 135-145.

KHYM, J.X., 1974. Analytical ion-exchange procedures in chemistry and biology: theory, equipment, techniques . Englewood Cliff: Prentice-Hall.

KOBUKE, Y., TANAKA, H. and OGOSHI, H., 1990. Imidedioxime as a significant component in so-called amidoxime resin for uranyl adsorption from seawater. *Polymer Journal,* **22**(2), 179-182.

KONGSRICHAROERN, N., POLPRASERT, C., 1996. Chromium removal by a bipolar electro-chemical precipitation process. *Water Science and Technology,* **34**(9), 109-116.

KONGSRICHAROERN, N., POLPRASERT, C., 1995. Electrochemical precipitation of chromium Cr(VI) from an electroplating wastewater. *Water Science and Technology,* **31**(9), 109-117.

KRISHNAN, K.A. and ANIRUDHAN, T.S., 2003. Removal of cadmium(II) from aqueous solutions by steam-activated sulphurised carbon prepared from sugar-cane bagasse pith: Kinetics and equilibrium studies. *Water SA,* **29**(2), 147-156.

KUNIN, R., 1960. Elements of Ion Exchange. New York: Reinhold Publishing Corporation.

KUNIN, R., 1976. The Use of macroreticular polymeric adsorbents for the treatment of waste effluents. *Pure & App!. Chem.,* **46**, 205-211.

KURNIAWAN, T.A., CHAN, G.Y.S., LO, W. and BABEL, S., 2006. Physico–chemical treatment techniques for wastewater laden with heavy metals. *Chemical Engineering Journal,* **118**(1-2), 83-98.

LEINONEN, H. and LEHTO, J., 2000. Ion-exchange of nickel by iminodiacetic acid chelating resin Chelex 100. *Reactive and Functional Polymers,* **43**(1-2), 1-6.

LIAN, N., CHANG, X., ZHENG, H., WANG, S., DONG, Y. and LAI, S., 2005. Synthesis and efficiency of a chelating fiber for preconcentration and separation of trace Au(III) and Pd(IV) from solution samples. *Annali di Chimica,* **95**(9-10), 677-683.

LIESER, K.H., 1979. New Ion Exchangers, Preparation, Properties and Application. *Pure Appl. Chem,* **51**, 1503.

LIN, L., LI, J. and JUANG, R., 2008. Removal of Cu(II) and Ni(II) from aqueous solutions using batch and fixed-bed ion exchange processes. *Desalination,* **225**(1-3), 249-259.

LIU R., LI Y., TANG, H., 2002. Synthesis and characteristics of chelating fibers containing imidazoline group or thioamide group. *J. Appli. Polym Sci,* **83**, 1608-1616.

LIU, M., DENG, Y., ZHAN, H. and ZHANG, X., 2002. Adsorption and desorption of copper(II) from solutions on new spherical cellulose adsorbent. *Journal of Applied Polymer Science,* **84**(3), 478-485.

LIU, R., LI, Y.I. and TANG, H., 1999. Application of the modified polyacrylonitrile fiber with amino-carboxyl-tetrazine groups for the preconcentration of trace heavy metal ions. *Journal of Applied Polymer Science,* **74**(11), 2631-2636.

LIU, R.X., ZHANG, B.W. and TANG, H.X., 1999. Synthesis and characterization of poly(acrylaminophosphonic-carboxyl-hydrazide) chelating fibre. *Reactive and Functional Polymers,* **39**(1), 71-81.

LLOYD, P.J., 2002. *Coal and the environment. JBA: Durban Energy Institute, University of Cape Town.* University of Cape Town: Durban Energy Institute,.

LUTFOR, M.R., SILONG, S., MD ZIN, W., AB RAHMAN, M.Z., AHMAD, M. and HARON, J., 2000. Preparation and characterization of poly(amidoxime) chelating

resin from polyacrylonitrile grafted sago starch. *European Polymer Journal,* **36**(10), 2105-2113.

MADAENI, S.S., MANSOURPANAH, Y., 2003. COD removal from concentrated wastewater using membranes. *Filtration and Separation,* **40**(6), 40-46.

MAUGUIN, G. and CORSIN, P., 2005. Concentrate and other waste disposals from SWRO plants: characterization and reduction of their environmental impact. *Desalination,* **182**(1-3), 355-364.

MCCOMB, M.E. and GESSER, H.D., 1997. Passive monitoring of trace metals in water by in situ sample preconcentration via chelation on a textile based solid sorbent. *Analytica Chimica Acta,* **341**(2-3), 229-239.

MICKLEY, M., HAMILTON, R., GALLENGOES, L. AND TRUESDALL, J., 1993. *Membrane concentration disposal.* Denver, Colorado: American Water works Association Research Foundation.

MOHAMED, A. M. O., AND ANTIA, H. E., 1998. Geoenvironmental Engineering. , 707-757.

MOHAMED, A.M.O., MARAQA, M. and AL HANDHALY, J., 2005. Impact of land disposal of reject brine from desalination plants on soil and groundwater. *Desalination,* **182**(1-3), 411-433.

MOROI, G., BILBA, D. and BILBA, N., 2004. Thermal degradation of mercury chelated polyacrylamidoxime. *Polymer Degradation and Stability,* **84**(2), 207-214.

NEDERLOF, M.M. and HOOGENDOORN, J.H., 2005. Desalination of brackish groundwater: the concentrate dilemma. *Desalination,* **182**(1-3), 441-447.

NILCHI, A., BABALOU, A.A., RAFIEE, R. and SID KALAL, H., 2008. Adsorption properties of amidoxime resins for separation of metal ions from aqueous systems. *Reactive and Functional Polymers,* **68**(12), 1665-1670.

OMICHI, H., KATAKAI, A., SUGO, T. and OKAMOTO, J., 1985. NEW TYPE OF AMIDOXIME-GROUP-CONTAINING ADSORBENT FOR THE RECOVERY OF URANIUM FROM SEAWATER. *Separation Science and Technology,* **20**(2-3), 163-178.

PAK, A. and MOHAMMADI, T., 2008. Wastewater treatment of desalting units. *Desalination,* **222**(1-3), 249-254.

PEREIRA LUIS S., CORDERY, IAN and IACOVIDES, I., 2002. *Coping with water scarcity.* No. 58. Paris: UNESCO.

PESAVENTO M., BIESUZ R. & CORTINA J. L., 1994. Sorption of Metal Ions on a Weak Cation-Exchange Resin Containing Carboxylic Groups. *Analytica Chimica Acta,* **298**, 225-235.

QIN, J.-J., WAI, M.-N., OO, M.H., WONG, F.S., 2002. A feasibility study on the treatment and recycling of a wastewater from metal plating. *Journal of Membrane Science,* **208**(1-2), 213-221.

RENGARAJ, S., YEON, K. and MOON, S., 2001. Removal of chromium from water and wastewater by ion exchange resins. *Journal of hazardous materials,* **87**(1-3), 273-287.

RIJSBERMAN, F.R., 2006. Water scarcity: Fact or fiction? *Agricultural Water Management,* **80**(1-3), 5-22.

RIVAS, B.L., MATURANA, H.A. and VILLEGAS, S., 2000. Adsorption behavior of metal ions by amidoxime chelating resin. *Journal of Applied Polymer Science*, **77**(9), 1994-1999.

RUBIO, J., SOUZA, M.L., SMITH, R.W., 2002. Overview of flotation as a wastewater treatment technique. *Minerals Engineering*, **15**(3), 139-155.

SAEED, A., IQBAL, M. and AKHTAR, M.W., 2005. Removal and recovery of lead(II) from single and multimetal (Cd, Cu, Ni, Zn) solutions by crop milling waste (black gram husk). *Journal of hazardous materials*, **117**(1), 65-73.

SAMCZY SKI Z. & DYBEZY SKI R., 1997. Some Examples of the Use of Amphoteric Ion-Exchange Resins for Inorganic Separations. *Journal of Chromatography A*, **789**, 157-167.

SÁNCHEZ, J.M., HIDALGO, M. and SALVADÓ, V., 2001. The selective adsorption of gold (III) and palladium (II) on new phosphine sulphide-type chelating polymers bearing different spacer arms: Equilibrium and kinetic characterisation. *Reactive and Functional Polymers*, **46**(3), 283-291.

SANDEEP, S., WALKER, S., DREWES, J. AND PEI, XU, 2006. Existing and Emerging concentrate minimization and disposal practices for membrane systems. *Florida Water Resources Journal*, 38-48.

SAPARI, N., IDRIS, A. and HAMID, N.H.A., 1996. Total removal of heavy metal from mixed plating rinse wastewater. *Desalination*, **106**(1-3), 419-422.

SCHLACHER, T. A. & WOOLDRIDGE, T. H., 1996. Ecological responses to reductions in freshwater supply and quality in South Africa's estuaries: lessons for management and conservation. *Journal of Coastal Conservation*, **2**, 115-130.

SCHOEMAN, J.J. and STEYN, A., 2001. Investigation into alternative water treatment technologies for the treatment of underground mine water discharged by Grootvlei Proprietary Mines Ltd into the Blesbokspruit in South Africa. *Desalination,* **133**(1), 13-30.

SENGUPTA, A.K., ZHU, Y. and HAUZE, D., 1991. Metal(II) ion binding onto chelating exchangers with nitrogen donor atoms: Some new observations and related implications. *Environmental Science and Technology,* **25**(3), 481-488.

SHIN, D.H., KO, Y.G., CHOI, U.S. and KIM, W.N., 2004. Design of High Efficiency Chelate Fibers with an Amine Group to Remove Heavy Metal Ions and pH-Related FT-IR Analysis. *Industrial and Engineering Chemistry Research,* **43**(9), 2060-2066.

SHUNKEVICH, A.A., AKULICH, Z.I., MEDIAK, G.V. and SOLDATOV, V.S., 2005. Acid–base properties of ion exchangers. III. Anion exchangers on the basis of polyacrylonitrile fiber. *Reactive and Functional Polymers,* **63**(1), 27-34.

SING, K. S. W., EVERETT, D. H., HAUL, R. A. W., MOSCOU, L., PIEROTTI, R. A., ROUQUEROL, J., SIEMIENIEWSKA, T., 1985. Reporting physisorption data for gas/solid systems with Special Reference to the Determination of Surface Area and Porosity. *Pure & App!. Chem.,* **57**(4), 603—619,

SOLDATOV, V. S., ELINSON, I. S., AND SHUNKEVICH, A. A., 1986. Purification of Air from Acid Gases (SO_2) by Non-Woven Strong-Base Filtering Materials. *Studies in Environmental Science,* **29**, 369-386.

SOLDATOV, V.S., SHUNKEVICH, A.A., WASAG, H., PAWLOWSKI, L., AND PAWLOWSKA, M., 2004. *Environmental engineering studies*. In: PAWLOWSKI ET AL., ed, New York: Plenum Publishers, pp. 153.

SOLDATOV, V.S., SHUNKEVICH, A.A., WASAG, H., PAWLOWSKI, L., AND WASANG, H., 1996. *Chemistry for the protection of the environment. No. 2*. In: PAWLOWSKI, ed, New York: Plenum Publishers, pp. 55.

SOLDATOV, V.S., 1984. New Fibrous ion Exchangers for Purification of Liquids and Gases, A.J.V.A.W.J.L. L. PAWLOWSKI, ed. In: *Studies in Environmental Science,* 1984, Elsevier pp353-364.

SOLDATOV, V.S., SHUNKEVICH, A.A., ELINSON, I.S., JOHANN, J. and IRAUSHEK, H., 1999. Chemically active textile materials as efficient means for water purification. *Desalination,* **124**(1-3), 181-192.

SOLDATOV, V.S., SHUNKEVICH, A.A. and SERGEEV, G.I., 1988. Synthesis, structure and properties of new fibrous ion exchangers. *Reactive Polymers, Ion Exchangers, Sorbents,* **7**(2-3), 159-172.

STRATTON, C. L. AND LEE, G. F., 1975. Cooling Towers and Water Quality. *Journal (Water Pollution Control Federation),* **47**(7), 1901-1912.

STREAT, M., 1984. Kinetics of slow diffusing species in ion exchangers. *Reactive Polymers, Ion Exchangers, Sorbents,* **2**(1-2), 79-91.

SULE, P.A. and INGLE, J.D., 1996. Determination of the speciation of chromium with an automated two-column ion-exchange system. *Analytica Chimica Acta,* **326**(1-3), 85-93.

SZLAG, D. C. AND WOLF, N. J., 1999. Recent advances in ion exchange material and processes for pollution prevention. *Clean Technologies and Environmental Policy,* **1**(2), 117-131.

TANG, W. and NG, H.Y., 2008. Concentration of brine by forward osmosis: Performance and influence of membrane structure. *Desalination,* **224**(1-3), 143-153.

TSIOURTIS, N.X., 2001. Desalination and the environment. *Desalination,* **141**(3), 223-236.

TUREK, M., 2004. Electrodialytic desalination and concentration of coal-mine brine. *Desalination,* **162**, 355-359.

TUREK, M., DYDO, P. and KLIMEK, R., 2008. Salt production from coal-mine brine in NF — evaporation — crystallization system. *Desalination,* **221**(1-3), 238-243.

VALERDI-PÉREZ, R., LÓPEZ-RODRÍGUEZ, M. and IBÁÑEZ-MENGUAL, J.A., 2001. Characterizing an electrodialysis reversal pilot plant. *Desalination,* **137**(1-3), 199-206.

VARSHNEY, K.G., 2003. Synthetic ion exchange materials and their analytical applications: Past, present and future.

VATUTSINA, O.M., SOLDATOV, V.S., SOKOLOVA, V.I., JOHANN, J., BISSEN, M. and WEISSENBACHER, A., 2007. A new hybrid (polymer/inorganic) fibrous sorbent for arsenic removal from drinking water. *Reactive and Functional Polymers,* **67**(3), 184-201.

VERNON, F. and SHAH, T., 1983. The extraction of uranium from seawater by poly(amidoxime)/poly(hydroxamic acid) resins and fibre. *Reactive Polymers, Ion Exchangers, Sorbents,* **1**(4), 301-308.

VEVERKA, P. and JERABEK KAREL, 2004. Influence of hyper crosslinking on adsorption and absorption on or in styrenic polymers. *Reactive & functional polymer,* **59**(1), 71-79.

VLAD, C., POINESCU, I. and COSTEA, E., 1996. Comments on the Porous Structure of Poly(methyl mthacrylate esters) networks. *European Polymer Journal,* **32**(9), 1067-1071.

WANG, Y., LIN, S. and JUANG, R., 2003. Removal of heavy metal ions from aqueous solutions using various low-cost adsorbents. *Journal of hazardous materials,* **102**(2-3), 291-302.

WANGNICK, K., *International Desalination Association Worldwide Desalting Plant Inventory produced by Wang Consulting for IDA.* Gnarrenburg, Germany: 2002.

WEI, J.F., WANG, Z.P., ZHANG, J., WU, Y.Y., ZHANG, Z.P. and XIONG, C.H., 2005. The preparation and the application of grafted polytetrafluoroethylene fiber as a cation exchanger for adsorption of heavy metals. *Reactive and Functional Polymers,* **65**(1-2), 127-134.

WILLIS, J.P., 1987. Variation in the composition of South African fly ash. Ash - a valuable resource. *Council for science and Industrial research,* **3**, 2-6.

WINTERS, J.C. and KUNIN, R., 1949. Ion Exchange in the Pharmaceutical Field. *Industrial & Engineering Chemistry*, **41**(3), 460-463.

WONG, K.K., LEE, C.K., LOW, K.S. and HARON, M.J., 2003. Removal of Cu and Pb by tartaric acid modified rice husk from aqueous solutions. *Chemosphere,* **50**(1), 23-28.

WU, R.S.S. and LAU, T.C., 1996. Polymer-ligands: a novel chemical device for monitoring heavy metals in the aquatic environment *Marine pollution bulletin,* **32**(5), 391-396.

YAVUZ, O., ALTUNKAYNAK, Y., and GUZEL, F., 2003. Removal of copper, nickel, cobalt and manganese from aqueous solution by kaolinite, *Water research*, **37**(4), 948-952.

ZAGORODGNI, A.A., 2007. Ion Exchange Materials: Properties and Application. London: Elsevier Oxford.

ZHANG, L., ZHANG, X., LI, P. and ZHANG, W., 2009. Effective Cd^{2+} chelating fiber based on polyacrylonitrile. *Reactive and Functional Polymers,* **69**(1), 48-54.

7 Appendix

7.1 Analysis of Calcium, Magnesium, Sodium, and Copper by Atomic Absorption Spectroscopy

7.1.1 Determination of Calcium and Magnesium

Instrument: Atomic absorption spectrophotometer (AAS), model PU9100 Philips AAS

Instrument Conditions:

Element	**Ca**	**Mg**
Mode	Absorption	Absorption
Wavelength	422.7 nm	285.2 nm
Band pass	0.2-0.5 nm	0.2-0.5 nm
Air flow	5 L/min	5 L/min
Flue flow	5 L/min	5 L/min
Lamp current	max 10 mA	max 4 mA
Burner height	10 mm	10 mm

7.1.1.1. Stock solution of 1000 ppm for Ca and Mg: 3.6682 g $CaCl_2$ and 8.3645 g $MgCl_2$ were dissolved in deionized water and made up to the mark in a 1000 mL volumetric flask.

7.1.1.2. Stock solution of 100 ppm for Ca and Mg: 10 mL of 1000 ppm stock solution was taken in a 100 mL volumetric flask and was made up to the mark with deionized water.

7.1.1.3. Working Standards: 20, 40, 60, 80 and 100 ppm of working standards for Calcium were prepared by taking 20, 40, 60, 80, and 100 ppm stock solution in a series of 100 mL volumetric flasks. For Magnesium, 1, 2, 3, 4 and 5 ppm of working standards were prepared by taking 1, 2, 3, 4 and 5 ppm stock solution in a series of 100 mL volumetric flasks.

A.1.4. Procedure: Atomic absorption spectrophotometer was set according to the above mentioned conditions for Ca and Mg separately. The cathode lamp for both Ca and Mg were turn on to warm up for at least 10 minutes. The instrument was then calibrated and standardized with the working standards of 20 to 100 ppm for Ca and 1 to 5 ppm for Mg, respectively. All the working standards were run as unknown and their actual concentration was verified. The sample solutions were run on the atomic absorption and the concentrations of Ca and Mg in ppm were noted for each sample.

7.1.2 Determination of Sodium

Instrument: Atomic absorption spectrophotometer (AAS), model PU9100 Philips AAS

Instrument Conditions:

Element	**Na**
Mode	Absorption
Wavelength	589 nm
Band pass	0.2-0.5 nm
Air flow	5 L/min
Flue flow	5 L/min
Lamp current	max 8 mA
Burner height	20 mm

7.1.2.1. Stock solution of 1000 ppm for Ca and Mg: 2.5435 g NaCl was dissolved in deionized water and made up to the mark in a 1000 mL volumetric flask.

7.1.2.2. Stock solution of 100 ppm for Ca and Mg: 10 mL of 1000 ppm stock solution was taken in a 100 mL volumetric flask and was made up to the mark with deionized water.

7.1.2.3. Working Standards: 1, 2, 3, 4 and 5 ppm of working standards for Na were prepared by taking 1, 2, 3, 4 and 5 ppm stock solution in a series of 100 mL volumetric flasks.

7.1.2.4. Procedure: Atomic absorption spectrophotometer was set according to the above mentioned conditions for Na. The cathode lamp for both Na was turned on to warm up for at least 10 minutes. The instrument was then calibrated and standardized with the working standards of 1 to 5 ppm for Na. All the working standards were run as unknown and their actual concentration was verified. The sample solutions were run on the atomic absorption and the concentration of Na in ppm was noted for each sample.

7.1.3 Determination of Copper

Instrument: Atomic absorption spectrophotometer (AAS), model PU9100 Philips AAS

Instrument Conditions:

Element	**Cu**
Mode	Absorption
Wavelength	325.8 nm
Band pass	0.2-0.5 nm
Air flow	5 L/min
Flue flow	1 L/min
Lamp current	max 4 mA
Burner height	10 mm

7.1.3.1. Stock solution of 1000 ppm for Cu: 2.4005 g $CuCl_2$ was dissolved in deionized water and made up to the mark in a 1000 mL volumetric flask.

7.1.3.2. Stock solution of 100 ppm for Cu: 10 mL of 1000 ppm stock solution was taken in a 100 mL volumetric flask and was made up to the mark with deionized water.

7.1.3.3. Working Standards: 10, 20, 30, 40 and 50 ppm of working standards for Cu were prepared by taking 10, 20, 30, 40 and 50 ppm stock solution in a series of 100 mL volumetric flasks.

7.1.3.4. Procedure: Atomic absorption spectrophotometer was set according to the above mentioned conditions for Cu. The cathode lamp for both Cu was turned on to warm up for at least 10 minutes. The instrument was then calibrated and standardized with the working standards of 10 to 50 ppm for Cu. All the working standards were run as unknown and their actual concentration was verified. The sample solutions were run on the atomic absorption and the concentration of Cu in ppm was noted for each sample.

7.2 Equilibrium Adsorption Isotherms

This section contains table of results and graphs showing the equilibrium adsorption isotherm for calcium, magnesium and sodium. It also contains the Langmuir and Freundlich modeling results for the isotherms.

Table 7.1: Equilibrium concentration versus metal ion adsorption for Calcium by Amberlite 252 RFH resin, Alkali-treated Amidoxime and Amidoxime fibres

Concentration (mg/L)	Amberlite 252 RFH Resin		Amidoxime fibre		Alkali-treated Amidoxime fibre	
	C_e	q_e	C_e	q_e	C_e	q_e
100	22.7273	37.7722	88.6364	5.5541	86.3636	6.6454
200	59.0909	68.7037	177.2727	11.0779	170.4545	14.3693
300	104.5455	94.8855	263.6364	17.6694	252.2727	23.1675
400	193.1818	104.8951	352.2727	23.1686	338.6364	29.7475
500	279.5455	108.8471	434.0909	31.9327	415.9091	40.7417
600	345.4545	119.9616	511.3636	42.8865	500.0000	48.4006
800	529.5455	127.0998	688.6364	53.6951	672.7273	61.3944
1000	727.2727	126.2103	886.3636	54.7128	872.7273	61.1010

Table 7.2: Equilibrium concentration versus metal ion adsorption for Magnesium by Amberlite 252 RFH resin, Alkali-treated Amidoxime and Amidoxime fibres

Concentration (mg/L)	Amberlite 252 RFH Resin		Amidoxime fibre		Alkali-treated Amidoxime fibre	
	C_e	q_e	C_e	q_e	C_e	q_e
100	51.6484	26.0086	87.3626	8.2203	81.4186	11.0511
200	126.3736	40.5630	178.0220	14.8214	166.2538	20.2132
300	214.2857	48.7631	271.4286	20.0085	253.2468	28.3014
400	307.1429	54.4937	361.5385	26.7636	339.6603	36.6069
500	401.0989	59.4683	445.0549	36.6462	409.5904	53.0614
600	494.5015	64.6154	538.4615	41.2733	506.9930	56.1697
800	692.3077	69.9206	747.2527	41.0997	709.7902	58.2990
1000	901.0989	69.3651	950.5405	43.5259	909.5904	61.4298

Table 7.3: Equilibrium concentration versus metal ion adsorption for Sodium by Amberlite 252 RFH resin, Alkali-treated Amidoxime and Amidoxime fibres

Concentration (mg/L)	**Amberlite 252 RFH Resin**		**Amidoxime fibre**		**Alkali-treated Amidoxime fibre**	
	C_e	q_e	C_e	q_e	C_e	q_e
100	54.1045	22.7984	95.6938	7.1201	63.0435	18.2762
200	117.5373	40.9334	193.7799	13.0535	147.8261	25.6762
300	184.7015	57.0554	291.8660	18.8745	239.1304	29.8088
400	257.4627	69.8955	370.8134	34.1416	330.4348	33.9717
500	339.5522	78.4052	454.5455	46.7826	413.0435	42.2940
600	429.1045	82.6370	550.2392	53.5569	500.0000	48.5724
800	623.1343	85.9293	741.6268	67.2763	695.6522	50.6257
1000	820.8955	86.4577	956.9378	68.9106	891.3043	51.9381

NB. A plot of equilibrium concentration versus metal ion concentration adsorbed at equilibrium will give the equilibrium adsorption isotherm in the 100 to 1000 mg/L concentration range.

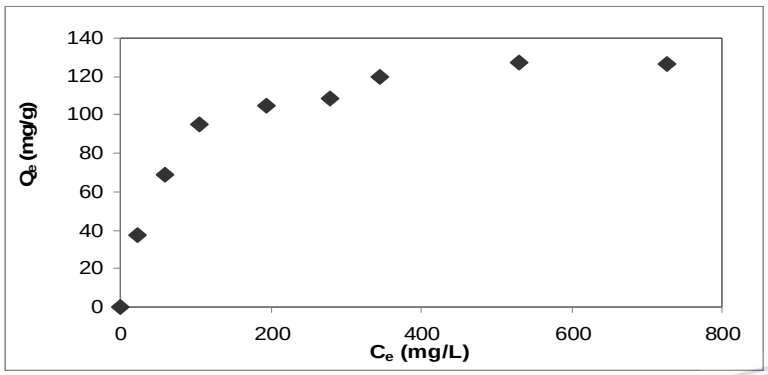

(a)

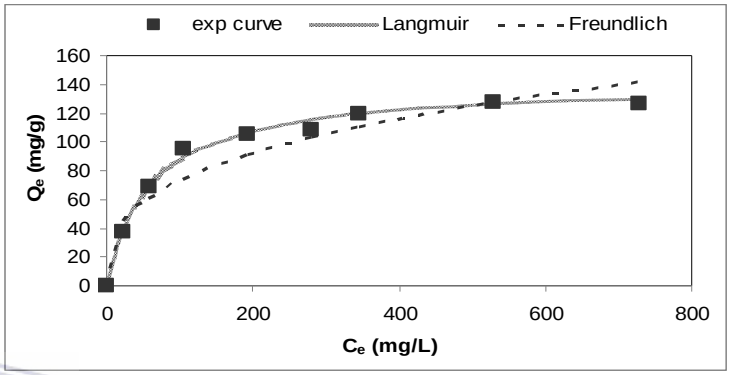

(b)

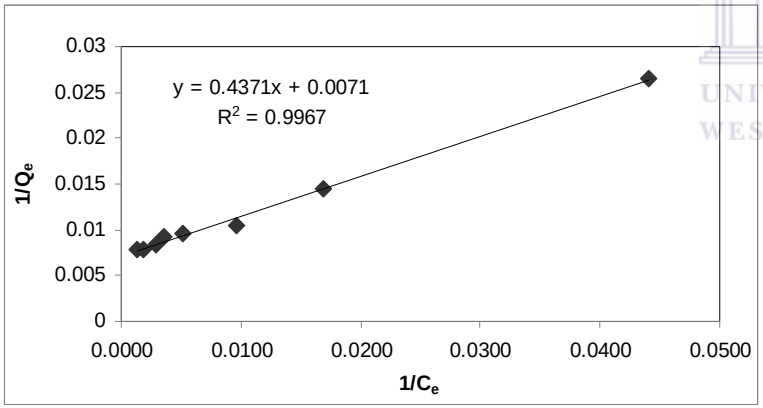

(c)

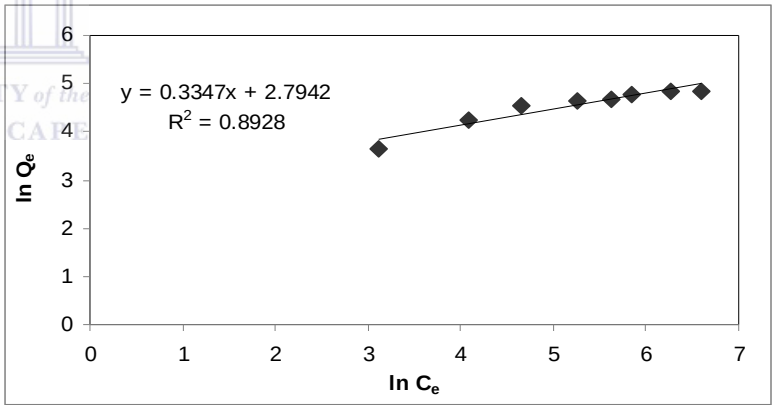

(d)

Figure 7.1: (a) Equilibrium adsorption isotherm, (b) The comparison of the experimental and theoretical curves for Langmuir & Freundlich models, (c) linearized form of Langmuir and (d) linearized form of Freundlich for adsorption of Ca^{2+} ions by Amberlite 252 RFH resin.

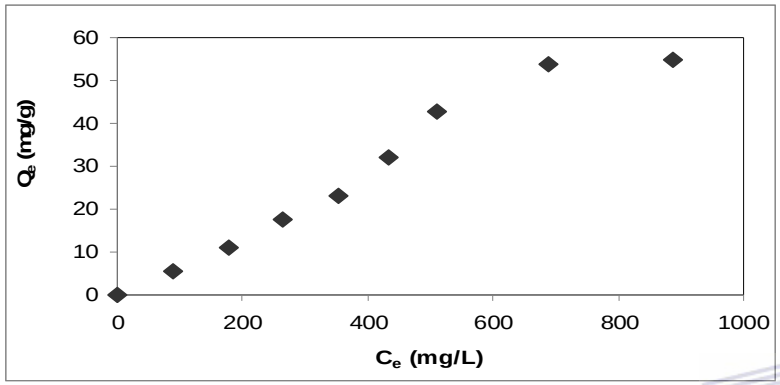

(a)

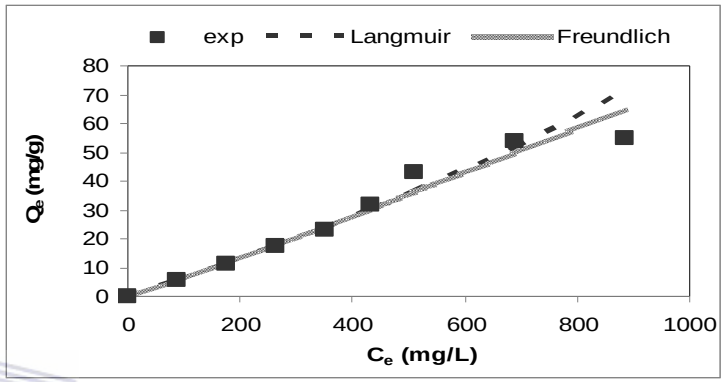

(b)

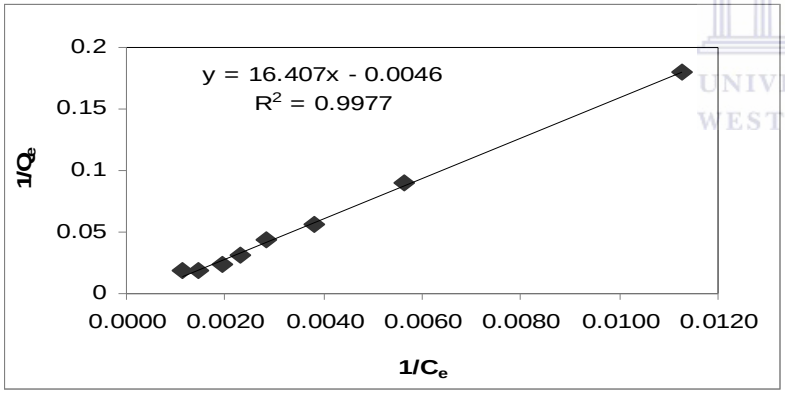

(c)

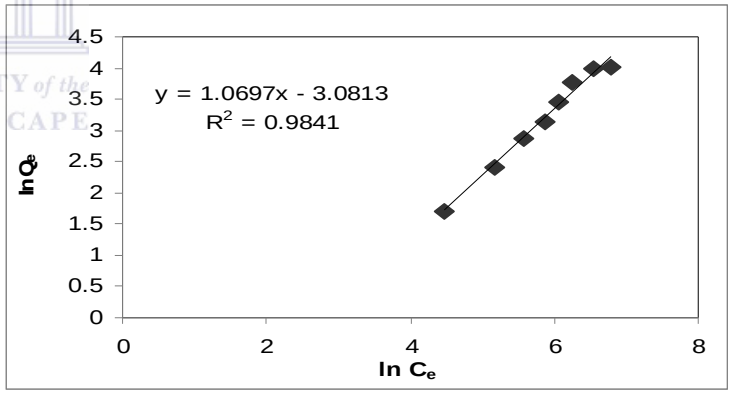

(d)

Figure 7.2: (a) The comparison of the experimental and theoretical curves for Langmuir & Freundlich models, (b) Equilibrium adsorption isotherm, (c) linearized form of Langmuir and (d) linearized form of Freundlich for adsorption of Ca^{2+} ions by Amidoxime fibres.

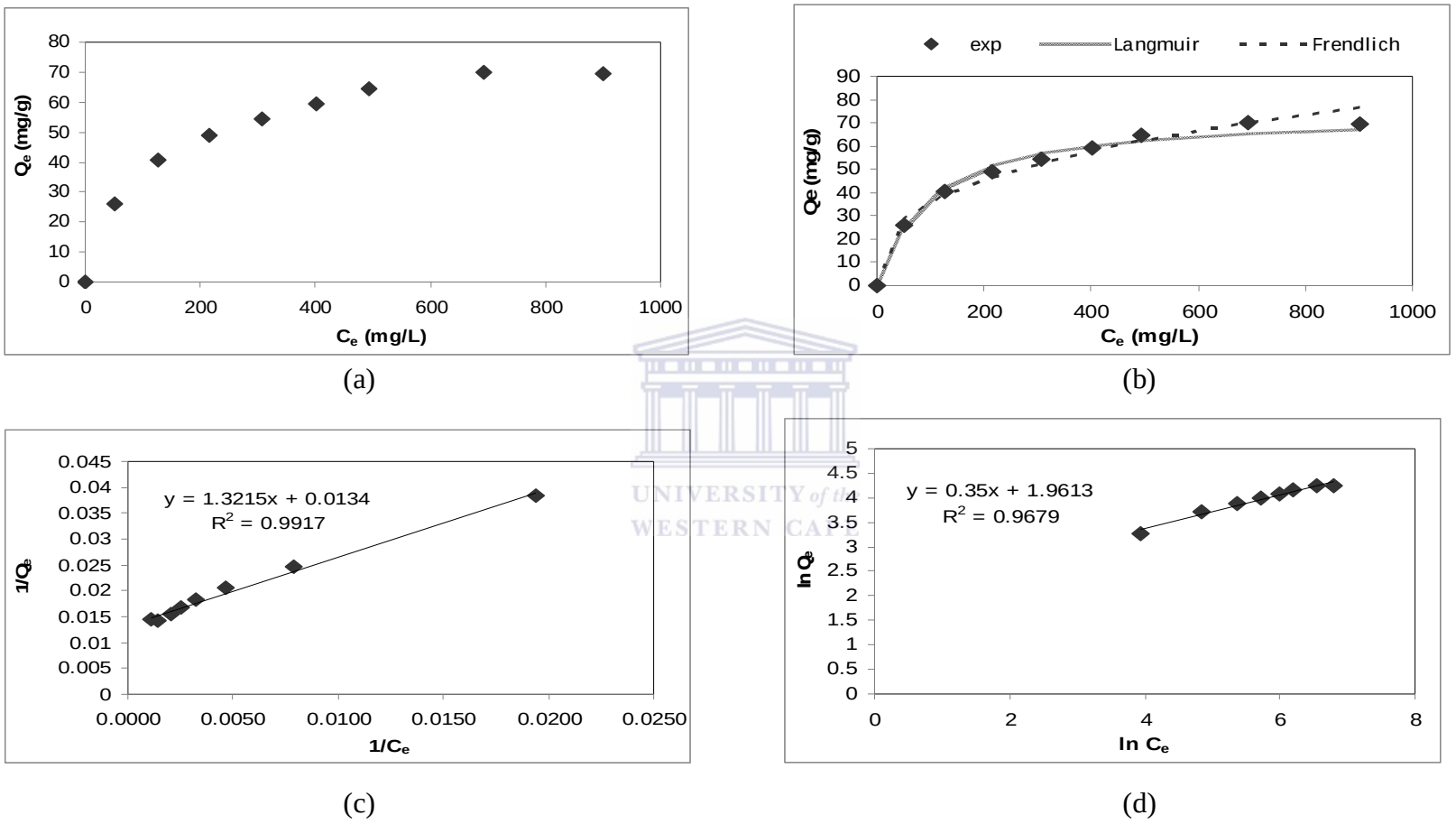

Figure 7.3: (a) Equilibrium adsorption isotherm, (b) The comparison of the experimental and theoretical curves for Langmuir & Freundlich models, (c) linearized form of Langmuir and (d) linearized form of Freundlich for adsorption of Mg^{2+} ions by Amberlite 252 RFH resins.

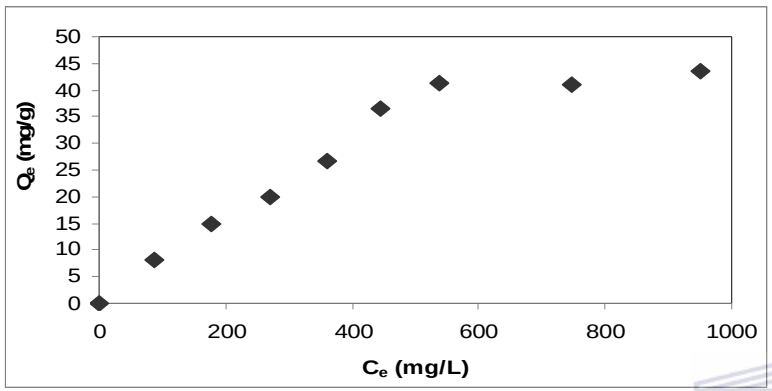

(a)

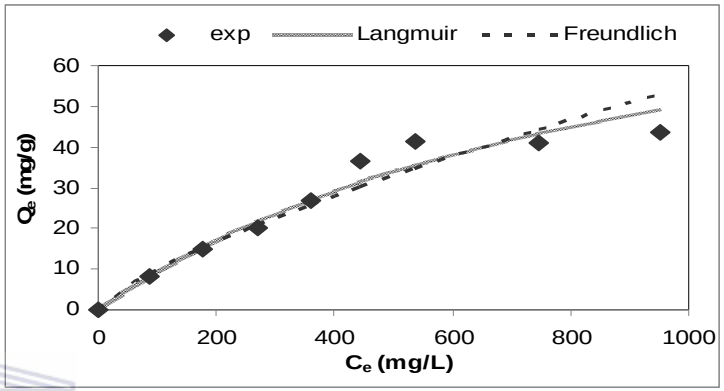

(b)

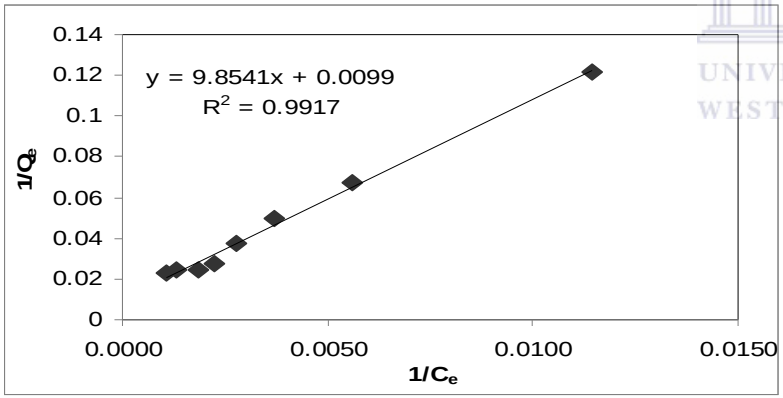

(c)

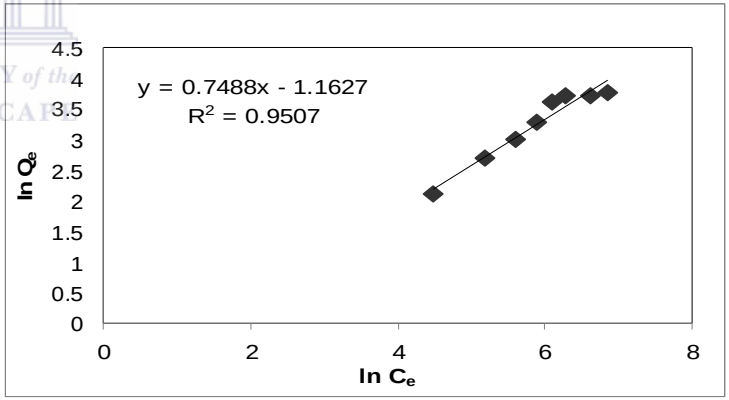

(d)

Figure 7.4: (a) Equilibrium adsorption isotherm, (b) The comparison of the experimental and theoretical curves for Langmuir & Freundlich models, (c) linearized form of Langmuir and (d) linearized form of Freundlich for adsorption of Mg^{2+} ions by Amidoxime fibre.

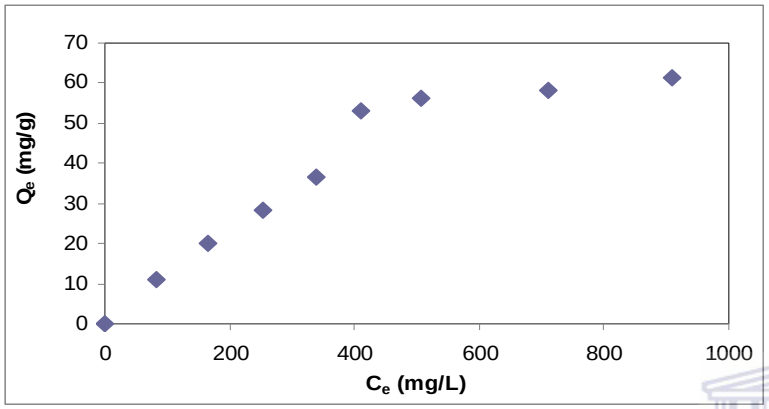

(a)

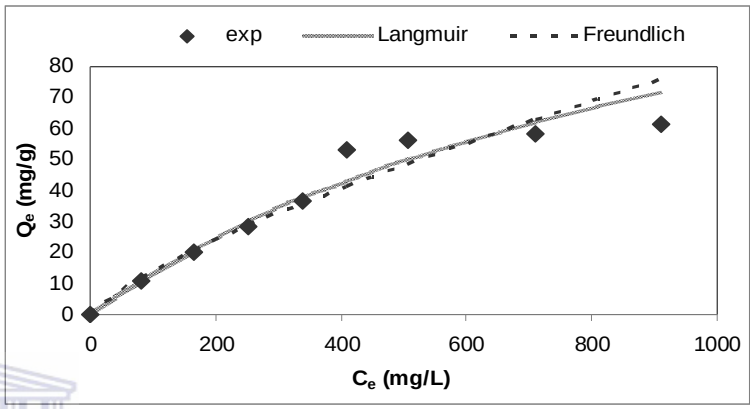

(b)

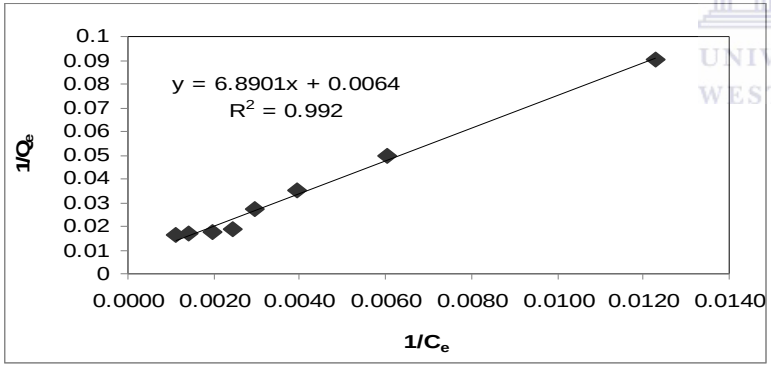

(c)

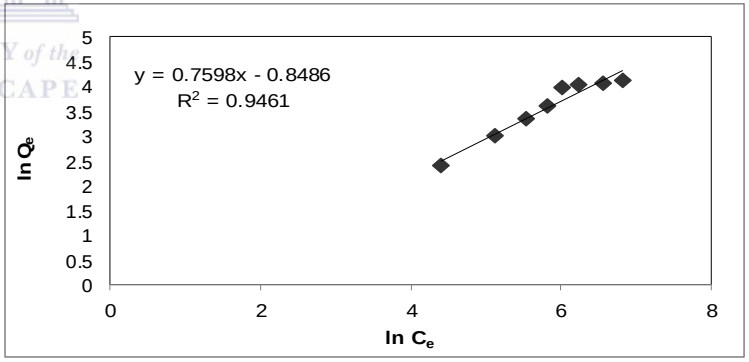

(d)

Figure 7.5: (a) Equilibrium adsorption isotherm, (b) The comparison of the experimental and theoretical curves for Langmuir & Freundlich models, (c) linearized form of Langmuir and (d) linearized form of Freundlich for adsorption of Mg^{2+} ions by Hydrolyzed Amidoxime fibres.

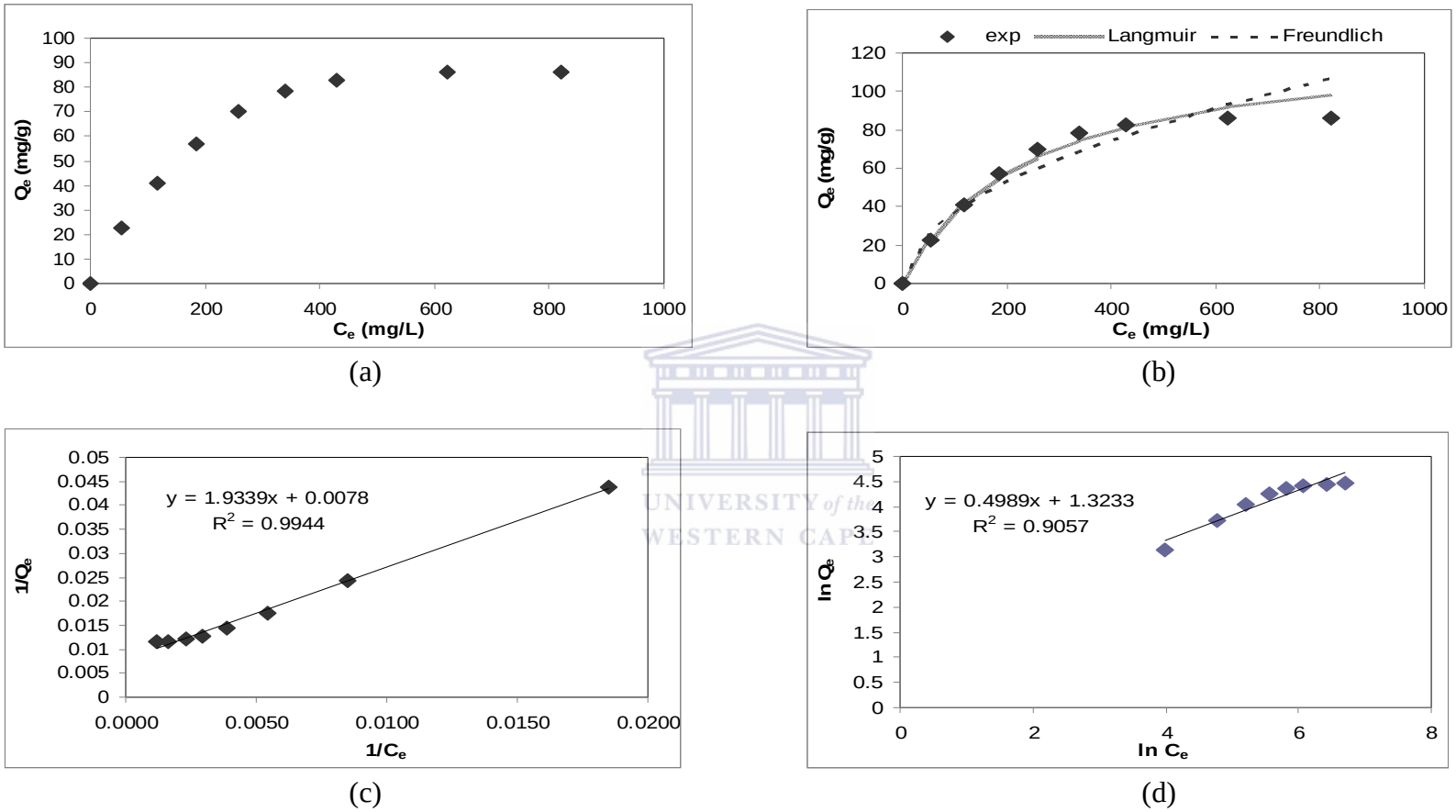

Figure 7.6: (a) Equilibrium adsorption isotherm, (b) The comparison of the experimental and theoretical curves for Langmuir & Freundlich models, (c) linearized form of Langmuir and (d) linearized form of Freundlich for adsorption of Na^+ ions by Amberlite 252 RFH resins.

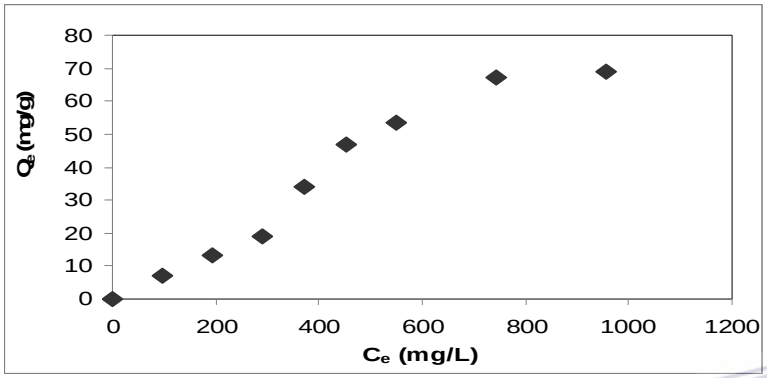

(a)

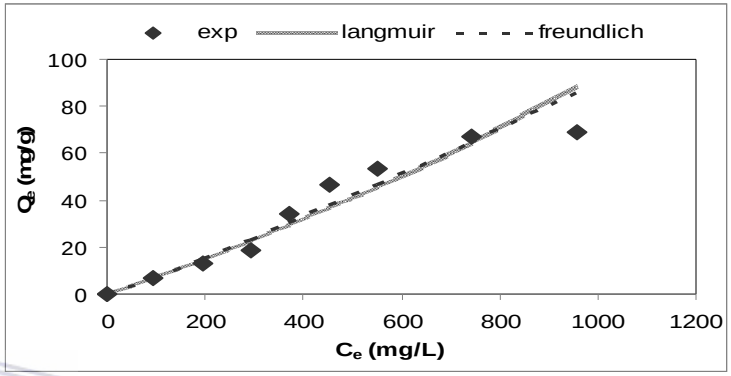

(b)

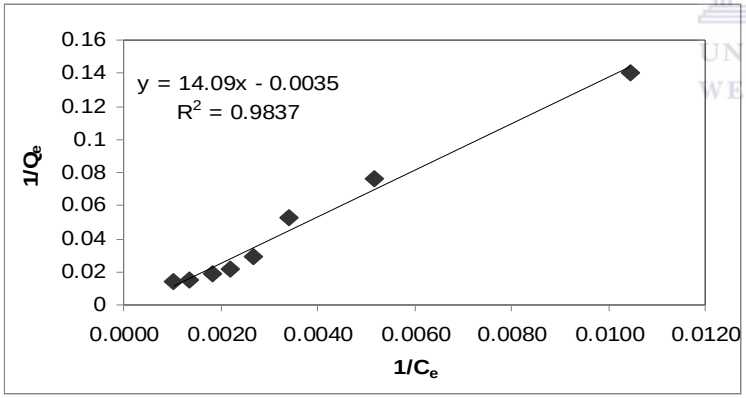

(c)

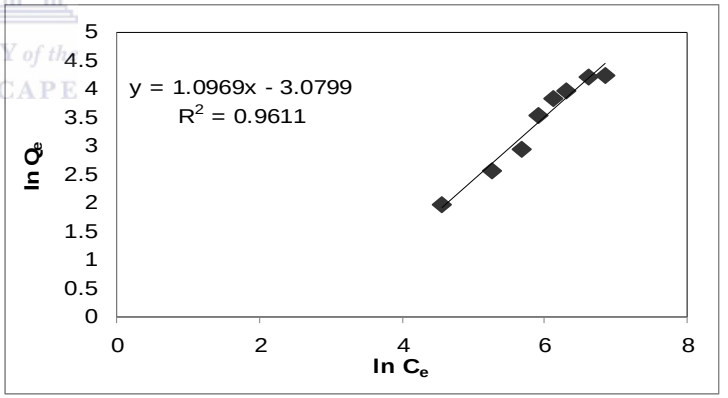

(d)

Figure 7.7: (a) Equilibrium adsorption isotherm, (b) The comparison of the experimental and theoretical curves for Langmuir & Freundlich models, (c) linearized form of Langmuir and (d) linearized form of Freundlich for adsorption of Na^+ ions by Amidoxime fibre.

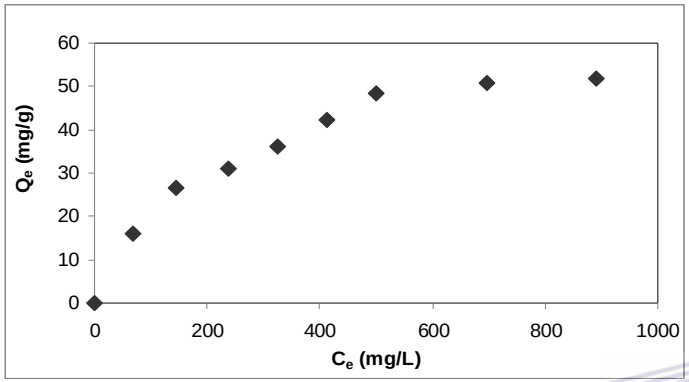

(a)

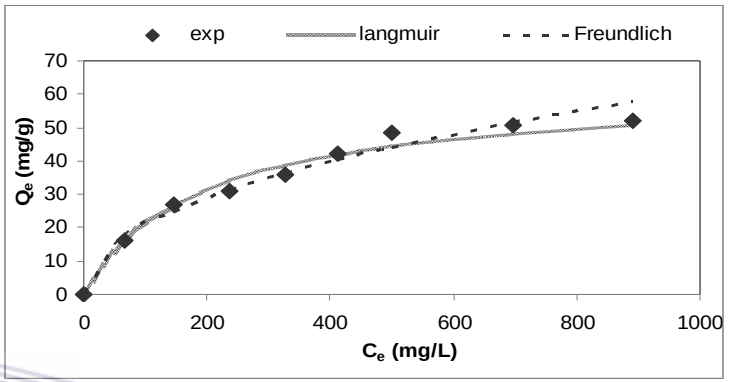

(b)

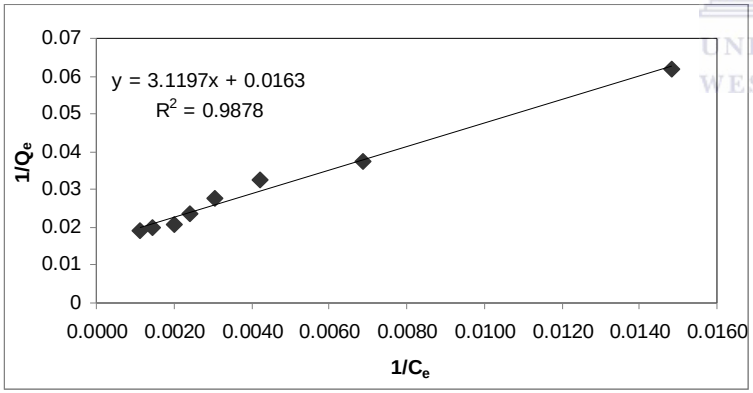

(c)

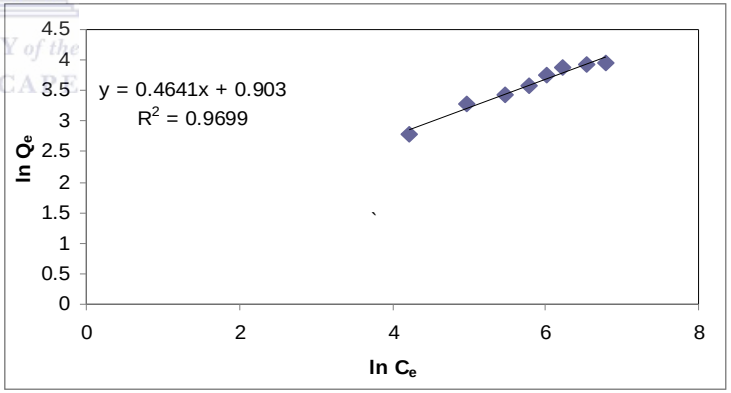

(d)

Figure 7.8: (a) Equilibrium adsorption isotherm, (b) The comparison of the experimental and theoretical curves for Langmuir & Freundlich models, (c) linearized form of Langmuir and (d) linearized form of Freundlich for adsorption of Na^+ ions by Hydrolyzed Amidoxime fibres.

7.3 Kinetics of Adsorption

This section contains the adsorption kinetics table of results and the graphs showing the adsorption rates for Ca^{2+}, Mg^{2+} and Na^{+} adsorption by Amberlite 252 RFH resins, Alkali-treated Amidoxime fibres and Amidoxime fibres. It also presents the kinetics modelling graphs showing the best fit between first and second order reaction rates for the kinetics adsorption expriments.

Table 7.4:

Time (mins)	Ca^{2+} (mg/g)			Mg^{2+} (mg/g)			Na^{+} (mg/g)		
	Amberlite resin	Alkali-treated Amidoxime	Amidoxime	Amberlite resin	Alkali-treated Amidoxime	Amidoxime	Amberlite resin	Alkali-treated Amidoxime	Amidoxime
1	27.4620	10.9848	7.3457	8.0373	12.3252	1.6081	12.5524	13.6683	1.9999
5	32.7923	19.1302	12.2070	17.9428	15.4775	4.8174	20.1324	15.1692	5.8361
10	33.9257	21.7120	14.1642	24.4308	17.5867	6.9247	23.0244	16.3301	6.5884
15	35.1960	27.0739	15.6250	28.1125	19.1206	8.5269	24.4618	16.7171	7.3469
20	36.5155	27.0475	15.3514	31.1759	19.0837	8.4697	25.1904	16.6762	7.3398
25	41.7610	26.9426	15.5642	34.3065	18.9375	8.3686	25.7679	16.6273	7.3291
30	42.9415	26.8385	15.4814	34.2732	18.8833	8.3369	25.6185	16.5455	7.2554
40	42.9208	26.8255	15.4291	34.2566	18.6959	8.3408	25.6185	16.5707	7.2211
50	42.7969	26.7480	15.2964	34.1410	18.5122	8.2509	25.4954	16.5146	7.2855
60	42.7350	26.7094	15.2672	34.0401	18.4948	8.2238	25.4708	16.4746	7.2675
90	42.7550	26.7655	15.3215	34.2656	18.5433	8.2815	25.4955	16.5235	7.2831
120	42.7815	26.7355	15.2716	34.2417	18.5222	8.3015	25.4875	16.5677	7.2627
150	42.7745	26.7650	15.2829	34.2775	18.5466	8.3012	25.4825	16.5478	7.2315
180	42.7565	26.7426	15.2615	34.2532	18.5566	8.2950	25.4855	16.5575	7.2515

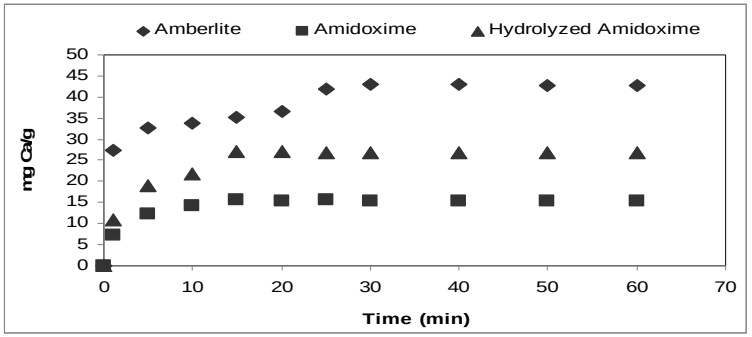

(a)

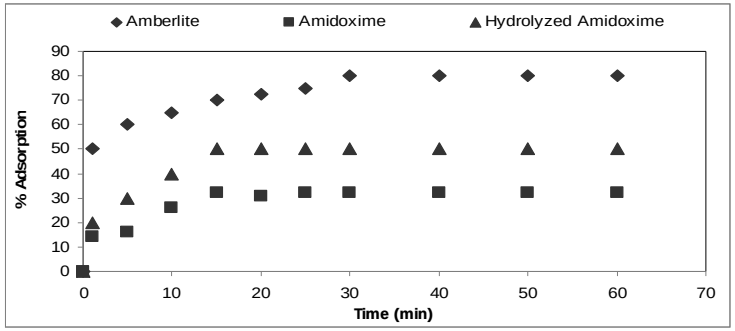

(b)

Figure 7.9: (a) Adsorption kinetics of Ca^{2+} ions from an initial concentration of 100 mg/L by Amberlite resin, Amidoxime fibre and hydrolyzed Amidoxime fibre and (b) % Adsorption of Ca^{2+} ions from an initial concentration of 100 mg/L by Amberlite resin, Amidoxime fibre and hydrolyzed Amidoxime fibre.

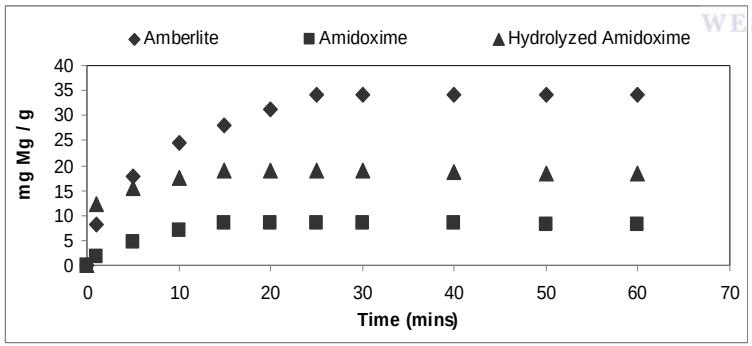

(a)

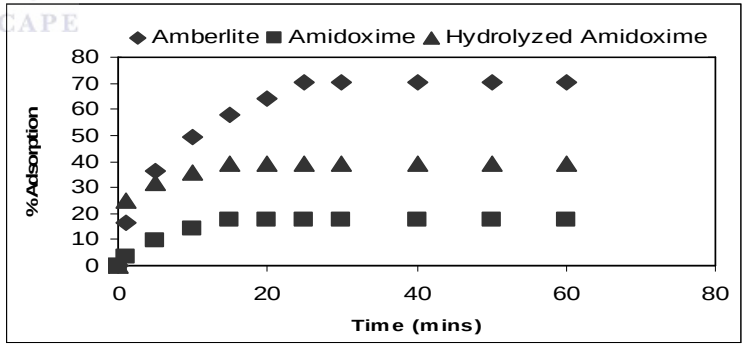

(b)

Figure 7.10: (a) Adsorption kinetics of Mg^{2+} ions from an initial concentration of 100 mg/L by Amberlite resin, Amidoxime fibre and hydrolyzed Amidoxime fibre and (b) % Adsorption of Mg^{2+} ions from an initial concentration of 100 mg/L by Amberlite resin, Amidoxime fibre and hydrolyzed Amidoxime fibre.

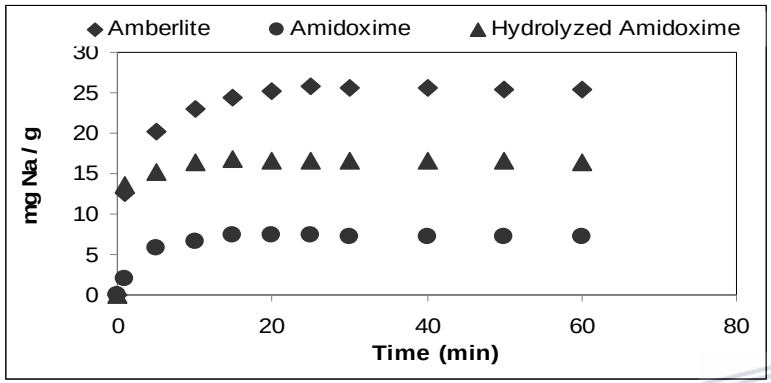

(a)

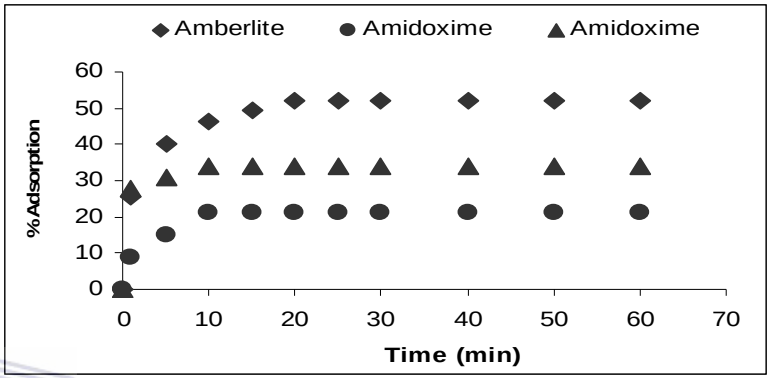

(b)

Figure 7.11: (a) Adsorption kinetics of Na^+ ions from an initial concentration of 100 mg/L by Amberlite resin, Amidoxime fibre and hydrolyzed Amidoxime fibre and (b) % Adsorption of Na^+ ions from an initial concentration of 100 mg/L by Amberlite resin, Amidoxime fibre and hydrolyzed Amidoxime fibre.

7.3 1st & 2nd Order Modelling of Kinetics Adsorption data

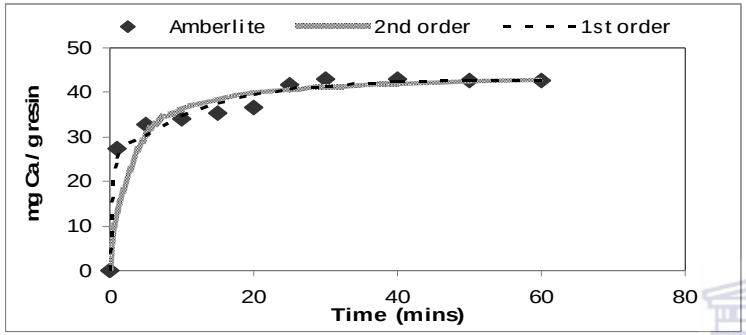

(a)

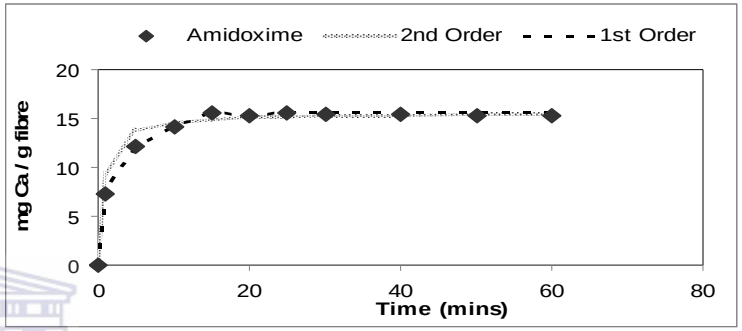

(b)

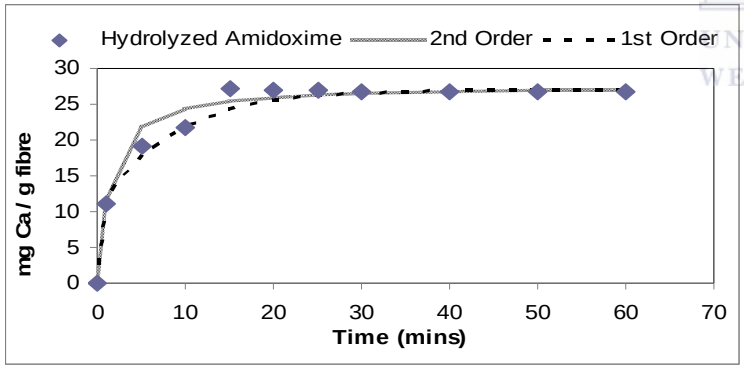

(c)

Figure 7.12: Plot of sorbed capacity versus time for the sorption kinetics of Ca^{2+} onto (a) Amberlite resin, (b) Amidoxime fibres and (c) alkali-treated Amidoxime fibres and modelled as 1st and 2nd order reaction rate.

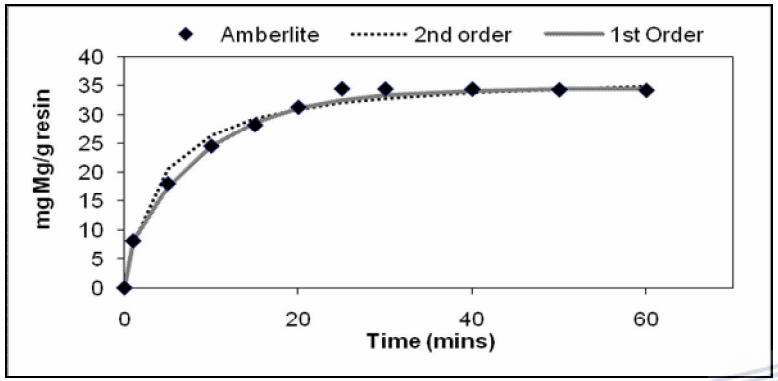

(a)

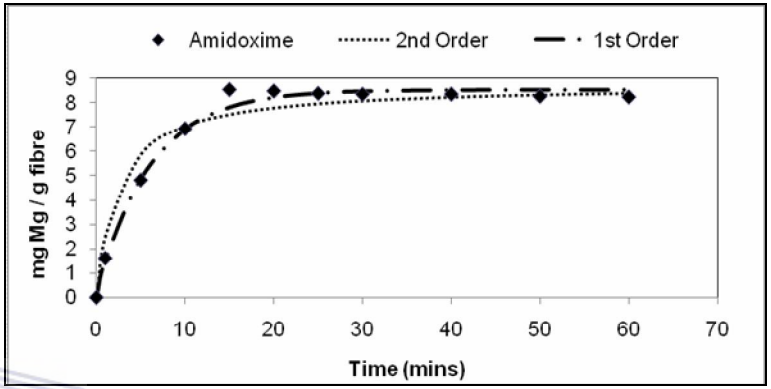

(b)

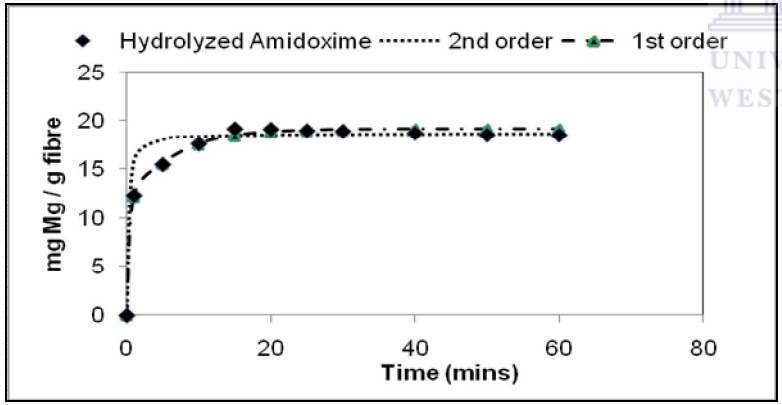

(c)

Figure 7.13: Plot of sorbed capacity versus time for the sorption kinetics of Mg^{2+} onto (a) Amberlite resin, (b) Amidoxime fibres and (c) alkali-treated Amidoxime fibres and modelled as 1st and 2nd order reaction rate.

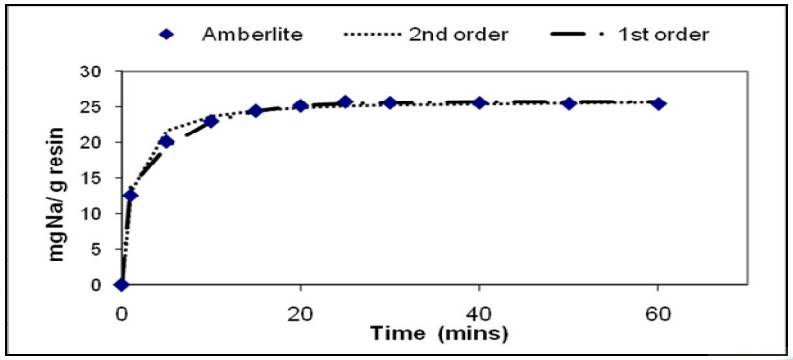

(a)

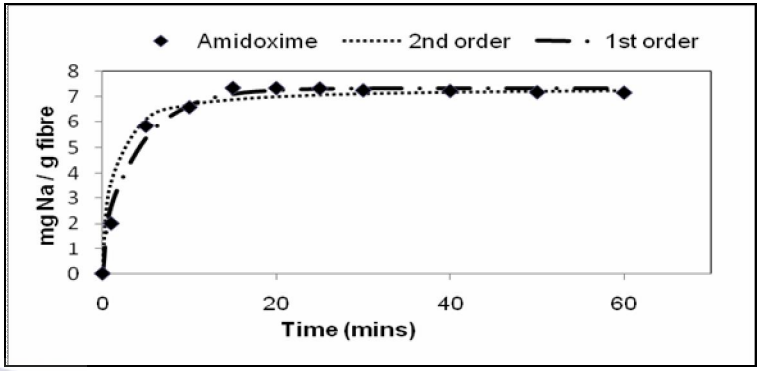

(b)

(c)

Figure 7.14: Plot of sorbed capacity versus time for the sorption kinetics of Na^+ onto (a) Amberlite resin, (b) Amidoxime fibres and (c) Hydrolyzed Amidoxime fibres and modelled as 1st and 2nd order reaction rate.